X-RAY DIFFRACTION ANALYSIS
OF THE STRUCTURE OF DEOXYRIBONUCLEIC ACID

by

Harold Winfield Wyckoff

B.S. Antioch College
(1949)

SUBMITTED IN PARTIAL FULFILLMENT
OF THE REQUIREMENTS FOR THE
DEGREE OF DOCTOR OF
PHILOSOPHY

at the

MASSACHUSETTS INSTITUTE OF TECHNOLOGY
June, 1955

Signature of Author

Department of Biology, June 6, 1955

Certified by

Thesis Supervisor

Accepted by

Chairman, Departmental Committee on Graduate Students

ABSTRACT

X-RAY DIFFRACTION ANALYSIS OF THE STRUCTURE OF DEOXYRIBONUCLEIC ACID

by

Harold Winfield Wyckoff

Submitted to the Department of Biology on June 6, 1955 in partial fulfillment of the requirements for the degree Doctor of Philosophy.

Three distinct types of X-ray diffraction pattern were obtained from DNA isolated from calf thymus by the Schwander-Signer method. One of these, obtained with the specimen immersed in 85 per cent ethanol, was indistinguishable from the patterns in the literature of type A. A pattern (designated B_3) similar to the B pattern of the literature but exhibiting much more detail was obtained with the specimen immersed in 70 per cent ethanol and held under mild tension. The axial repeat period was 34.2 A and the spacing between helix axes (in a hexagonal array) was 25.2 A. A lattice containing a frequent quantized defect was derived. A pattern (designated B_2) resembling the B pattern more closely than the A pattern was obtained from DNA immersed in 85 per cent ethanol and stretched 55 per cent. The axial repeat period was 32.5 A. The specimen was crystalline. Mechanical and optical studies were used to correlate the A to B_2 transition observed by X-ray diffraction with the mechanical and optical studies in the literature. Completely reversible 2 fold elongation was observed.

A molecular model for DNA in the B_3 form was derived. It is in substantially better agreement with the X-ray data than the Watson and Crick model. The basic assumptions of the latter are maintained. It was necessary to hypothesize a new configuration for the deoxyribose. In the model the two backbone chains are helically arranged outside the base pairs with 10 residues per 34 A turn. The phosphorus atoms are located on helices of 9.9 A radius axially displaced from each other by 0.442 turns. The centers of all of the atoms of the base pair (except two hydrogens) are within 5.1 A of the axis.

Many aids to analysis were developed that will be of use in any structure determination involving nucleic acid, including refinement of optical diffraction technique and instrumentation, a method for taking the water of hydration into account by modifying the weights of the atoms of the main structure, simplification and graphical representation of the diffraction equations, and design of a three dimensional model kit.

X-ray diffraction patterns were obtained from DNA stained with acridine orange that exhibited the same type of lattice as that derived for the B_3 pattern. The axial repeat was 34 A and the distance between helix axes was 21.4 A. A plausible type of structure was derived for the complex and correlated with the results of complexing studies carried out in dilute solution. Denaturation vastly

Biol., Nov. 22, 1955

changed the complexing in solution.

The results of spectroscopic studies on the complexing of acriflavine and $MgCl_2$ are reported and data concerning the "solubility" of DNA in alcoholic solutions is presented.

Thesis Supervisor: Richard S. Bear
Title: Professor of Biophyical Chemistry

ACKNOWLEDGEMENTS

I wish to express by gratitude to Professor Richard S. Bear for his constant advice and encouragement and his patience with a neophyte. I wish to thank Dr. Jesse F. Scott for many discussions concerning the biological and spectroscopic properties of DNA. I am grateful to Miss Rosalin Franklin for the suggestion that a lattice defect might explain some of my data. I wish to express my thanks to all of the members of the Biology Department staff for their efforts and good will in attempting to transmute a physicist into a biophysicist. I am also indebted to Misses Carolyn Cohen, May I. Chow, and Barbara Hall for invaluable help in the development and application of the optical diffraction technique. I wish to thank Mr. William Strovnik and Mr. James Dunell for aid in the design and construction of the optical diffractograph and the three dimensional model kit.

TABLE OF CONTENTS

	Page
Title page	1
Abstract	2
Acknowledgments	4
Table of Contents	5
Table of Plates, Figures, and Tables	8
Introduction	11
Experimental	25
Preparation of DNA from calf thymus	25
1. Methods used	25
2. Details of two preparations	26
X-ray techniques	32
1. Specimen preparation and mounting	32
2. Subtleties of fiber formation	34
3. Immersion of the specimen in alcoholic solutions	36
Optical diffractograph	38
1. Design of the optical diffractograph	38
2. Technique	40
Three dimensional model	42
Results	44
X-ray diffraction patterns	44
Tension elongation and birefringence	56
The solubility of DNA in alcoholic systems	63
The ultraviolet absorption coeficient of DNA as a function of the presence and concentration of salts and as a function of denaturation	69

TABLE OF CONTENTS (Continued)

The binding of acridine derivatives to DNA 70

1. Experimental method 70
2. Experiments with "normal" DNA 71
3. Experiments with denatured DNA 74

Analysis of the X-ray Data 76

Lattice 76

1. The B_3 DNA pattern 76
2. Acridine orange stained DNA pattern 81
3. The B_2 DNA pattern 82

The form factor and molecular structure; general considerations for the DNA system 83

1. Diffraction from helices; systems with a dyad axis 83
2. Diffraction from helical systems of the DNA components; an optical diffractograph study 87
3. Treatment of the diffraction from the extensive water of hydration in DNA 95
4. Comparison of the optical diffractograph "sections" with x-ray "rotation" patterns 107

The form factor and molecular structure; the DNA B_3 pattern 112

1. Analytic description of the DNA B_3 pattern 112
2. Evaluation of the Watson and Crick model as a source of the DNA B_3 pattern 115
3. Evaluation of modifications of the Watson and Crick model 118
   a. Phase maps in the $\phi - z$ plane 119
   b. The effects of motion of the components of DNA on the diffraction pattern 121
   c. Radial parameters and the equatorial intensity problem 122
   d. Calculation of certain stearic limitations to modification of the model 127

TABLE OF CONTENTS (Continued)

    - e. Configuration of the pentose; configuration of non-resonant-ring structures with five members 131
- 4. A molecular model for DNA with a modified deoxyribose configuration 133
    - a. Modification of the furanose ring 133
    - b. Model building with the hypothetical deoxyribose 134
    - c. Model #4.0 137
    - d. Model #4.0 and the DNA B_3 pattern 142
- 5. Consideration of the acridine-orange-stained-DNA diffraction pattern in terms of the DNA model #4.0 150

Summary 153

Bibliography 158

Biography 161

TABLE OF PLATES, FIGURES, AND TABLES

Plates

Plate 1 a through i. X-ray patterns obtained from DNA under various conditions of hydration and tension. 46

Plate 2, a, b, d, e, g. X-ray patterns from DNA under various conditions of hydration and tension.

c. X-ray pattern from DNA stained with mercury.

f, h, i. X-ray patterns from DNA stained with acridine orange. 48

Plate 3 a. X-ray pattern of a mixture of DNA in the "A" and "B_2" forms.

b. X-ray pattern of DNA in the "B_2" form. 49

Plate 4 a, b. X-ray patterns of DNA in the "B_3" form. 113

Figures

1. Optical Diffractograph 39

2. Three dimensional model 43

3. Equatorial spacings vs. hydration 55

4. a. Elongation vs. hydration (X-ray specimen)

b. Elongation vs. tension (X-ray specimen)

c. Elongation vs. tension (mechanical study) 57

5. a. "Solubility" of DNA in ethanol

b. "Solubility" of DNA in butanol—ethanol—water system 64

6. Optical density of DNA vs. $MgCl_2$ content 68

7. a. Complexing of acriflavine (N.F.) with DNA

b. Complexing of acridine orange with DNA 73

8. Lattice for DNA in the B_3 form 80

Figures (Continued)

9. Optical diffractograph patterns of the components of DNA in the Watson and Crick positions (Dyad axis projection) 88

  a. Phosphate—atomic c. Deoxyribose (partial) atomic

  b. Phosphate—schematic d. Deoxyribose (partial) schematic

10. Same continued 91

  c. PO_4 + D'rib – atomic a. Base pair—atomic

  d. PO_4 + D'rib – schematic b. Base pair—schematic

11. Same continued 94

  a. PO_4 + D'rib + Bases—atomic c. PO_4 + D'rib + Bases—atomic—basal projection

  b. PO_4 + D'rib + Bases—schematic d. PO_4 + D'rib + Bases—schematic—basal projection

12. Volume assignments for the atoms of the base pair 98

13. Phase maps on the Z vs. ϕ plane 120

14. Partial structure factors for the components of DNA at two equatorial sampling positions 124

15. Optical diffractograph pattern from a large diameter, eleven residue per turn, DNA model 126

16. Van der Waals and "backbone length" exclusions in the ϵ vs. y_B plane with components in the "standard" configurations 130

17. Van der Waals and "backbone length" exclusions in the ϵ vs. y_B plane with a hypothetical deoxyribose 136

18. XY plot of model # 4.0 with elevations and with atom notations indicated 139

19. Optical diffractograms from two projections of model # 4.0 143

20. Optical diffractograms from components of model # 4.0 and two projections of complete model 144

21. Positions of diffractions from X-ray DNA B_3 patterns and optical diffractograph projections of model #4.0, with "parent" lattice points indicated. 148

Tables

1. The effects of additives on the fiber forming properties of DNA 35

2. Data relevant to the x-ray patterns of Plate 1 45

3. Data relevant to the x-ray patterns of Plate 2 47

4. Derivation of lattice constants from the coordinates of the reflections on the DNA B_3 pattern 77

5. Summary of the optical diffractograph study of diffraction from the components of DNA 93

6. Treatment of diffraction from the water in DNA; the volume assignments, corrections, and reduced scattering power of the atoms by groups 99

7. Weighting factors and spot sizes used in making optical diffractograph masks for the atoms of DNA with the "water correction" applied 103

8. Calculation of corrections to be applied to the atomic weighting factors for diffraction to the 11th layer line 104

9. Weighting factors and spot sizes for the atoms of DNA with both water and atomic structure factor corrections applied 105

10. Scattering powers of the components of DNA with and without the various corrections applied 106

11. Coordinates for the atoms in model #4.0 140

12. Bond angles and lengths in the backbone and major Van der Waals conflicts in model #4.0

13. Diffraction from the components of DNA in the model #4.0 positions at two equatorial positions as sampled in the case of DNA stained with acridine orange and in the case of DNA in the B_3 form 150

INTRODUCTION

Deoxyribonucleic acid (DNA) is a remarkable material. This thesis is concerned with its molecular structure (physical). A large variety of types of information has contributed to the development of the present concepts of this structure. Some of this material will be cited here without detailed references since Chargaff and Davidson's book The Nucleic Acids; Chemistry and Biology reviews all of this material adequately.

All nucleate living organisms contain DNA in their nuclei and where chromosomes are observed it is associated with them. Where bands are observed on chromosomes they contain DNA and by combined genetic and histological observations the bands can be associated with genes. In pneumococci, genetic strains can be converted from one to another by growing them in a medium containing purified DNA (protein content less than 0.02 per cent) isolated from the appropriate pneumococci. In the case of bacterial virus (which have genetic characteristics) it can be shown with radio active tracer experiments that only the nucleic acid from the infecting bacteriophage enters the host bacterium. These three bodies of information suggest very strongly that the genetic material is either wholly or in part nucleic acid.

Chemically the nucleic acids are distinctly different from other biological polymers in that they are poly di pentose esters of phosphoric acid containing "side chains" of a very limited number of purines and pyrimidines. By the same token they are closely related to the coenzymes which are low molecular weight materials containing the same components.

Recently as chromatographic techniques have become refined it has become apparent that DNA from various sources contain different amounts of the various bases. (It also has been shown that DNA is heterogeneous.) The early 20th century idea of a tetranucleotide structure for DNA had long since given way to the ideas of polytetranucleotides and statistical tetranucleotides. These now vanished but a new and intriguing quantitative relationship between the bases gradually came to light. In DNA the amount of thymine is always the same as adenine and the amount of cytosine (+ 5 methyl cytosine) is the same as guanine. The relative amounts of the two pairs vary from species to species over a range from 0.4:1 to 1.9:1. And yet it was shown from fractionation and analysis of enzymatic hydrolysates (di and tri nucleotides determined and estimated) that these pairs were not simply dinucleotide building blocks for the larger structure. Todd and co-workers(Brown, Michelson, Todd, 1954) [illegible] have recently completed the chemical identification of the nucleotides from DNA as β-D-deoxyribofuranosides.

Titration and viscosity experiments on high molecular weight preparations have shown another peculiarity of DNA. The initial forward and back titration curves are markedly different if the pH is taken above 11 or below 5. The conclusions drawn from these results are that all of the amino and hydroxyl groups are unaccessible to titration until the DNA is denatured by the acid or base. Viscosity was found to behave in a manner parallel to the titration data.

Since these original results suggesting "denaturation" were obtained a large variety of evidence has accumulated suggesting a number of stages and types of denaturation too involved to discuss here. The types of data include biological activity (Zamenhof, Griboff and Marullo, 1954), sensitivity of viscosity to time and temparature (same authors), light scattering (Reichman, Bunce and Doty, 1953), viscosity itself, ultraviolet absorption (Thomas, 1954, a,b; Laland, Overend and Peacocke, 1954; Overend, Peacocke, Stacey, 1954), infrared absorption (Blout & Lenormant, 1954), effects of salts on the absorption (Shack, Jenkins, and Thompsett, 1953), and dye binding (Thomas, 1954). The denaturing agents include acid, base, heat, enzymes, sonic radiation, dialysis, dilution, drying, and time. Most of these changes involve no change in the molecular weight (Doty, and Rice, 1955; Peacocke and Schachman, 1954; Doty and Schachman, private communications.)

Measurements of sedimentation and diffusion, electrophoretic mobility, viscosity, and light scattering show that the molecule is heavy, distended, asymmetric, and highly charged. The molecular weight of material obtained by the Mirsky-Pollister method is of the order of 1 to 2 million and of that prepared by the Signer and Schwander method is 6 to 8 million. In dilute solution (0.14 M NaCl) the end to end separation is of the order of 5,000 A and the root mean square radius is about 2,000 A (Reichman, Bunce, and Doty, 1953).

Electronmicrographs show the molecule to be linear, unbranched, thousands of Angstroms long, and about 20 A in diameter (Williams, 1952).

Surface films of DNA can be formed on 1 M NaCl and these have a thickness of 20 A to 25 A based on interference methods or on estimation of the amount of DNA in a film stripped from a measured area (James and Mazia, 1953).

The dielectric dispersion in dilute solutions has been interpreted by Jacobson (1953) to indicate that the DNA induces a high degree of order into the surrounding water.

DNA fibers can be formed by withdrawing a rod from a stiff gel and the mechanical and optical properties of these yield information relative to the structure of the molecule. Wilkins, Gosling, and Seeds (1951) observed that when stretched at 50 per cent relative humidity the fibers elongated and that part of this process was accompanied by an unequal reduction of diameter in various parts of the fiber. "Necks" formed and moved along the fibers. A two-fold stretching was obtained and when the tension was released and the hydration increased, a shrinkage by a factor of 1.5:1 occurred. The normal fiber was crystalline and exhibited strong negative birefringence and perpendicular ultraviolet dichroism (BR -0.05, dichroic ratio 4:1 at 2650 A, Wilkins, 1951). The necked portions exhibited much lower negative birefringence (-0.02) and on further stretching became positive (+ 0.02). The stretched material is non-dichroic in the ultraviolet and amorphous when examined by X-ray diffraction. These results were interpreted to indicate that the molecule was reversibly extensible and that in the process the purine and pyrimidine bases tilted about 45° from a position perpendicular to the fiber axis.

Fraser and Fraser (1951) have observed infrared dichroism in stretched and normal oriented films of DNA. In the unstretched material the bands which were tentatively assigned to double bonds in the bases, and to N-H, C_1'-O_1'-C_4', and P-O-C stretching showed perpendicular dichroism. In the stretched material (no relative humidity specified) these all exhibited parallel dichroism. A band tentatively assigned to P = O exhibited no dichroism in either case and this was taken to indicate that the P = O bond was at about 54° to the fiber axis.

The most detailed data relative to the physical structure of DNA comes from the surprisingly high quality X-ray patterns that can be obtained from synthetic fibers of hydrated DNA.

The first X-ray patterns to be obtained from DNA were those of Astbury and Bell (1938 a,b) by the "film pack" method. The patterns obtained turned out later to be a mixture of two patterns from different hydration states (and were not of present-day excellence) but the very strong "3.4 A meridional" spacing was sufficiently striking for Astbury to suggest that the structure resembled a stack of coins with 3.4 A axial spacing. The higher spacings were taken as possibly indicating a tetranucleotide effect.

After 1945 a number of detailed crystallographic analyses of purines and pyrimidines derived from nucleic acids or closely related to these compounds were carried out by Pitt (1948), Clews and Cochran (1947, 1948, 1949), Broomhead (1948, 1951), Cochran (1951), and Parry (1954).

Furberg (1950) analyzed the first nucleoside, cytidine, (Zussman, 1953, reports another nucleoside structure) and derived that the furanose ring was nearly perpendicular to the plane of the base. (Astbury had assumed the whole molecule to be planar.) This led him to consider how such units might be arranged in a polynucleotide. He proposed (Furberg, 1952) two types of arrangement that would be expected to give a strong 3.4 A reflection on the meridian and be compatible with his structure for cytidine. One of these had the bases arranged in a helical fashion, parallel to each other and spaced at 3.4 A along the axis. The pentose and phosphate backbone was on a larger diameter helix and the phosphates were near the plane of the bases. There were eight residues per turn and the phosphorus was at a radius of approximately 5.2 A.

In 1951 Riley and Oster obtained powder patterns of DNA at various hydrations ranging from material dried over P_2O_5 in a vacuum to wet gels containing 3 per cent DNA. They found that there was a crystalline region with spacings ranging from 2.97 A to 19.1 A and that order persisted in the 3 per cent gel as evidenced by a 72 A spacing. (Interpreted to be equatorial) At hydrations slightly lower than the latter a 190 A spacing was observed. They came to the conclusion that there was a two-dimensional swelling in the gel and suggested that at the higher hydrations an open lattice of "seven molecule micelles" with internal hexagonal spacing existed. Their smallest "micelle band" spacing was 20.8 A but the extrapolation of their curves to zero hydration was interpreted to indicate a unit 16 A in diameter.

Early in 1953 Pauling and Corey proposed a three-chain helical structure for DNA with the phosphate ions close packed in the center of the molecule and the bases pointing outward. At this time Wilkins and co-workers and Gosling and Seeds had obtained but not published oriented patterns of a crystalling DNA (in the form of fibers) and also had patterns of a "paracrystalline" form. Pauling's model did not fit the more refined data.

Cochran, Crick had and Vand(1952) recently developed the theory of diffraction from helical systems,

¶The paracrystalline patterns of Wilkins and co-workers exhibited in a striking fashion some of the characteristic features of diffraction from a helix as derived in this work. The fact that the crystalline DNA pattern was so rich in spots indicated that a degree of order existed that was on first appearance inconsistent with the biochemical idea of a random order of purines and pyrimidines along the backbone, i.e. a random order of large and small "side chains."

Watson and Crick (Watson, colloquium at Harvard University, January 1955) were particularly impressed with the latter fact and reasoned that the chemically regular part of the structure was the backbone and that this might provide a regularity for the physical structure. Since the bases were "large" and "small" they would most likely be in pairs in a regular structure. Pairing the bases in a regular way, adenine with thymine and guanine with cytosine, each in its most probable tautomeric form, provided the most extensive system of optimum hydrogen bonds (two for the former pair and two or three for the latter). The bonding could also be done in such a way that the $N-C_1'$ bonds to the pentoses were diad related so that the connection to two backbone chains could be identical and independent of which base was attached to which backbone.

In this manner a regular structure could be built with a random order of the bases. The double structure would contain two complementary molecules and this was appealing in that it suggested a method for self-replication -- a characteristic of genes! The specific pairing of the bases would explain the quantitative pairing found chemically. The extensive hydrogen bonding clarifies the titration data. The length of the molecule based on 3.4 A per base pair and the known molecular weight would be 26,000A and the viscosity behavior is reasonable in the light of this. The hydrogen bonding might well stiffen the molecule and physical chemical changes, as found, with denaturation would be expected. The size of the base pairs makes reasonable a molecule-pair diameter of 15 A to 25 A in accord with the data cited above.

A double helical structure of two units of the type suggested by Furberg was therefore considered by Watson and Crick and they were able to build a model that was stereochemically feasible and that had a number of residues per turn and a pitch consistent with Wilkins' X-ray data. A description of the model was presented by them in April 1953 (Watson and Crick, 1953, a) and later atomic coordinates were published (Crick and Watson, 1954). This is the only detailed model for DNA that has been published, other than that of Pauling and Corey mentioned above.

At the same time that the Watson and Crick model was proposed Wilkins, Stokes and Wilson (1953) and Franklin and Gosling (1953,a) published patterns of "type B" and discussed the interpretation of these in terms of schematic helical structures. They also referred to the "A type" pattern and some of the conclusions that they had drawn from it.

Wilkins, Stokes, and Wilson (1953) inferred from the spread of intensity on the layer lines that the helix had an integral number of residues in one turn (compared with two or three turns) and thus the pitch was 34 A. There were ten residues per turn of each helix and two or three coaxial molecular chains could be present from volume considerations. From the angle of the central X the diameter was approximately

20 A. From the narrowness of the layer-line streaks a large fraction of the mass had to be at approximately 20 A. Although the central X in the pattern corresponded to a 20 A diameter helix the higher layer-line reflections corresponded to a 12 A diameter helix. This was interpreted to mean that the central portion of the structure was more sharply divided into a 3.4 A periodicity than the outer portions. [The validity of this point remains obscure to the author, especially as they used it.] The strong reflection at approximately 17 A on the equator suggested hexagonal packing of cylinders 20 A in diameter and a "sharp spot" on the inner edge of the second layer-line streak indicated that some crystalline order existed.

In this report and earlier (see cited reference for others) Wilkins and co-workers cited X-ray data from sperm heads and bacteriophage, as well as from material having transforming principle activity and preparations from a variety of sources with varying base contents. They came to the conclusion that the basic features of the B pattern were general to all of these (under proper hydration conditions) and therefore it was not an artifact or special case.

Franklin and Gosling (1953a) came to a very similar set of conclusions emphasizing slightly different points. They concluded that the structure was probably helical with exactly ten residues in 34 A and with the phosphates (or phosphorus) at 10 A radius. The equatorial intensities at 24 A (strong), 9.0 A (weak, sharp), and 5.5 A and 4.0 A (weak, diffuse) were interpreted to be evidence that the pentose and bases were turned inward. They point out that a cylinder of radius 10 A and height 34 A would contain 32 nucleotides on the basis of the dry density but that in dry material there might be some interpenetration of helices. On the basis of an 8 A radius there would be 20 nucleotides per unit. Thus two or three chains might be present. They discussed the A to B pattern reversible transition with hydration and having deduced a two-chain structure from the A pattern inferred that the B material is similar.

Since these three papers were published Watson and Crick have published three papers (Watson and Crick, 1953b,c; Crick and Watson, 1954) dealing with the details of their model, their reasons for proposing it and the biological implications.

Franklin and Gosling (1953b,c,d, 1955) have published four papers. One of these is concerned mainly with the presentation of the variety of patterns obtained as the water content is varied. The others deal with the A pattern data and with the interpretation of the two and three dimensional Patterson functions derived from them. With regard to the B pattern they suggest that the phosphorus radius should be 8.5 A instead of the originally suggested 10 A. Their previous argument concerning the number of nucleotide chains in B material is more fully developed and substantiated than in the first account but the conclusions are not changed.

In their works the A pattern lattice and space group are derived and the interpretation of the Patterson function centers mostly on P-P vectors. The number of residues per turn is concluded to be 11. From the three-dimensional data the rotational orientation of the helices is determined and the intermolecular approaches can therefore be examined in more detail than otherwise. They propose that the phosphorus atoms are located directly above one another on two coaxial helices of 9 A radius and spaced exactly one half a unit cell apart in the z direction. The molecular approach is such that two P-P distances occur. Four exygen atoms pack closely together with the two associated sodium atoms lying outside the tetrahedron. Inside of the two helical backbone chains the bases are assumed paired and coplanar and the pattern is interpreted to indicate that such units would be tilted at about 65° to the axis.

The validity of interpreting the Patterson peaks in terms of phosphorus atoms or phosphate groups is somewhat questionable when one considers the concentration of electrons in the five-membered rings present in DNA. However, when the effect of the water is taken into account by applying corrections to the atomic scattering powers (see page 95, 106, this thesis) the effective electron density in the phosphate group is enhanced considerably. (Franklin and Gosling recognized that this would be so.) The concentration of electrons in the sodium ion is particularly significant and the "center of gravity" of the $NaPO_4$ group may be more properly associated with peaks than the phosphorus position. This would be a minor change in the over-all picture but would alter the PO_4-PO_4 approaches significantly.

Wilkins, Seeds, Stokes, and Wilson (1953) have provided the richest DNA A pattern (obtained from mouse sarcoma DNA) and presented the data obtained from the original in graphical form. The unit cell dimensions which they derived differed by a few tenths of an Angstrom from Franklin's values for calf thymus DNA. They conclude that the structure is helical and not pseudo-helical, that much of the structure is at a sharply defined diameter of 18 A, and that this portion lies on two helices spaced nearly equally along the axis. The lack of reflection from the 18 A helices on the 4th layer line was taken to indicate a thickness of the helices in the axial direction of at least 3.5 A. They also proposed that "spaced centrally between the two 18 A diameter helices is one helix of mean diameter about 10 A." This is interpreted to correspond to the bases in which "the nucleotide shape resembles that of a rod inclined to the axis" and in agreement with Franklin and Gosling they place the angle at approximately 65°. From the location of intensity on the 4th and higher layer lines Wilkins and co-workers deduce that there are 11 residues per turn in the A structure.

In discussing the B pattern Franklin and Gosling proposed that the two helices are separated by 3/8th of a repeat period to explain a 4th layer-line absence of intensity. Wilkins and co-workers took a 4th layer-line absence in the A pattern to indicate that the individual helices were at least 1/8th of a period thick. The reflections from two helices spaced at any odd eighths of the repeat period will cancel on the 4th layer line. These two alternative explanations of absences on the 4th layer line, applied by different investigators to different patterns, exemplified the nature of much of the discussion of schematic interpretations of the DNA patterns. It may well be that other considerations led to the selection of the specific explanation invoked where the one datum was ambiguous. Space and the reader's patience would not permit complete coverage of all the factors involved. This emphasizes, however, the need for consideration of detailed molecular models if a satisfactory evaluation of the structure of DNA is to be reached.

There is general agreement (Franklin and Gosling, 1953; Wilkins, Seeds, Stokes and Wilson, 1953; Feughelman, Langridge, Seeds, Stokes, Wilson, Hooper, Wilkins, Hamilton and Barclay, (1955) ~~in press~~; Franklin, private communication; Wilkins, private communication; Watson, private communication) that the Watson and Crick model does not fit the details of the X-ray data. There is also agreement that a model of their type appears promising and that perhaps rather minor changes will substantially improve the situation. Wilkins and co-workers refer to model building and testing being in progress and state that "the model as a whole corresponds closely with the structure deduced from the X-ray data" referring mainly to the A pattern analysis discussed above.

The research reported in this thesis ran parallel to much of the work reported above and in many instances similar results and conclusions have been derived independently. In particular Wilkins and co-workers (Feughelman, et al, 1955) ~~(private communication)~~ have recently obtained B type patterns that have shown the same evidence of a systematically defective lattice as those reported here. (Rich also obtained some indication of this, private communication.) They have also obtained a pattern exhibiting a less defective B lattice and the interpretation of this leads them to a slightly different emphasis in discussing the systematic defects than is employed in this thesis.

Very recently Wilkins and co-workers (Feughelman, et al, 1955) ~~(private communication)~~ have arrived at the conclusion that the pentose ring must be distorted to make a molecular model in agreement with the X-ray B pattern. With the ring made planar such a model was achieved and a paper dealing with this and certain DNA protein and protamine complexes was recently published ~~is in press~~. (Feughelman, Langridge, Seeds, Stokes, Wilson, Hooper, Wilkins, Hamilton, and Barclay, 1965). The conclusion that the pentose must be changed has also been derived in the following but a different change has been made and a correspondingly different model has been derived.

Details of the model derived by Wilkins and co-workers are not available and a critical comparison of the two therefore cannot be made at present. It would appear that in the two works similar problems were considered and similar but slightly different solutions were found. Both show substantial improvement in the correlation of a model with the X-ray data of the DNA B patterns. It is gratifying to the author that such agreement has been obtained in the solution of such a provocative problem and that the results support the Watson and Crick synthesis of the diversified data reviewed above.

EXPERIMENTAL

Preparation of DNA from calf thymus

1. Methods employed.

Two methods were used to prepare the DNA used in this thesis, one by Mirsky and Pollister (1946) and the other by Schwander and Signer (1950).

In the Mirsky and Pollister procedure the nucleo_protein is isolated and partially purified by alternate solution of the nucleoprotein in 1 M NaCl with removal of the residual debris and precipitation of the nucleo_protein by dilution to 0.14 M NaCl with removal of the supernatant. The protein is then removed by shaking or blending the NaCl solution (1 M) with chloroform and octanol (Sevag). The proteins form a gel in the chloroform phase and the DNA remains in the aqueous solution. The DNA is finally precipitated with ethanol and rinsed thoroughly with ethanol—water solutions and finally with ether. The total procedure spans about 24 hours. The yields are very variable in more or less an all or none fashion. The final materials can vary with respect to the state of denaturation and salt impurities. For these reasons a detailed account of the procedure used is given below.

The Schwander—Signer procedure differs from the Mirsky—Pollister method in two main respects. The nucleo_protein is much less rigorously purified in the former and the protein is removed in a different manner. The thymus gland material is repeatedly dispersed in 1 M NaCl and precipitated by dilution as in the Mirsky—Pollister method but only the supernatant from the precipitation is discarded. This serves to remove hemoglobin and RNA but leaves many proteins behind in addition to the nucleo protein. The DNA is then freed from protein by denaturing and precipitating the latter with NaCl solution (saturated) and time and removal of the precipitate by filtration. The DNA is precipitated with alcohol and thoroughly washed as in the Mirsky-Pollister procedure. The complete procedure spans one month. The preparation described in detail below covered a much longer period and the filtration and final precipitation steps were not exactly those specified by Signer and Schwander.

As mentioned in the introduction (pg. 13) the molecular weight of these two types of preparation differ markedly. Frick (1954 a,b) has recently reported on "a critical study of some commonly used methods of preparing DNA" concerned mostly with chemical purity and yields. There is also evidence in the literature pertaining to denaturation (see pg 12) that the Mirsky-Pollister material is partly denatured.

2. Details of two preparations.

The details of one typical preparation of DNA by the Mirsky-Pollister method are as follows: A calf thymus was obtained at a kosher slaughterhouse immediately after slaughter, wrapped in aluminum foil and packed in dry ice. (In this case, the lot was stored in dry ice for two months before the preparation was started.) The remainder of the procedure was carried out at 4°C. Fifty grams of material was cut and chipped into small (1/4") pieces and mixed with 500 ml. of 0.14 M NaCl* in a Waring blender for 1 minute. Three drops of octanol

*All salt solutions contained sodium citrate (.01 M).

were used to break the foam and the lot was spun in an International Centrifuge, size 2, at 1400-1500 rpm for 10 minutes. The supernatant and floating debris were decanted and discarded. The residue was taken up in 500 ml. of 0.14 M NaCl, blended for 30 seconds, spun 10 minutes at 1400-1500 rpm, and the supernatant and debris were again discarded. This was repeated 3 more times. The final residue was suspended in 750 ml. of 0.14 M NaCl. Then 750 ml. of 2 M NaCl was added while stirring. A gelatinous mass resulted and this was stirred 19 hours. A 5oo ml. batch of this solution was mixed with 200 ml. $CHCl_3$ and 50 ml. octanol for 30 seconds in a Waring blender. A white gelatinous mass formed and this replaced the entire chloroform-octanol layer when spun down at 1500-1600 rpm for 10 minutes. Supernatant amounting to 465 ml. was recovered. The procedure was repeated 3 more times yielding 435 ml. of supernatant. Two equal batches were then mixed and 25o ml. of chloroform and octanol were added and blended in for 90 seconds and spun for 15 minutes. The amount of gel forming was small and one more cycle left only a partial layer of gel at the interface between the clear layers. The overall recovery of supernatant from these "Sevag" operations was 790 ml. out of 1 L. The supernatant from this last separation was decanted carefully and poured into 5 volumes of reagent (or 95 per cent pure) ethanol. The fibrous precipitate was collected on a stirring rod as it formed. The "boule" was rinsed repeatedly in 80 per cent, 95 per cent, and absolute ethanol and with ether. This was air dried to yield 0.52 gm. "DNA". Since all of the 50 gm. preparation was not carried through, the calculated yield is 18 mg/gm thymus. This is a high yield and some of the weight might be sodium citrate. It was found later that when 5 volumes of ethanol are added to a 0.01 M sodium citrate solution in 1 M NaCl some of the citrate precipitates. The citrate was omitted from the final DNA solution in the preparations that followed.

The details of the one preparation carried out by the Schwander-Signer method are as follows:

Calf thymus was obtained from animals slaughtered probably within the hour. The tissue was frozen by packing a large mass in dry ice and then stored at -15°C for four days. The mass was then cracked into pieces ranging from pea size to one inch and 45 grams of glandular material was selected. This was ground in a pestle and mortar with dry ice and passed through a 20 mesh sieve. The dry ice was allowed to sublime off at -15°C. To this was added 400 ml. of 1 M NaCl solution* at 0°C and the mixture was stirred vigorously for 12 hours, followed by 3 days of more gentle stirring Of the resulting pink and turbid "solution," 440 ml. was poured into 5 volumes of ice cold water while stirring. A gelatinous mass formed on the stirrer and fibrous material formed in the solution. The supernatant solution was poured off and the combined precipitates were washed four times with 200 ml. batches of 1 per cent NaCl, by

*Unless it is noted to the contrary,
*all salt solutions contained sodium citrate (0.01 M).

violent shaking, 10 minutes settling, and pouring off the supernatant solution. Solids left in the supernatants were collected by centrifugation, washed and combined with the main mass. This procedure spanned an 8 hour period.

The precipitate from above was taken up in 400 ml. of 1 M NaCl solution and stirred at 0°C for 3 days. The mixture was poured in a fine stream into 5 volumes of water while stirring. In this operation most of precipitate collected on the stirring rod and was easily removed from the mother liquor. The precipitate was washed 6 times with 1 per cent NaCl and again dispersed in 400 ml. 1 M NaCl. This operation took only 1 hour. Stirring was continued another 3.5 days and then precipitation was carried out as before. The precipitate was taken up in 500 ml. of 1 M NaCl. Saturated NaCl (100 ml.) was added with stirring and then 170 gm, of solid NaCl were mixed in to saturate the solution. (Sodium citrate was added to maintain the concentration at 0.01 M.) This was stirred slowly for 5 days and stored for 2 months at 4°C before filtration.

Filtration was attempted according to the Schwander-Signer method, except for use of a smaller Buchner funnel with batches scaled down accordingly. The filtration did not proceed as smoothly as they imply. In one batch the initial filtrate was clear and a second step was not employed on this fraction. Material labeled sslc3 was obtained from this single filtrate as follows. Filtration was carried out with vacuum through a bed of John's Mansville Celite 545 filter aid. (4.8 gm. of this had been dispersed in 150 ml. of saturated NaCl by violent stirring for 20 hours and then deposited by filtration on a filter paper in a 9 cm. Buchner funnel.) To 245 ml. of this filtrate 50 ml. of reagent ethanol was added. The precipitate was removed by centrifugation. An additional 50 ml. of reagent ethanol was added. The precipitate was removed by centrifugation. An additional 50 ml. of alcohol was added and again the precipitate was collected. The third addition of 50 ml. of alcohol produced copious precipitation with apparently no NaCl precipitating. The precipitate was collected. The supernatant had an optical density of only 0.4 (1 cm, $\lambda = 2600$ A) and further addition of alcohol precipitated a little DNA and some salt.

The third precipitate was taken up in 25 ml. of 0.12 M NaCl and stored at 4°C overnight. Purified isopropanol (12.5 ml.) was added and some local precipitation took place which later reversed. There remained 4.0 ml. of an apparent gel phase and 33 ml. of solution. Twenty-two ml. of the mixture was diluted with one volume of 0.5 M NaCl and the gel persisted. Addition of 21 ml. of isopropanol produced essentially complete precipitation of the DNA. This was teased apart in 80 per cent reagent ethanol, rinsed, and stored overnight in 80 per cent ethanol. The alcohol was replaced again and the lot stored 13 days at 4°C. The DNA was then rinsed with 95 per cent pure ethanol, soaked in 95 per cent ethanol 1 hour, soaked in absolute alcohol 1 hour, and transferred to ether for one hour. It was then dried overnight at room temperature in air of 30 per cent relative humidity.

The yield of this fraction was 0.116 gm. (wet wt.). Only part of the original material was precessed in this batch. It is estimated that the effective amount of starting material was 15.8 gm. for this and another smaller collection. Accordingly effective yield was 15.5 mg. DNA per gram of thymus.

The material labeled ss1b was obtained from another batch of filtrate, precipitated with ethanol, and washed exhaustively with alcohol according to a schedule similar to the above. The yield was roughly 13 mg. (wet wt.)/gm.

X-ray techniques

1. Specimen preparation and mounting.

The x-ray patterns of obtained from pure DNA by Franklin and Gosling, (1953 a, b, c) and Wilkins, and his co-workers (Wilkins, Stokes, and Wilson, 1953, Wilkins, Seeds, Stokes, and Wilson 1953) show that remarkedly well oriented crystallates exist in fibers formed from a stiff gel. In their technique the specimens were single fibers 30 microns in diameter or several such fibers, and micro focus x-ray tubes and micro cameras were employed. In the present study the specimen consisted of a bundle of tens of thousands of fibers one or two microns in diameter and standard "macro" x-ray equipment was adequate.

Such specimens are readily prepared as follows: A bit of air-dried DNA (10 - 30 mg) is placed in a glass cup 6 mm in diameter and 6 mm deep. A drop or two (50 - 100 mg) of distilled water is added and the material is stirred thoroughly with a glass rod. The initial gel is too wet to form fibers, but as stirring is continued portions on the lip soon dry enough so that stable 8 inch fibers can be formed with ease. A specimen is then started by drawing a fiber and quickly laying it down tangentially on a rotating four prong spindle.* It sticks and as it is wound around the spindle

* The perimeter is 35 mm and the spindle is rotated at approximately 4 revolutions per second.

new fibrous material is drawn from the gel both in the cup and on the stirring rod. The fibers are carefully watched (by dark field effect obtained with a 60 watt bulb 10 inches from the specimen and a black back drop) as they are formed and an attempt is made to prevent globs of gel from reaching the spindle. With good material fibers will spin out for 2 to 7 seconds (25 to 100 cm.) before breaking, at which time a new pair of fibers are quickly started. After half an hour the gel remaining in the cup will be too dry to spin well and more water must be added. In one hour a circular bundle of parallel fibers weighing about one milligram is obtained. The bundle is removed from the spindle by sliding the fibers along each prong a fraction of a millimeter at a time by pushing with a strong glass needle rounded at the end.

Since the fibers form a closed loop they can be pulled into a two ply bundle with two loops of thread and the plier can be readily held taught and parallel.

The DNA fibers are remarkedly strong. A four ply bundle weighing 3.0 mg per cm (ca 1 mm dia) will support well over a kilogram. On a weight basis the DNA hydrate is thus as strong as annealed iron wire or one tenth as strong as the strongest steel.

As x-ray patterns are being obtained, then, the DNA fibers can be kept under appreciable tension by hanging suitable weights on the attached thread. The tension improves the orientation of molecules within the fiber and can be also used to stretch the fibers considerably. The x-ray patterns obtained from highly stretched DNA under the proper hydration conditions shows that the molecules themselves are elongated. This stretched DNA pattern is a new set of data pertinent to the structure and properties of DNA obtained with this technique.

2. Subtleties of fiber formation.

Some of the subtleties of spinnability are indicated by the following data. DNA prepared from calf thymus by the Signer-Schwander method spins very well. If the Mirsky-Pollister method is used and care is taken that sodium citrate does not co-precipitate with the DNA when the alcohol is added, a material which will not form fibers is obtained. Adding NaCl, $CaCl_2$, $HgCl_2$, sodium citrate, or acriflavine (N.F.) will make the material readily spinnable. The various additives have vastly different efficacy as shown in Table 1. The values in the table indicate the number of equivalents of cation that must be added to calf thymus DNA prepared by the Mirsky-Pollister method in order to obtain fibers of the

stipulated lengths. The additives in solution were added to the stiff DNA gel and the length recorded is the maximum that was obtained as the wet gel was stirred to dryness with repeated testing.

Arbitrarily large amounts of the NaCl can be added with little effect after the initial slow improvement is complete. On the other hand, $HgCl_2$ in increasing amounts decreased and finally destroyed the ability to form fibers after slightly improving the spinnability of a preparation that initially gave 4 to 8 inch fibers. Acriflavine or acridine orange will precipitate the DNA from a wet gel if added in too concentrated a solution and this material can not be spun at all. When added in very small amounts they greatly enhance spinnability. When a dilute solution of acridine

Table 1

Fiber	Equivalents of cation added per phosphate					
length	NaCl	NaCit	NaOH	$CaCl_2$	$HgCl_2$*	AO†
0 – 1/4"	0	0	0– .27	0	.54	.2
1"	.02					
2"	.04 – .09	.02				
4"	.13	.04				0
8"	.19 – .24			.05	0.28	
>8"	.30 – .35	.09		.10	.05	.02

*added to a preparation that initially formed 8" fibers.

†acridine orange, added to preparation that formed 4" fibers.

orange was added to a dilute solution of DNA such that the final weight ratio was 1:6 (AO:DNA) some precipitate formed where local concentration ratios were adverse but most of the material remained in solution (as a complex). The precipitate was removed and the supernatant was lyophilized. A non-spinnable material was obtained. (Whether the acridine orange or lyophilization was responsible is unknown.) When NaOH was added to a non-spinnable DNA preparation no improvement was obtained no matter what the amount of additive.

Amounts of additive sufficient to give good spinnability did not result in noticeable x-ray diffraction from free additive. However, badly arced but definitely oriented sharp diffractions were observed arising from sodium citrate co-precipitated with the DNA when, in the Mirsky-Pollister's preparation, the DNA was precipitated with alcohol (80 per cent final concentration) from a 1M NaCl, solution containing 0.01M sodium citrate.

3. Immersion of the specimen in alcoholic solutions.

The x-ray pattern obtained from DNA varies markedly with the hydration of the specimens and thus depends under equilibrium conditions on the milieu in which the specimen finds itself. Riley and Oster (1951) studied gels in sealed capilaries containing a fixed amount of water. Wilkins and co-workers and Franklin and Gosling have immersed the specimen in moist air, helium, or hydrogen of controlled relative humidity. In this study the specimen was usually immersed in ethanol-water mixtures, which were constantly dripping over the fibers (15 to 60 drops/minute). In some cases an inorganic salt or organic solute was added to the immersion fluid to "stain" the DNA or exchange the cation. The x-ray scattering power of the "aqueous phase" or water of hydration would also be altered by additions to the immersion fluid.

The effects of varying the alcohol concentrations will be discussed later. It suffices here to say that, judging the x-ray patterns obtained, and the data of Wilkins and co-workers and Franklin and Gosling, 85 per cent ethanol is roughly equivalent to 75 per cent relative humidity and 70 per cent ethanol is equivalent to 92 per cent relative humidity.

The results of "staining" experiments are reported later. Additives do enter the specimen as evidenced by the change in x-ray pattern and in solubility of the DNA. The ability to introduce additives when the specimen is in a known state of organization, hydration, and strain is useful. Furthermore, well ordered specimens can not always be prepared in the presence of additives.

The Optical Diffractograph*

The DNA molecule and proteins contain so many atoms that optical diffraction studies should be very useful in interpreting X-ray data. The method is based on the fact that the diffraction of light in passing through a mask is analogous to the diffraction of X-rays from matter. The wavelengths are so different and the structures are so different in size in the two cases that the angle of diffraction is also vastly different in practical apparatus, being extremely small in the optical case. The involved models present peculiar problems that required the development of special technique and a suitable optical diffractograph was developed.

1. Design of the Optical Diffractograph

The design of the final apparatus is diagramed in Figure 1.

The light gun is straight forward. F_1, F_2, and L_0 are spaced to eliminate broad interference fringes. F_3 can be omitted in which case some red light reaches the eye of an observer but is not recorded on the orthochromatic film. The intention was to define the wavelength more closely but this does not seem necessary. The guard aperture minimizes stray light in the system and yet allows equivalent illumination of all parts of the lens L_1 taking diffraction into account.

The pinhole is of brass and no dielectric or guard apertures are between it and the lens L_1.

Lenses L_1 and L_2 must be of high quality and of homogeneous glass but no aspherizing is necessary. Third order theory calculation as well as ray tracing show that the longitudinal spherical aberration

*See Lipson and Cochran(1953)pages 75, 236, and 245 for discussion of optical diffraction methods and applications, and for references.

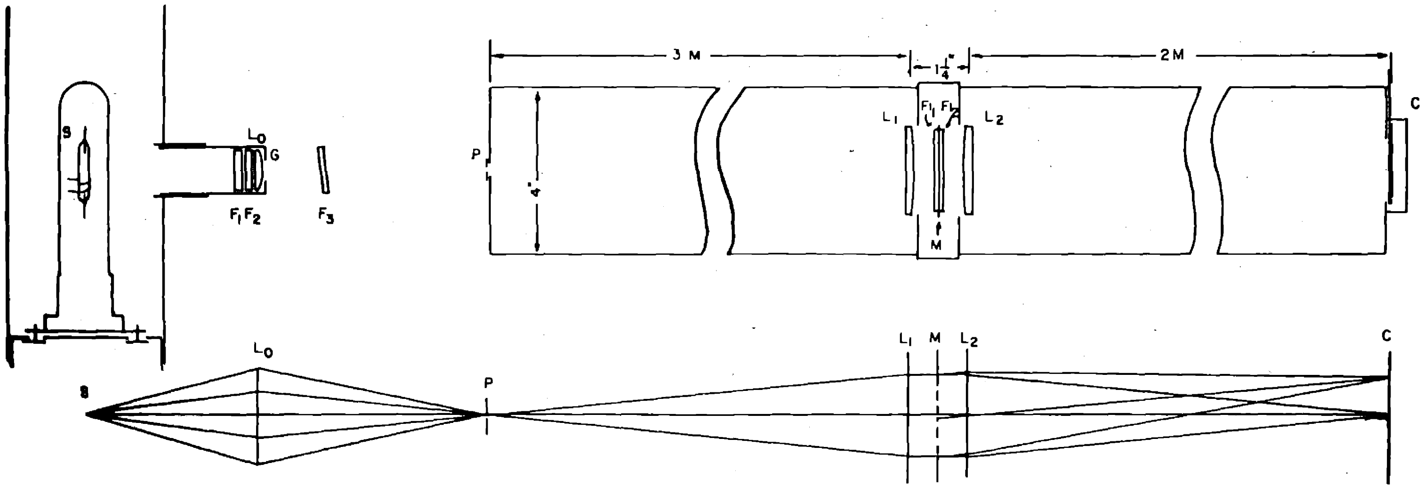
S
L_0
G
F_1F_2
F_3
3 M
$1\frac{1}{4}$"
2 M
P
4"
L_1
F_{l_1} F_{l_2}
L_2
M
C
S
L_0
P
L_1 M L_2
C

FIGURE 1

S - source GE AH3 Hg arc
F_1, F_2 - glass filters (Corning C.S. #3-69 and C.S. #1-60)
L_o - glass lens, 63 mm. f.l.
G - guard aperture
F_3 - multilayer interference filter (Baird Hg Green)
P - entrance pinhole, 0.1-0.3 mm. dia.
L_1, L_2 - crown glass lenses; 3 M & 2 M f.l. respectively, ca 6 mm. thick
Fl_1, Fl_2 - 1/8" plate glass flats
M - photographic mask immersed in oil, n - 1.51
C - cassette

constant of the total system is of the order of 0.5 mm. The distance between L_1 and L_2 is not critical, i.e. 6" is completely acceptable as well as 1".

The mask is made by photographic reduction and usually consists of a set of transparent holes on a black background. The film is immersed in oil between two glass flats in order to minimize the effects of variations in the optical thickness of the film, (Bragg and Stokes, 1945). This is necessary if a usable image is to be obtained and seems to be sufficient, (see Hooper, Seeds, and Stokes, 1955, for an alternative.)

The flats which are highly selected 1/8" plate glass are flat to better than a quarter wave length and are sufficiently homogeneous so that good images are obtained. Care must be taken not to distort these thin flats with the spring load that is used to hold them together (Distortion changes the thickness of the oil).

The diffraction image is recorded on Kodak super ortho press film with exposure times of $\frac{1}{2}$ to 120 minutes or it can be observed directly with the aid of a simple 2X eye piece.

The apparatus is mounted at three stations on a cinder block wall. Since the optical path is not folded with a relay mirror the system has a minimum sensitivity to vibration and no trouble has been encountered in this respect.

2. Technique

The original model from which the masks are made usually consists of a plot of a projection of a single unit cell of an atomic (or schematic) three dimensional model. Each atom is represented by a black spot on a vellum paper and the first photographic reduction (7X) is made with transmitted light. The various atoms are assigned weights (after correction for water, etc.) ranging from one to sixteen in integral steps (Punches of area 1, 2, 3, 4, 5, 6, 8, 10, 12, and 16 are used to cut the spots out of gummed paper). The scale of the original plot is 1 cm. to 1 A and the smallest spot is 3 mm. in diameter. Overlapping spots are usually combined into one at the "center of gravity" of the originals.

The final mask usually contains a row of six unit cells. These are incorporated in an intermediate size model by contact printing a number of units and assembling them or by projection printing the unit repeatedly as the print paper is moved. The final reduction (10X) is made using a very high contrast film (Kodak Kodalith Ortho, Type 2, thin base) so that a very dense background can be obtained with relatively clear holes. The focusing and exposure time are rather critical at this point if faithful reproduction of the spot sizes are to be obtained.

This mask is then placed in the optical diffractograph and the diffraction image is recorded as described above. The patterns presented in this thesis (with the exception of the half page enlargements) are 10X enlargements of the originals made in two steps.

Three Dimensional Model

A three dimensional schematic model kit on a scale of 1 inch to 1 A, was made to facilitate model building.

The bases are represented by flat plates with small holes indicating the center of each atom. Larger holes are present where ever an external chemical or hydrogen bond may exist.

The atoms in the backbone chain are represented by adjustable joints (aluminum) consisting of two units locked in position with the aid of a sand paper "lock" washer and a thumb screw. Each half of the joint receives a rod (hardened drill rod) in which a groove has been machined near each end. The distance between the grooves determines the bond length and the joints can be allowed to rotate freely on the rod or locked into any rotational position. The half joints can be connected directly to the plates representing the bases and the rods can be received by connectors on the deoxyribose unit.

The deoxyribose unit is complicated by the fact that the external bonds to the furanose ring are not coplanar. The plate representing the deoxyribose was made to pass through the atoms that receive external bond (other than hydrogen) and special connectors were machined to join this plate at the proper angles. The positions of the other atoms are indicated by the ends of screws protruding from the plate.

Polystyrene—foam balls can be mounted on the model when desired to obtain a better concept of the space filling properties and Van der Waals approaches.

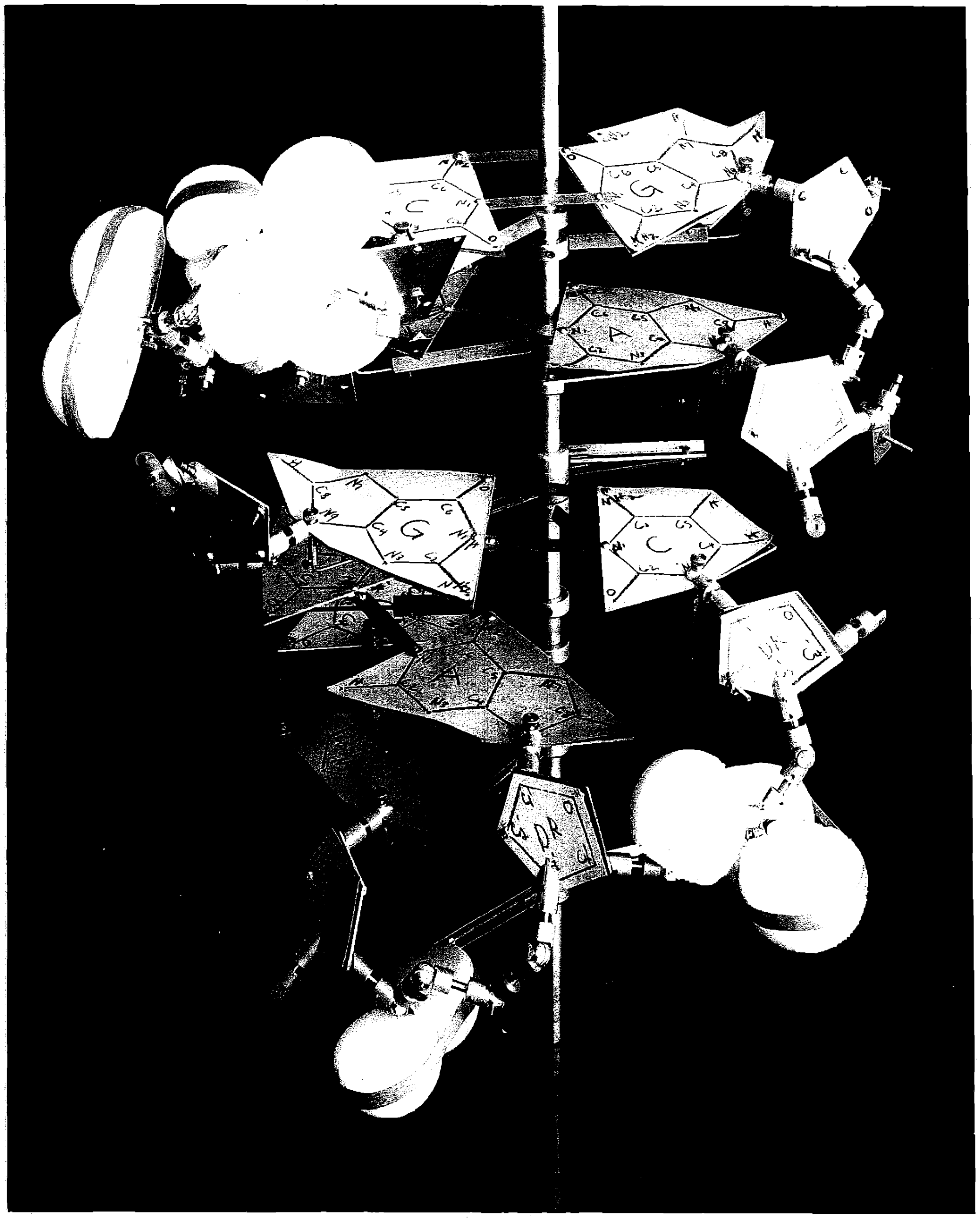
C
G
A
G
C
A
DR
DR

Figure 2

RESULTS

X-ray diffraction patterns

The X-ray diffraction patterns obtained from DNA under various conditions of immersion and tension are surveyed in plates 1 and 2 (pg. 46 and 48 see also plates 3 and 4 pg. 49 and 113 for enlargements of 1d, 2a, and 1b). The significance of the history as well as the momentary conditions is illustrated and effects of "staining" with mercuric ion and acridine orange are shown. Detailed data concerning each pattern are tabulated on the preceding pages in corresponding positions (pg. 45 and 47). The sharp rings at 4.06 A in the patterns of plate 1 are from contaminating Celite filter aid.

The specimens as prepared at 20 to 40 per cent relative humidity show mainly amorphous rings as noted by Franklin and Gosling (1953 [illegible]). With the specimen immersed in 95 per cent ethanol equatorial spots are discernable in the haze, with spacings as indicated later.

If the tension is kept low and the ethanol concentration is changed to 85 per cent the pattern 1a (plate 1) is obtained. No difference has been noted between this pattern and the typical "A" pattern obtained by ~~Wilkins and~~ Franklin and Gosling (1953c) and Wilkins, Seeds, Stokes, and Wilson (1953) at 75 per cent relative humidity.

Decreasing the alcohol concentration to 70 per cent, brings about a complete A to B transition (see pattern 1b, plate 1 pg. 46 and plate 4) equivalent to changing the relative humidity to 92 per cent. The B pattern obtained is different than any previously published pattern

TABLE 2

Film#23/54 Exp. 4.1 hr Spec.#SS/b-1 Exp.# 3 Formed wt. 2.96 mg/cm Immersion 85 o/o ethanol Tension/(formed/wt/cm) gm/(mg/cm) 61 Elong. 0 Dia. mm. Spec. filmdist. 5.0 cm. Tilt ca 5° Layer-line spacing A Eq. Spacings A A Pattern Type A	Film#57/54 Exp. 5.4 hr. Spec.#SS/b-3 Exp.# 6 Formed wt. 2.63 mg/cm Immersion 70 o/o ethanol Tension/(formed/wt/cm) gm/(mg/cm) 86 Elong. 37 o/o Dia. 0.76mm. Spec. filmdist. 5.0 cm. Tilt 4.4° Layerline spacing A Eq. Spacings A 21.7 A Pattern Type B_3	Film#61/54 Exp. 7.3 hr. Spec.#SS/b-3 Exp.# 8 Formed wt. 2.63 mg/cm Immersion 65 o/o ethanol Tension/(formed/wt/cm) gm/(mg/cm) 129 Elong. 78 o/o Dia. 1.21 mm. Spec. filmdist. 5.0 cm. Tilt 4.4° Layer-line spacing A Eq. Spacings 12.9A 22.2 A Pattern Type B_3
Film#24/54 Exp. 4.0 hr. Spec.#SS/b-1 Exp.#4 Formed wt. 2.96 mg/cm Immersion 85 o/o ethanol Tension/(formed wt/cm) gm/(mg/cm) 115 Elong. 55 o/ o Dia. mm. Spec. filmdist. 5.0 cm. Tilt ca 5° Layer-line spacing A Eq. spacings A A Pattern Type B_2	Film#26/54 Exp. 4.8 hr. Spec.#SS/b-1 Exp.#6 Formed wt. 2.96 mg/cm Immersion 85 o/o ethanol Tension/(formed wt/cm) gm/(mg/cm) 7 Elong. Dia. mm. Spec. filmdist. 5.0 cm. Tilt ca 5° Layer-line spacing A Eq. spacings A A Pattern Type A	Film#28/54 Exp. 4.0 hr. Spec.#SS/b-1 Exp.#8 Formed wt. 2.96 mg/cm Immersion 85 o/ o ethanol Tension/formed wt/cm) gm/(mg/cm) 115 Elong. Dia. mm. Spec. filmdist. 5.0 cm. Tilt ca 5° Layer-line spacing A Eq. spacings A A Pattern Type B_2
Film#75/54 Exp. 4.1 hr. Spec.#SS/b-4 Exp.#3 Formed wt. 4.46 mg/cm Immersion 85 o/ o ethanol Tension/(formed wt/cm) gm/(mg/cm) 122 Elong. 76 o/o Dia. 0.80mm. Spec. filmdist. 5.0 cm. Tilt 4.4° Layer-line spacing A Eq. spacings 12.8 A 19.2 A Pattern Type B	Film#76/54 Exp. 5.9 hr. Spec.#SS/b-4 Ext.#4 Formed wt. 4.46 mg/cm Immersion 80 o/o ethanol Tension/(formed wt/cm) gm/(mg/cm) 122 Elong. 85 o/o Dia. 0.80mm. Spec. film dist. 5.0 cm. Tilt 4.4° Layer-line spacing A Eq. spacings 12.8 A 19.8 A Pattern Type B	Film#77/54 Exp. 6.9 hr. Spec.# SS/b-4 Exp.#5 Formed wt. 4.46 mg/cm Immersion 75 o/o ethanol Tension/(formed wt/cm) mg/(mg/cm) 122 Elong. 90 o/o Dia. 0.83 mm. Spec. film dist. 5.0 cm. Tilt 4.4° Layer-line spacing A Eq. spacings 12.8 A 20.3 A Pattern Type B

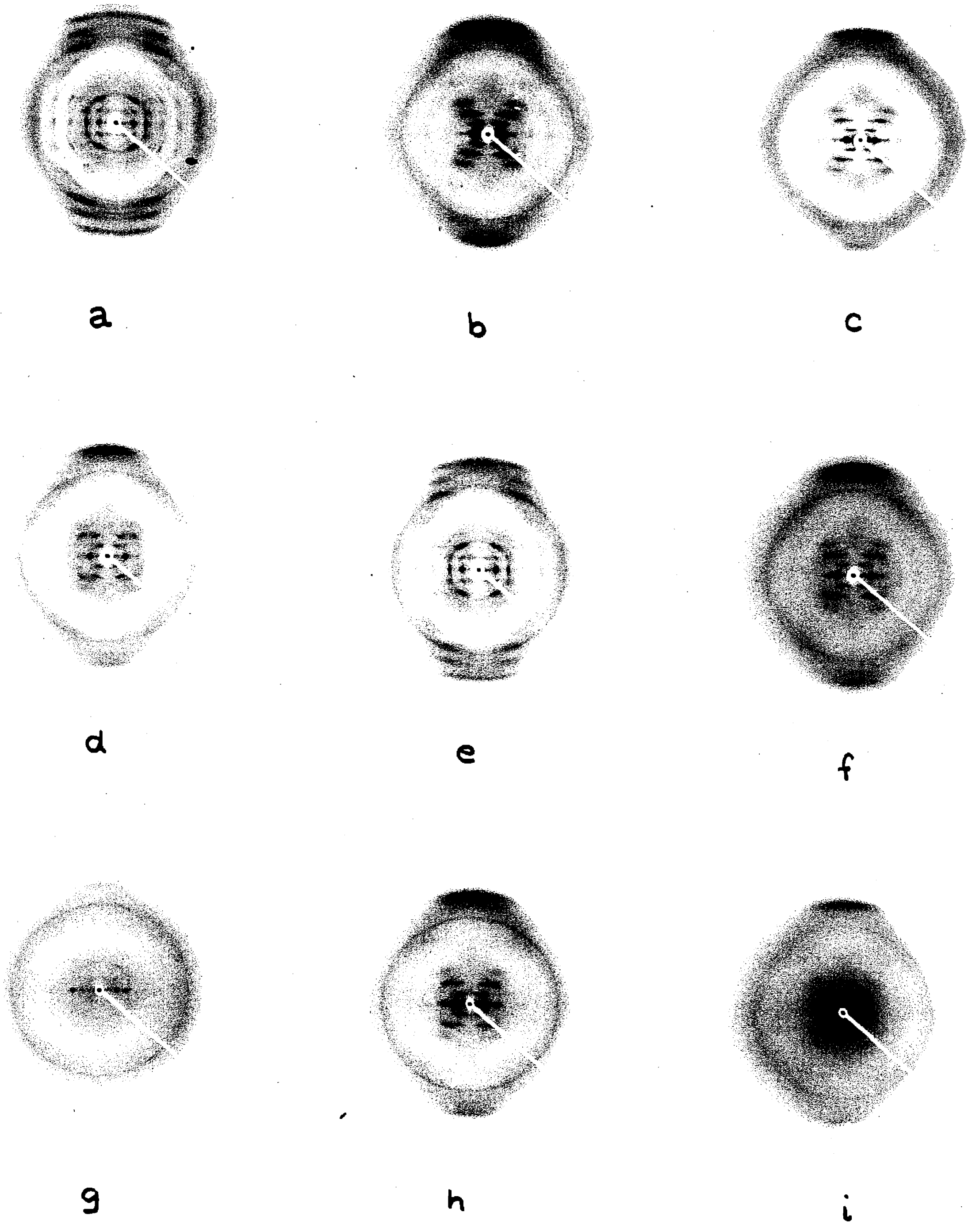

PLATE 1

TABLE 3

Film#99/54 Exp. 8.8 hr. Spec.#SS/c3–2 Exp.#1 Formed wt. 1.26 mg/cm Immersion 85 o/o ethanol Tension/(formed wt/cm) gm/(mg/cm) 80 Elong. Dia. 0.68 mm. Spec. film dist. 5.0 cm. Tilt 4.4° Layer-line spacing A Eq. spacings A A Pattern Type A and B_2	Film#131a/54 Exp. 72 hr. Spec.#SS/c3–6 Exp.#2b Formed wt. 0.92 mg/cm Immersion 85 o/o ethanol Tension/(formed wt/cm) gm/(mg/cm) 131 Elong. 35 o/o Dia. mm. Spec. filmdist. 7.50 cm. Tilt 4.4° Layer-line spacing A Eq. spacings A A Pattern Type A and B_2	Film#95/54 Exp. 17.5 hr. Spec.#SS/c3–1 Exp.#11b Formed wt. 4.34 mg/cm Immersion 60 o/o ethanol Tension/(formed wt/cm) gm/(mg/cm) 101 Elong. 87 o/o Dia. 0.99 mm. Spec. filmdist. 4.9 cm. Tilt 4.4° Layer-line spacing A Eq. spacings A 24.6 A Pattern Type Hg stained
Film#159a/54 Exp. 46 hr. Spec.#SS/c3–7 Exp.#1b Formed wt. 0.86 mg/cm Immersion 70o/o ethanol Tension/(formed wt/cm) gm/(mg/cm) 58 Elong. Dia. mm. Spec. filmdist. 7.50 cm. Tilt 1.04° Layer-line spacing 34.1 A Eq. spacings – A 21.9 A Pattern Type B_3	Film#161/54 Exp. 48 hr. Spec.#SS/c3–7 Exp.#2 Formed wt. 0.86 mg/cm Immersion 70 o/o ethanol Tension/(formed wt/cm) gm/(mg/cm) 58 Elong. Dia. mm. Spec. filmdist. 7.50 cm. Tilt 13° Layer-line spacing A Eq. spacings A A Pattern Type B_3	Film#18a/54 Exp. 7.2 hr. Spec.#MW1C–1 Exp.# 1 Formed wt. — mg/cm Immersion 20 o/o ethanol, AO Tension/(formed wt/cm) gm/(mg/cm) Elong. — Dia. / mm. Spec. filmdist. 5.0 cm. ~~Tilt~~ powder ~~Layer-line~~ spacing 3.4 A ~~Eq~~. spacings – A 31 A Pattern Type AO stained
Film#114/54 Exp. 2.1 hr. Spec.#SS/c3–5 Exp.#1 Formed wt. 0.8 mg/cm Immersion 70 o/o ethanol Tension/(formed wt/cm) gm/(mg/cm) 68 Elong. 21 o/o Dia. 0.58 mm. Spec. filmdist. 5.0 cm. Tilt 4.4° Layer-line spacings 34.0 A Eq. spacings – A 21.7 A Pattern Type B_3	Film#116/54 Exp. 11 hr. Spec.#SS/c3–5 Exp.#2b Formed wt. 0.8 mg/cm Immersion 70 o/o Et. 0.1 o/o AO Tension/(formed wt/cm) gm/(mg/cm) 68 Elong. 25 o/o Dia. 0.39 mm. Spec. filmdist. 5.0 cm. Tilt 4.4° Layer-line spacing 34.0 A Eq. spacings 10.4 A 18.2 A Pattern Type AO stained	Film#118/54 Exp. 8.0 hr. Spec.#SS/c3–5 Exp.#3b Formed wt. 0.8 mg/cm Immersion 50 o/o ethanol Tension/(formed wt/cm) gm(mg/cm) 68 Elong. 28 o/o Dia. 0.42 mm. Spec. filmdist. 5.0 cm. Tilt 4.4° Layer-line spacing 34.0 A Eq. spacings – A 20.4 A Pattern Type AO stained

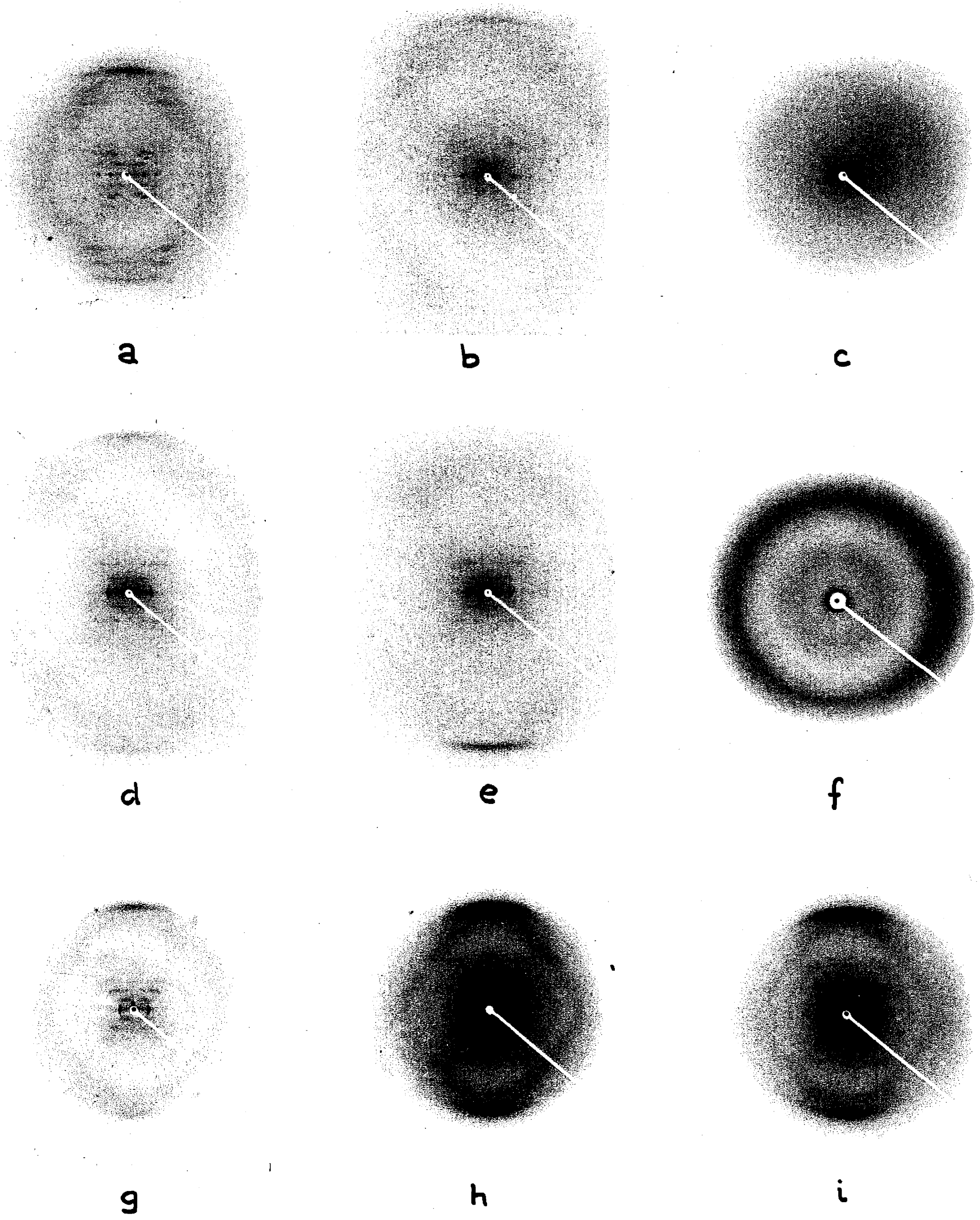

a b c

d e f

g h i

PLATE 2

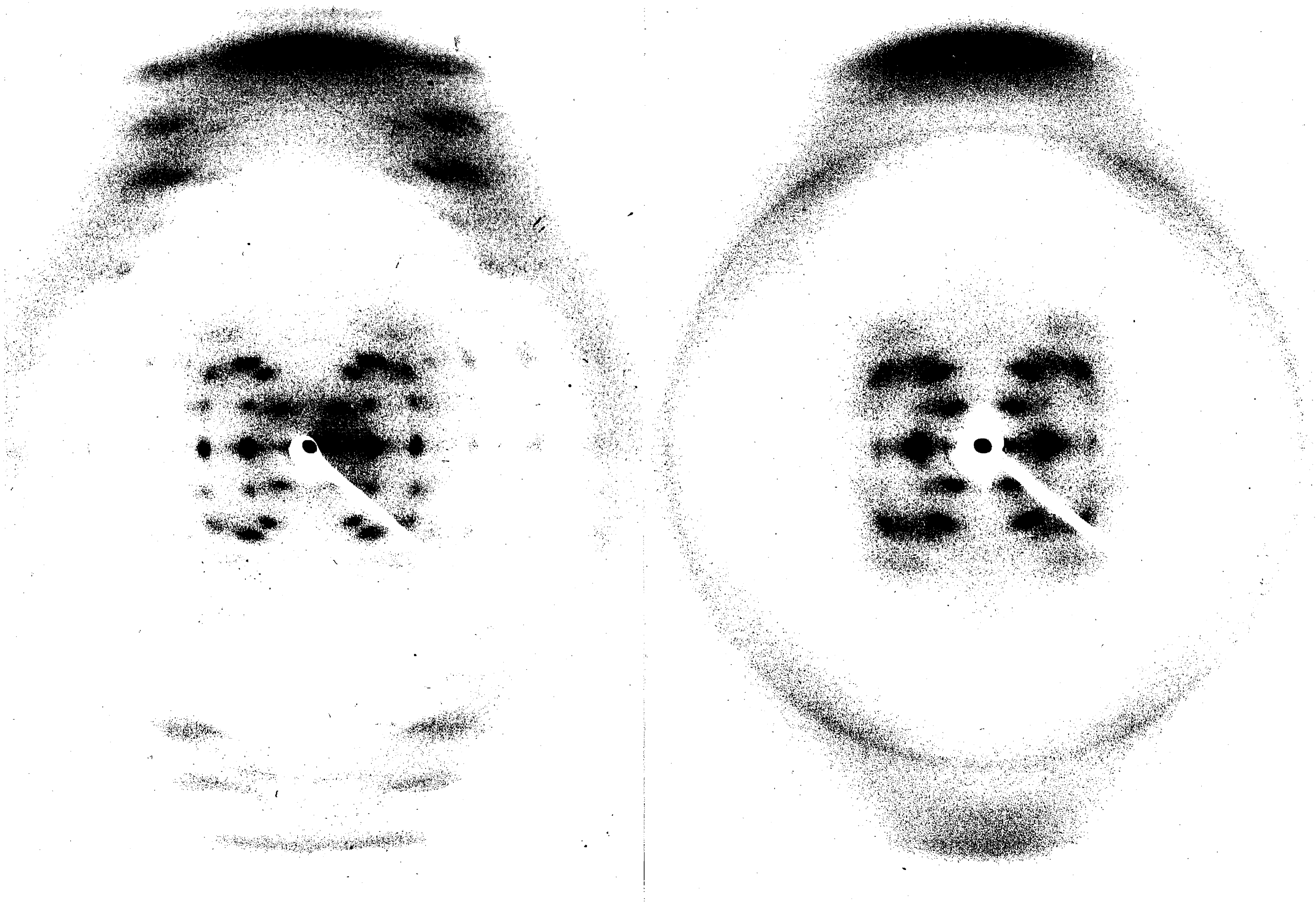

a (2a)

b (1d)

PLATE 3

in that three well-resolved spots appear on the 2nd layer line. The very strong equatorial spot is well resolved and single, (see patterns 2d, e and g pg. 48). There is no evidence of the 1st or 3rd layer lines being sampled by a lattice. An analytical description of the intensity distribution of this pattern is given on pg. 112 through 115. On decreasing the alcohol concentration still further to 65 per cent, along with increased tension, pattern 1c was obtained with evidence of lateral swelling and the appearance of a second sharp but weak equatorial spot at 1.72 times the radius of the first. The 2nd layer line spots are slightly more diffuse than at 70 per cent ethanol. The specimen gradually weakened and broke at this hydration level. Wilkins and co-workers have recently obtained a pattern very similar to the 70 per cent ethanol pattern which they refer to as "paracrystalline B." The designation used hereafter in this thesis will be B_3.

When the tension applied to a specimen in 85 per cent ethanol is increased the specimen stretches and the pattern changes from pattern 1a to 1d (pg. 46 and pg. 113). The layer line spacing is increased from 28.1 A to 32.5 A. In the 3A region the transition is typical of that from A to B. The second layer line is sampled by a lattice with only two spots clearly visible. On the 1st layer line a spot appears at what would be the inner edge of the B_3 pattern streak. The intensity on the equator shifts from the 2nd spot to the 1st spot and that remaining at the larger radius may be from some material remaining in the A state. This pattern is designated B_2, since it is more like the ordinary B pattern than the A, but it is clearly distinct from the published patterns and from B_3 above. When the tension was reduced so that the conditions were the same as those that formerly yielded a nearly pure A pattern a mixed pattern was obtained. Further reduction of tension allowed nearly complete reverse to the A pattern 1e (pg. 46). Increasing the tension again restored the B_2 pattern presented as 1f. The transition from A to B_2 is thus readily reversible but does exhibit pronounced hysteresis.

Pattern 2a (pp. 48 and 49) shows a mixture of the A and B_2 patterns obtained at intermediate tension with the specimen in 85 per cent ethanol. The change in layer line spacing and spot positions is clearly demonstrated. The presence of both patterns at once, clearly resolved from each other, indicates that the transition is discrete in nature, just as the ordinary A to B transition appears to be. Pattern 2b (pg. 48) is a high resolution pattern of a mixture of A and B_2, illustrating the same points.

Whether the transition from B_2 to B_3 is continuous or discrete is not clear because the two dovetail in such a way that a mixture could not readily be resolved. Patterns 1g, 1h, and 1i (pg. 46) were obtained at high tension at three alcohol concentrations. At low tension A or mixed A and B_3 patterns would have been obtained under these conditons. Further hydration weakened the specimen to the breaking point.

Patterns 2d and 2e are diffractograms of the normal B_3 pattern taken with a high resolution camera with the specimen tilted 1° and 13° respectively. These indicate the sharpness of the layer lines and the equatorial spot although the spots on the second layer line does not show well in the reproduction. Clearly the lattice is extensive (at least 10 unit cells) with no indication of small crystal broadening on the equator, and measurements can be precise. The 13° tilt brings the center of the tenth layer plane into the sphere of reflection so that conditions are proper for detecting splitting of the 10th layer line streak. None is observed. (The second layer line spots were not so clearly resolved on this pattern as in the preceding picture, indicating possible age or motion effects.)

Patterns 2f, 2 g, 2h, and 2i show the effects of acridine orange staining of the specimen. Pattern 2g was obtained with the specimen under mild tension, immersed in 70 per cent ethanol. Acridine orange disolved in 70 per cent ethanol (0.1 per cent) was then allowed to flow over the specimen and after hours of equilibration the pattern 2h was obtained. The layer-line spacing is normal but the lattice points have shifted outward, indicating a smaller unit cell. The inner spot on the 2nd layer line is intermediate between the B_2 and B_3 patterns. The lattice is, however, sensibly isomorphous with B_3. The intensity distribution is noticeably altered on the equator and 2nd layer line. (This is partly but not entirely due to the change in sampling positions according to the analysis on pg. 150.)

Pattern 2i was obtained from the same specimen as 2g and 2h after prolonged washing with 50 per cent ethanol. The specimen did not dissolve as unstained material will at 60 per cent ethanol. The acridine orange was not washed out. The specimen did swell slightly. Another specimen, stained with an 85 per cent alcohol solution of acridine orange, did not dissolve in pure water but did swell enormously from less than 1 mm. in diameter to 5 mm. in diameter. It still supported its attached weight and was shaped like a squat foot ball. On increasing the tension slightly it would elongate and lifting the weight slightly would cause it to round up. No X-ray pattern was obtained from this due to its size and dilution ($<$ 2 per cent DNA). Pattern 2f shows a powder pattern obtained from DNA precipitated out of 20 per cent ethanol solution by the addition of acridine orange solution. It was immersed in the mother liquid in a glass capillary. The spacing of the central ring is 31 A.

Staining with mercuric chloride or silver nitrate caused general weakening and severe deterioration of the X-ray pattern. Pattern 2c was obtained from a specimen stained with 0.015 M mercuric chloride in 85 per cent ethanol while the specimen was stretched so that it was largely in the B_2 form. The specimen was then washed thoroughly with 60 per cent ethanol (the tension was maintained) and the exposure was taken under these conditions. An equatorial spot with abnormally high spacing (25 A) remains and haze more dense than the background extends from this spot to the region of the 1st layer line.

Three series of X-ray patterns were taken at constant tension and variable alcohol concentration. One specimen served for each series. The variations in the Bragg spacing for the innermost equatorial spots is shown in Figure 3 , along with the spacings obtained from other specimens with additives as indicated. The following discussion is concerned with these data. In each series the specimen was hung under tension and 95 per cent alcohol was applied as described above. After equilibrating for an hour or more the pattern was obtained with an exposure time of the order of 5 hours. The ethanol concentration was changed and after equilibration for an hour another exposure was started, etc. Each series took several days and some degradation might have occured during this time.

The 11.3 to 11.8 A equatorial spot is characteristic of the A pattern and is strongest at 85–80 per cent ethanol where the best A patterns are obtained. At 75 per cent ethanol it is very weak at low tensions and non-existant at moderate or high tension. The best B_3 patterns are obtained at 70 per cent ethanol and the good B_2 pattern was obtained by stretching A material at 85 per cent ethanol.

It can be seen from Figure 3 that the 15.4 A to 23 A spacing is present in all regions and appears to change smoothly with hydration. At least below 85 per cent ethanol with medium or high tension this would appear to be so. At low tension a stepwise variation may take place as suggested by Franklin and Gosling (1953 c) and Wilkins and co-workers[1](~~in press~~ private communication). Above 85 per cent ethanol the higher tension

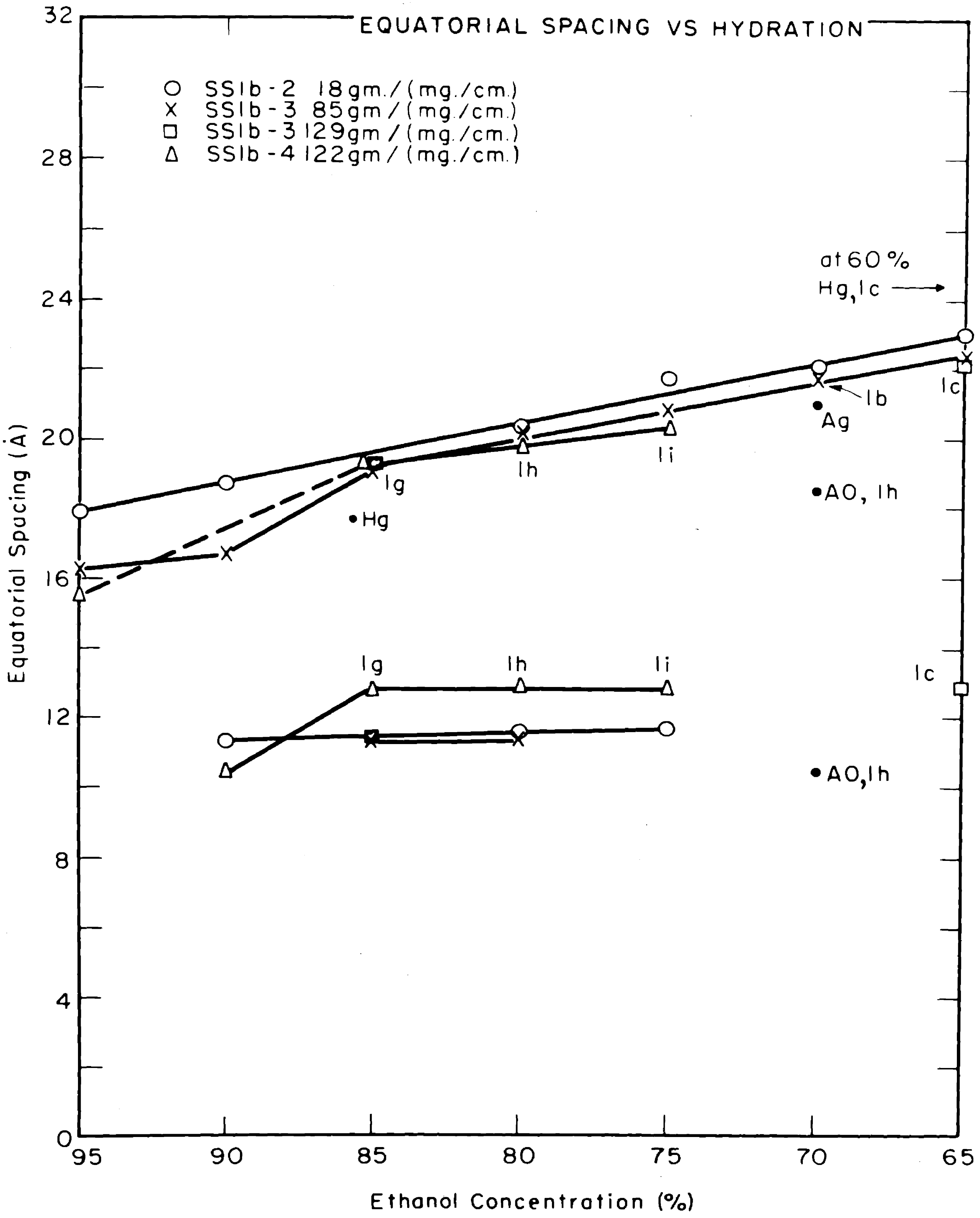
EQUATORIAL SPACING VS HYDRATION
○ SSIb-2 18gm./(mg./cm.)
× SSIb-3 85gm/(mg./cm.)
□ SSIb-3 129gm/(mg./cm.)
Δ SSIb-4 122gm/(mg./cm.)
at 60%
Hg, Ic →
Equatorial Spacing (Å)
32
28
24
20
16
12
8
4
0
Ib
Ic
Ag
Ig
Ih
Ii
•Hg
•AO, Ih
Ig
Ih
Ii
Ic
•AO, Ih
95
90
85
80
75
70
65
Ethanol Concentration (%)

FIGURE 3

curves break as the structure becomes disorganized. On the high tension curve one spot is absent and this may indicate a structure factor at zero. That the smaller spacing curve obtained at higher tension is markedly different from the others is evidence of the individuality of the configuration which gives rise to the B_2 pattern.

Adding mercuric chloride or silver nitrate to the immersion fluid, as stated above, generally disrupted the X-ray pattern. The equatorial spot in the 15 A to 23 A range remained. Its spacing, however, corresponded to that which would normally be obtained at an alcohol concentration about 5 per cent higher than that of the immersion fluid. The presence of these additives also made the DNA insoluble at low alcohol concentrations. One spot obtained from a mercury stained specimen in 60 per cent ethanol is represented in the Figure. Its Bragg spacing is the largest on the Figure, being 25.2 A.

Acridine orange staining had a much more striking effect in that the sharp pattern was changed rather than destroyed by it. The decrease in the 15 to 25 A spot spacing was equivalent to that which would have been obtained with a 20 or 25 per cent change in alcohol concentration. In this case it appears that the lattice shrunk markedly but the structure did not collapse into disorder.

Tension, elongation, and birefringence.

The length of the specimen (between the supporting threads) was measured while the series of X-ray patterns were being obtained under the various conditions given above. Figure 4a (pg 57) shows

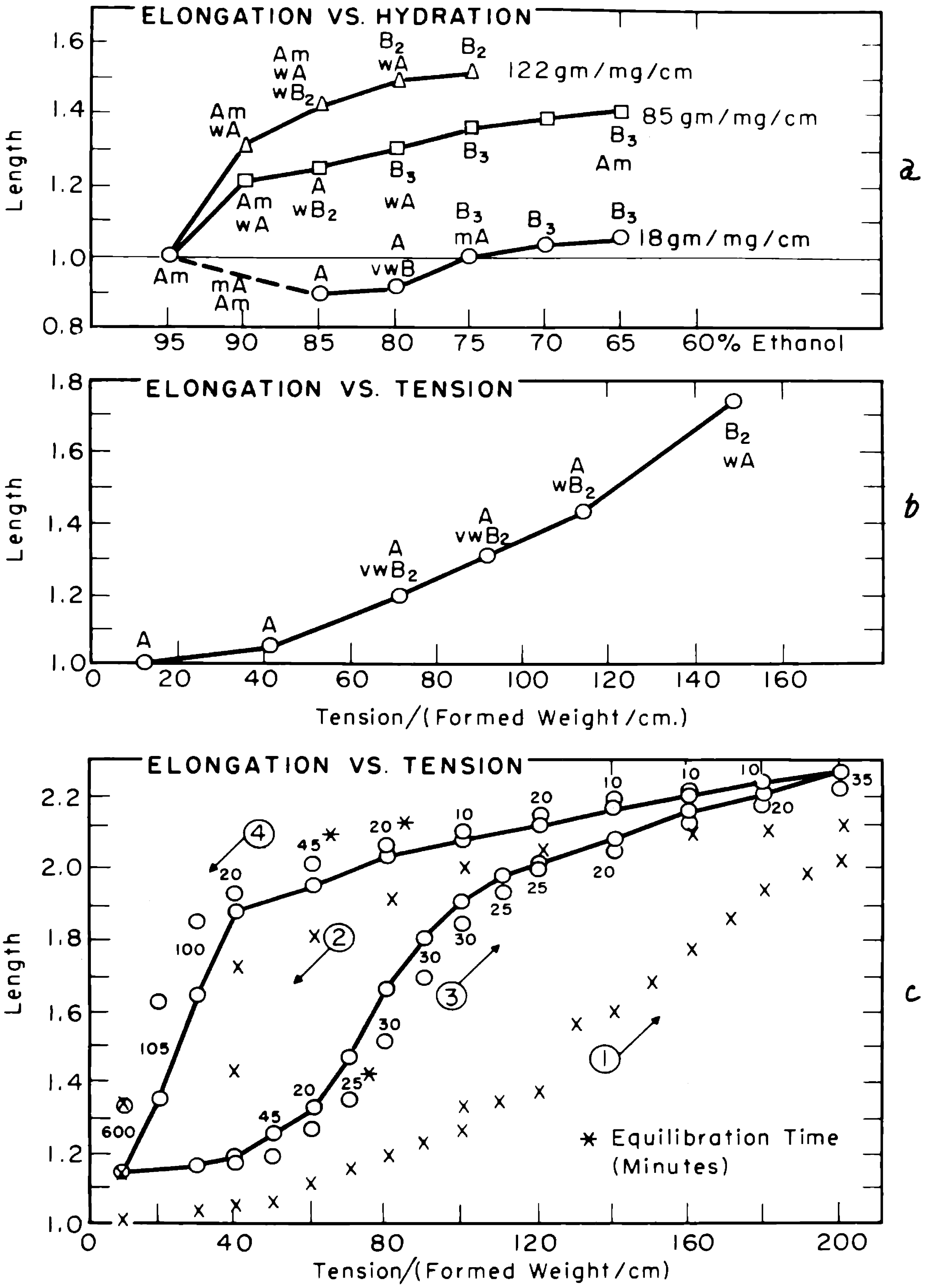
ELONGATION VS. HYDRATION
Length
1.6
1.4
1.2
1.0
0.8
95
90
85
80
75
70
65
60% Ethanol
122 gm/mg/cm
85 gm/mg/cm
18 gm/mg/cm
Am
Am wA
Am wA wB2
B2 wA
B2
Am wA
A wB2
B3 wA
B3
B3 Am
mA Am
A
A vwB
B3 mA
B3
B3
a
ELONGATION VS. TENSION
Length
1.8
1.6
1.4
1.2
1.0
0
20
40
60
80
100
120
140
160
Tension/(Formed Weight/cm.)
A
A
A vwB2
A vwB2
A wB2
B2 wA
b
ELONGATION VS. TENSION
Length
2.2
2.0
1.8
1.6
1.4
1.2
1.0
0
40
80
120
160
200
Tension/(Formed Weight/cm)
④
②
③
①
600
105
100
20
45
20
10
20
10
10
35
20
25
25
30
30
30
20
25
20
45
20
* Equilibration Time (Minutes)
c

FIGURE 4

the percentage elongation based on the 95 per cent ethanol length for the three series of pictures whose equatorial spacings were discussed above. The type of pattern observed is given with rough relative intensities indicated when mixed. "Am." indicates amorphous rings and the other notations are as above.

At low tension the fiber bundle actually shortened 10 per cent on hydration to the A form from the amorphous (95 per cent ethanol) form. This may well be associated with strain in the fiber, as formed, that cannot be released until water "lubricates" the molecules and allows them to come to equilibrium. Of more interest is the fact that the fiber bundle elongated only 14 per cent while the X-ray pattern changed from pure A to pure B_3. The change in layer line spacing corresponds to an elongation of 19 - 21 per cent and the change from 11 to 10 residues per turn proposed by Franklin and Gosling (1953 a,b) and Wilkins and co-workers (1953) for the stress free A to B transition would imply an additional 10 per cent elongation which would compound to 32 per cent.

At medium tension the specimen elongated 20 per cent when the ethanol concentration was changed from 95 per cent to 90 per cent and only a weak A pattern was found then. At 85 per cent ethanol and 25 per cent elongation an A pattern with a small amount of B_3 was found. With another 5 per cent decrease in alcohol concentration and an accumulated elongation of 30 per cent a B_3 pattern was obtained. The change from A-with-weak-B_2 to B_3-with-weak-A involved only a 4 per cent change in length of the fiber bundle in this case.

At high tension no clear transition was observed. The elongation reached 52 per cent.

Figure 4b (pg. 57) shows the elongation vs. tension curved at 85 per cent ethanol observed with one specimen/and the corresponding changes in X-ray pattern are indicated. At 15 per cent elongation the first sign of B_2 pattern was seen and after 42 per cent elongation the B_2 pattern was still much weaker than the A. The pattern was predominately B_2 in the next exposure and the over-all elongation at this time was 76 per cent. The change in length during this major transition was thus 24 per cent. Whether or not the transition was complete before this much elongation occurred is unknown. The elongation corresponding to the layer line spacing shift is 16 per cent. An additional 10 per cent for change in the number of residues per unit cell would compound to 28 per cent overall.

Thus the transition from A to B type pattern obtained with a change in alcohol concentration was accompanied by an inordinately small change in the length of the fiber bundle. In contrast the change in length observed during the A to B transition brought about by stretching corresponds reasonably with the expected elongation. In both cases appreciable changes in length are observed with no A to B transition. It must be remembered that the X-ray pattern is obtained from a small segment of the bundle and conditions may not be homogeneous. Furthermore the sharp X-ray pattern may come from only a fraction of the material that is in the beam.

To illucidate further the stretching of DNA fibers and fiber bundles in the light of the X-ray pattern transition reported here and Wilkin's birefringence and "necking" observations (see pg. 14) obtained under different conditions, separate stretching experiments were carried out. A fiber bundle similar to those used as X-ray specimens but longer and thinner was mounted in an 85 per cent ethanol bath. One mounting thread was anchored at the bottom and the other connected to a beam balance at the top. The bath and anchor point could be raised and lowered so that the balance would read properly and the fiber bundle length was measured with a traveling microscope.

The results are shown in Figure 4c (pg. 57). The first stretching was done by increasing the tension by 10 gms. every 2 or 3 minutes and taking readings before and after each change. Several breaks are seen in the curve, labeled 1, corresponding to 10 or 20 minute time lapses. At the highest tension, 200 gms., an hour was allowed for equilibrium to be reached during which time the elongation increased from 100 per cent to 114 per cent. The tension was then rapidly stepwise decreased to 40 gm. with a return to 72 per cent elongation. After an hour at this tension the length was back to 141 per cent of the original. After a further decrease in tension and allowance of 45 minutes for shrinkage the bundle was only 17 per cent longer than the original specimen in 85 per cent ethanol. This was after having been stretched to 2.14 times the original length. During the next eight hours at constant tension 2 per cent additional shrinkage was observed.

The same specimen was stretched again, from 1.15 to 2.26 times the original length and returned to 1.15 after gradual release of the tension. During this stretching and relaxation, time was allowed for an approach to equilibrium at each tension. The elongation was obtained within a minute or two after changing the tension and periodically until only a 1 or 2 per cent change was observed in ten minutes or longer. The first and last of these points are presented in the Figure with the time lapse (in minutes) indicated. The curve is drawn through the latter points.

The equilibration is slow but a 95 per cent completely reversible elongation in the DNA fiber bundle was observed by allowing sufficient time for elongation and shrinkage.

The stretching curve is sigmoid, suggesting a transition between two phases each with its own extensibility and "rest" length. From the data of Figure 4b the A to B_2 transition in the X-ray pattern would appear to occur in the region of the inflection point (Figure 4c) or above it. The increase in length observed during the X-ray transition was 24 per cent and thus there remains a 40 per cent elongation before the transition and at least a 12 per cent elongation after the transition. Certainly before the transition the fiber bundle elongation is not reflected in a layer line spacing change.

The relaxation curve is not noticeably sigmoid and exhibits severe hysteresis effects. The B_2 to A pattern transition as noted on pp. 51 showed a similar hysteresis.

That the reversible extensibility is a property of the individual fiber rather than the bundle was demonstrated with a fiber 6 microns in diameter. It was stretched from 9 mm. to 18 mm. and returned to 9 mm. The relative humidity in this case was 72 per cent, but in order to speed the equilibration the fiber was breathed upon. An approximate determination of the tension applied to this fiber converted to the scale of Figure 4c gave a value of 80 gm. as compared to the 200 gm. applied there. The agreement is satisfactory. During this two-fold stretching and return the birefringence of the fiber changed from strong negative to weak negative and back to strong negative.

The sharp transition from the A to the B_2 X-ray pattern reported here would seem to be related to the sharp "necking" of fibers, with the concomitant change in birefringence reported by Wilkins, Gosling, and Seeds (see pg. 14) in relation to the less hydrated material. They reported a loss of sharp X-ray diffraction on necking but the discrepancy is undoubtedly due to the fact that they were working at a low relative humidity. They reported 100 per cent extensibility but only a partial return by a ratio of 1.5:1, as contrasted to the complete return reported above. This may have been due to low humidity and/or insufficient time. They reported a positive birefringence in the highly stretched material, which has been confirmed by others (Rich and Watson, private communications). This also seems to be obtained only at low hydration levels (see below).

The following observations concerning necking and birefringence were made with material used in this thesis.

At 50 per cent relative humidity sharp necks were seen in fibers, as formed, or when the necks were produced by breathing on a taught fiber. The normal birefringence was —0.05 to —0.10 when estimated from interference colors with and without the Red I plate. In only one fiber was positive birefringence seen and this was estimated at +0.02. Usually values between 0 and —0.02 were obtained in the "necked" portions.

At ap roximately 80 per cent relative humidity the necks were more gradual and no positive birefringence was ever observed. The birefringence measured with a quartz wedge compensator and micrometer eye piece was —0.068 in the thick region and —0.048 in the thin region at one "neck". At slightly higher humidity values of —0.086 and —0.066 were obtained, with still more gradual "necking". Other measurements at approximately 80 per cent relative humidity gave values of —0.075 and —0.038 for the unstretched and stretched regions, respectively.

The data indicate that DNA in the A and B_3 forms have nearly the same birefringence (ranging between —0.06 and —0.09) and in the B_2 form about half as much.

"Solubility" of DNA in alcoholic systems.

The solubility phenomena in the alcohol, water, DNA system are rather interesting of themselves and are pertinent to the X-ray technique of alcohol immersion employed in this thesis. Perhaps use

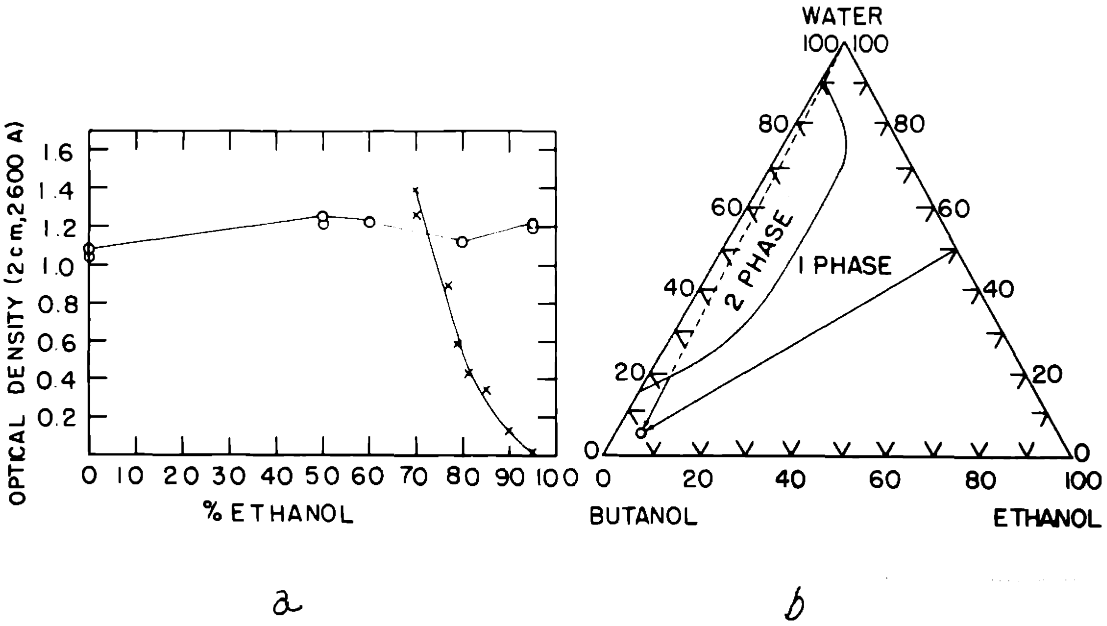

a.) DNA "Solubility" vs. Ethanol Concentration

⊖ 4.0 mg (ca. dry wt.)/100 ml. Ethanol added to water solution.

X 6.3 mg. (ca. dry wt.)/20 ml. Water added to solid DNA plus ethanol.

b.) DNA "Solubility" in Water—ethanol—butanol system.

Figure 5

can be made of the peculiar properties in fractionation procedures, physical chemical studies, or degradation studies. The results of several experiments concerning these phenomena are therefore reported below but no further comment will be made in later sections regarding these data.

If salt free DNA is dissolved in water and then mixed with any quantity of ethanol (this DNA was prepared by the Mirsky-Pollister method) an examination of the ultra violet absorption spectra gives no indication of precipitation. Such "solutions" can stand for weeks at 4°C with no change in the spectrum. If on the other hand air-dried DNA is placed in alcohol of 65 per cent or greater it does not dissolve extensively. Indeed fibers have appreciable tensile strength under these conditions as reported above.

Figure 5a,b (pg. 64) illustrates these two points. In the one experiment (curve labeled 1) 1 ml. of a given solution of DNA was mixed with appropriate amounts of water and then ethanol was added to 20 ml. The spectrum was recorded on the Cary Spectrophotometer immediately and in several cases after 3 days at 4°C. Precipitation would be indicated by loss of light due to scatter above 3000 A or a decrease in absorption at 2600 A. In the other experiment (curve 2) air-dried DNA was placed in 95 per cent ethanol, shaken violently and the spectrum was recorded as before. In this case solid material was present and it scattered light (O. D. of 0.1 at 3500 A). A rough correction was made for this scatter by extrapolating the curve. Water was added serially and a rough "solubility" curve was thus obtained. The final mixture was tested again after 3 days at 4°C with little increase in optical density. The optical density at 95 per cent ethanol would have been 24 if all the material were in solution. Thus after three days at 4°C in 70 per cent ethanol only 1/14 of the DNA was in solution.

Apparently there is a large energy barrier between the dispersed and aggregated states in salt—free alcohol above 65 per cent concentration and therefore thermodynamic equilibrium is never reached. It is interesting to note that within the range of 65 to 95 per cent ethanol the X—ray pattern, the elastic properties and rest length of fibers change appreciably, as reported elsewhere in this thesis, indicating different hydration states and pronounced changes in structure. One might suppose that these changes would take place also in the molecularly dispersed state presumably existing in the highly alcoholic solution. The variations in optical density of curve 1 may be significant in this respect. This finding is also pertinent to the interpretation of the dielectric dispersion data of Allgen (1954) obtained in alcoholic "solutions".

One further step in the alcohol solubility study is of interest. The DNA will apparently remain molecularly disperse in 90 per cent butanol, 5 per cent ethanol, 5 per cent H_2O if the mixing is done in such an order that a two phase system is never formed. This is done by mixing the ethanol with an aqueous solution of DNA and then adding the butanol with shaking. If on the other hand the butanol and ethanol are mixed and added to the aqueous DNA, the DNA will be precipitated quantitatively. Figure 5b shows the ethanol—butanol—water phase diagram at 26°C and illustrates the changes in composition with the two orders of mixing described above.

The results are explained using the energy barrier between the condensed and dispersed states within one liquid phase as hypo—

In this situation they are difficult to separate so that centrifugation is necessary. On the other hand they are very temperature sensitive and the difficulty of temperature control during centrifugation makes it undesirable.

In summary, DNA will apparently remain molecularly disperse in alcohol systems that will not dissolve solid DNA. The colloid is readily formed by dispersing the DNA in water and then adding the other solvents in such a way as to maintain a single solvent phase. Attempts to partition DNA between two liquid phases failed.

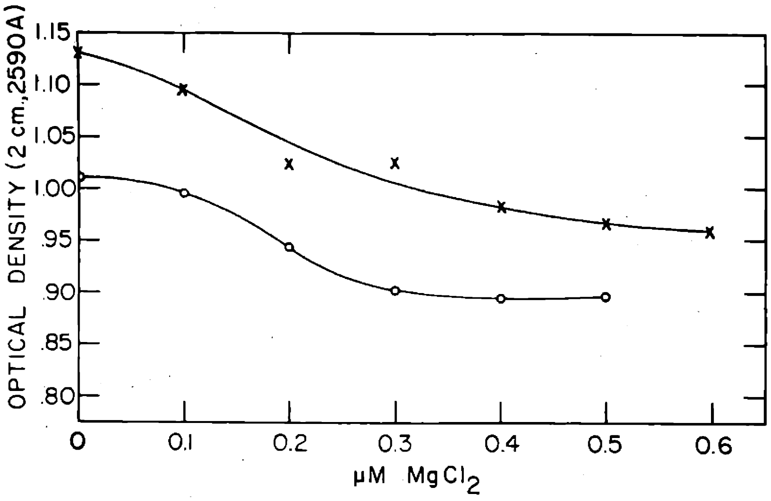

DNA Optical Density vs. $MgCl_2$

Θ Normal DNA 0.6 u M (P) in 10 ml.

X Boiled DNA

Figure 6

thesized above. If the system contains only one liquid phase at all times the molecules are never able to come together. On the other hand if a butanol—ethanol—water phase and a water—ethanol—butanol phase are in equilibrium, the DNA will partition essentailly completely into the water—rich phase. As more butanol is added the water—rich phase will decrease in volume. The DNA will become more concentrated and eventually either precipitate suddenly as the molecules are forced more strongly together or simply have all the water extracted except for whatever is bound in the "precipitate" state.

One can go still further with the DNA solubility in non—aqueous media by adding, for example, decalin in large quantities to the butanol—ethanol—water solution with no precipitation as long as a single phase is maintained. In this manner, combined with some concentration steps, a molecular dispersion of DNA in a non—polar solvent might be obtained and be of interest in relation to physical chemical studies.

Supposedly a fractionation of some sort might be obtained if DNA would partition between two phases in equilibrium. A partition ratio of 1:10 is the maximum disparity between two phases that seems to be practical even when using counter—current distribution methods. Experiments were attempted along these lines but the ratios were certainly greater than 1:10 if not infinite in all those experiments where poor temperature control did not seem to invalidate the results. The problem is that in order to obtain two phases nearly alike in affinity for DNA the two phases must apparently be almost identical.

The ultra violet absorbtion coefficient of DNA as a function of the presence and concentration of salts and as a function of denaturation.

In conjunction with an interest in the use of heavy metal staining to aid in X-ray diffraction analysis and an interest in the possible use of ion binding studies to support structure hypothesis preliminary observations were made concerning the relation of the ultra violet spectrum of DNA to the presence of several salts. Such observations may also serve as evidence concerning the state of denaturation (see references to denaturation literature on pg. 12). and the presence or absence of salts as impurities. The following data are therefore presented.

A stock solution of DNA from calf thymus prepared by the Mirsky-Pollister method was made by dissolving 49.5 mg. of air-dry (relative humidity 22 per cent) material from preparation 6 in 100 cc. of relatively anoxic distilled water. The following observations were made concerning the ultra violet absorbtion of this solution as diluted as a function of boiling and/or the addition of NaCl or $MgCl_2$. Measurements were made in the Cary Recording spectrophotometer with 2 cm. cells. Values of the optical density at the absorbtion maximum near 260^0 A are given.

The optical density (here after referred to as O. D.) of a 20 fold dilution was 1.01. When an aliquot was quickly heated to boiling and quickly cooled the O. D. had increased to 1.13.

A series of equal dilutions containing 0.0 M, 0.000003 M, 0.0001 M and 0.25 M NaCl had optical densities of 0.525, 0.520, 0.508, and 0.450 respectively.

The effects of serially adding $MgCl_2$ to the boiled and unboiled twenty fold dilution is shown in Figure 6 (pg. 68). The optical density data has been corrected for dilution with slight progressive error due to loss of bulk solution on repeated transfer. The ordinate is in u M of $MgCl_2$. The amount of DNA present assuming 20 per cent hydration of the "air dry" starting material is 0.6 u M (P).

The date for the $MgCl_2$ effect on unboiled DNA qualitatively but not quantitatively confirm Cavalieri's (1952) findings. (Since such small amounts of $MgCl_2$ have a pronounced effect there is probably very little $MgCl_2$ present in the DNA preparation.) Schachman (private Communication ,) found no such sensitive $MgCl_2$ effect with DNA prepared by a method giving a higher molecular weight product than that employed here. Results recently obtained in Doty's laboratory (private communication) seem to confirm the implication that the $MgCl_2$ effect is obtained only with partially denatured DNA. The results presented here obtained with boiled DNA show that denaturation of this kind modified the $MgCl_2$ effect but did not obliterate it. The rise in absorbtion with boiling is consistent with the literature (see pg. for references). This evidence would seem to indicate that the action of $MgCl_2$ and heat on the ultraviolet chromophore are largely disjunct.

The binding of acridine derivatives to DNA*

1. Experimental method.

The binding of acridine derivations to calf thymus DNA

---

*See Wiegand (1953)

(prepared by the Mirsky-Pollister method) in dilute solution was studied in a cursory way by a partition method. The acridines used were acridine, acriflavine (National Formulary) which is an unspecified mixture of pure acriflavine with proflavine, and acridine orange. These will be designated acridine, ACF and AO. The basis of the method is that in a two phase butanol-water system the acridines partition in favor of the butanol and the DNA remains entirely in the aqueous phase. From a measurement of the optical density of the butanol phase and a knowledge of the volumes of the phases the amount of free and bound acridine in the aqueous phase can be calculated if the total amount present is known as well as the individual partition coefficients and absorbtivities.

The acriflavine hydrochloride hydrate (N. F.) (Matheson Co., Inc. lot #6848) was tested and found to obey Beers law in water and in butanol saturated with water within the optical density range used (O. D. = 0 to 1.4 in 2cm. cell). The absorbtivities (k = O. D./cx with c in gm/cc. and x in cm.) found were: 1.50×10^5 at the 2620 A maximum in water, 1.00×10^5 at the 4500 A maximum in water, and 1.56×10^5 at the 4600 A maximum in butanol saturated with water. The partition ration (c in butanol phase/c in water phase) was found to be 2.93. No DNA partitions into the butanol phase.

2. Experiments with normal DNA.

When 5 ml. of a butanol-saturated-with-water solution of ACF with an O. D. of 3 x 0.96 was mixed with an equal volume of a given DNA solution, the O. D. of the butanol phase decreased to 0.17.

From these figures it was calculated that 43.5 μ g of ACF (HCL hydrated) was bound to DNA and 3.7 μ g was free. 1,000 μ g of DNA (estimated dry wt.) was present. The dilute solution had been stored at 4°C for 1 week.

When the solution was made 0.001 M in NaCl in a similar experiment no visibly noticeable effect was seen. Increasing the NaCl concentration to 0.0065 M resulted in 44 per cent of the ACF being freed. In a third experiment with 0.4 M NaCl it visually appeared as though all of the ACF was free.

A series of measurements were made of the O. D. of the butanol phase when solutions containing a fixed amount of ACF and various amounts of DNA were equilibrated with a fixed volume of butanol saturated with water. The results are presented in Figure 7a (pg. 73). The abscissa are the amounts of DNA present (assuming 20 per cent hydration at the time of weighing.), and the ordinates are the values of O. D. obtained from the butanol phase. If the initial and final straight line portions of the curves are extrapolated to their intersection this point may be interpreted as indicating the amount of DNA that would be necessary to bind all of the ACF if all of the binding cites were occupied.

The amount of the acriflavine hydrochloride hydrate present was 62.5 mg. Drying one batch of this lot of acriflavine hydrochloride hydrate at 160°C for 2 hours resulted in a weight loss of 19.6 per cent. Applying this correction, the dry weight of ACF becomes 50.3 mg. The molecular weight of pure acriflavine chloride

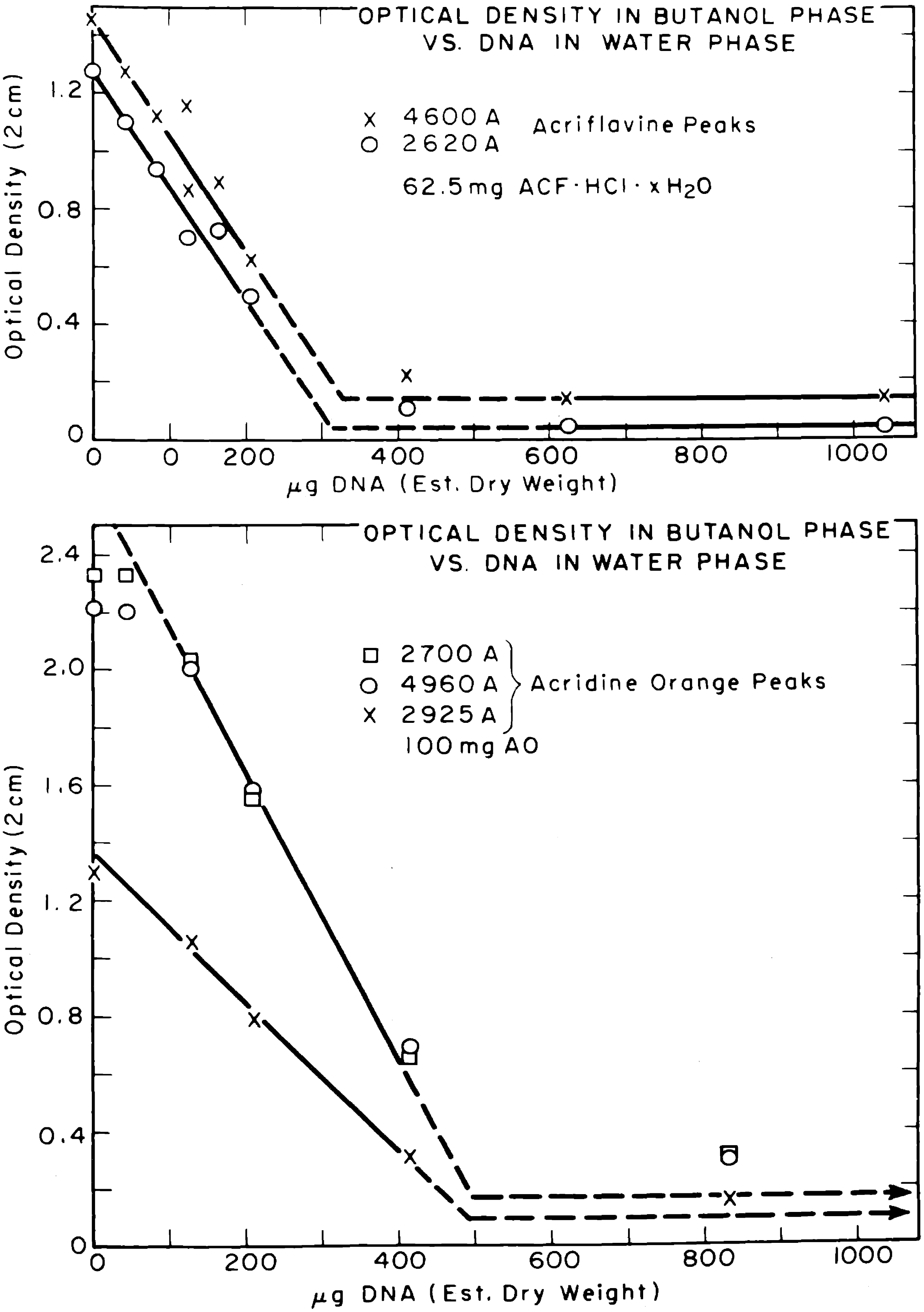
OPTICAL DENSITY IN BUTANOL PHASE
VS. DNA IN WATER PHASE
X 4600 A
O 2620 A
Acriflavine Peaks
62.5 mg ACF · HCl · x H_2O
Optical Density (2 cm)
1.2
0.8
0.4
0
0
0
200
400
600
800
1000
μg DNA (Est. Dry Weight)
OPTICAL DENSITY IN BUTANOL PHASE
VS. DNA IN WATER PHASE
□ 2700 A
O 4960 A
X 2925 A
Acridine Orange Peaks
100 mg AO
Optical Density (2 cm)
2.4
2.0
1.6
1.2
0.8
0.4
0
0
200
400
600
800
1000
μg DNA (Est. Dry Weight)

FIGURE 7 a, b

is 259.6 and that of proflavine is 210.1. If the mixture were 60:40 the average molecular weight would be 240. Thus 0.2 μ M of acriflavine would be bound to 0.96 μ M (P) of DNA. The molar ratio of P/ACF is thus calculated to be 4.6. This may readily be in error by as much as 25 per cent.

Using Acridine Orange (National Analine lot #11538) instead of acriflavine (N.F.) a set of experiments similar to the last series above was carried out. The data are presented in Figure 7b (pg. 75). The measurement was made twice at each concentration, the second value only being used. Measurements were read from the O. D. curve at three peaks–2700 A, 2925 A, and 4960 A. The optical densities at 2700 A and 4960 A never differed by more than 6 per cent and a single straight line is drawn to fit these data at low DNA content. If this line is extrapolated to the ordinate value of the lowest point the abscissa is 500 μ g DNA (dry weight est.) or 1.52 μ M (P). The amount of AO present is 100 mg. or .376 μ M assuming the starting material to be pure, dry, and not the hydrochloride. The calculated molar ratio P/AO is thus 4.0. From the O. D. data at 2925 A the same value is obtained. If the starting AO were hydrated when weighed or the DNA were less hydrated than assumed the ratio would be higher.

3. Experiments with denatured* DNA.

When a DNA solution was heated quickly to boiling and cooled

*$MgCl_2$ effects on the DNA spectrum with boiled and unboiled DNA were presented on pg. 70 and Figure 6 . Effects of adding NaCl to boiled DNA were found to be very similar to those reported for unboiled DNA on pg. 69 .

rapidly a large change occured in its ACF binding properties. When large amounts of DNA were present only about half of the ACF was removed from the butanol phase. When a dilute solution of DNA was stored at 4°C for 5 weeks a check on the binding of AO at one P/AO ratio showed that only about half as much AO was bound as would have been expected. The effect of severe denaturation is further evidenced by the fact that a green fluorescence was observed (by eye) in a solution of DNA, AO, and butanol in water while an identical solution containing boiled DNA showed no fluorescence. The spectral shifts in the dye in a water phase containing various amounts of boiled and unboiled DNA were found to differ in character.

ANALYSIS OF THE X-RAY DATA

Lattice

The X-ray pattern of DNA of the type A has a well defined lattice with no evidence of systematic defects. The detailed lattice parameters have been determined by Franklin and Gosling (1953 d) and by Wilkins, Seeds, Stokes, and Wilson (1953) from measurements of more than 60 spots.

1. The B_3 DNA pattern.

The B type pattern has been reported as paracrystalline with layer line sampling apparent but no transverse lattice effects obvious except for a spot on the equator and an intensification on the inner edge of the second-layer-line streak (Wilkins, Stokes, and Wilson, 1953). In plates 1, 2, and 4 (patterns 1b, 2d, 2e, 2g) the B_3 patterns presented show sharp sampling on the equator and second layer line and no evidence of sampling on the 1st, 3rd, 5th, or 10th layers. The reciprocal space coordinates of the sharpest spots and layers derived from measurements of exposure 1b of specimen sslc 3-7 (pattern 2d, pg. 48) are presented in Table 4. The specimen to film distance was 7.50 cm and the central beam diameter on the film was 0.40 mm. The resolving power corresponding to the spacing for twice this diameter is 290 A. The probable errors in the measured meridional and radial dimensions averaged 0.6 per cent for the 1st and 2nd layer-line measurements. Four measurements

Table 4

	Z^*	X^*	÷ by	a^*
Eq. 1st spot	0	.0702	$\sqrt{3}$	.04053
1st layer streak	.0453			
2nd layer 1st spot	.0904	.0403	1	.04030
2nd layer 2nd spot	.0906	.0821	2	.04105
2nd layer 3rd spot	.0890	.1077	$\sqrt{7}$	.04070
			Average	.04064
10th layer streak	.4492	.107		

were averaged for each spot. The strong equatorial spot measured 0.44 mm in diameter.

The layer line spacing calculated from 1st and 2nd layer line measurements was 34.1 A. The value obtained for the 10th layer line position was 9.96 times this layer line spacing.

If the lattice is assumed to be pseudo—hexagonal* and the X^* values are divided by the constants appropriate to the index assignments as indicated in the table, four values of a are obtained. They are equal within experimental error. The selection rule $h - k + l = 3\ m$ allows all of the spots observed and forbids many of the spots that are predicted from the lattice but not observed. When $l = 0$ this selection rule allows the identical spots that would be obtained from any lattice whose projection on to the plane perpendicular to the fiber axis (z axis) is hexagonal with $a^{*\prime} = \sqrt{3}\ a^*$. (Thus $a^{*\prime} = .0705$ and the separation of helix axes is 25.2 A) When $l = 2$ the appropriate selection rule is obtained if there are three equivalent units per lattice point with c projections as above and z coordinates at 0, 1/3, and 2/3 c respectively. Such a lattice is shown in the upper left corner of Figure 8 . The relationship of the units to one another in any adjacent pair is identical to that in any other pair, namely a translation perpendicular to c of 2/(3 a*) and a translation parallel to c of |1/3 c| . This is the simplest lattice that will fit the equatorial and second layer line spots. However any lattice derived from this by displacing units parallel to c systematically or at random (an infinite unit cell) by 1/2 c will result in the identical sampling points on the equator and second layer lines (see lower left of Figure 8).

---

*Since the individual helical units have a 10 fold screw axis the lattice can not be strictly hexagonal in the sense of a hexagonal space group. Equivalent points on the various helices can fall on a geometrically perfect hexagonal lattice within experimental error and hexagonal(omitting "pseudo") is used in this sense in the following discussion.

One simple systematic variation can be derived as follows. The original or "parent" lattice can be referred to a monoclinic system with two identical units per unit cell. This is a body centered lattice. (see Figure 8 rectangles labeled B.C.). If the central unit is displaced in z by 1/2 c the cell becomes face centered. (see Figure 8 cells labeled F. C.) The even order layer planes are identical for body and face centered cells with identical lattice parameters. The derivation of a face centered cell from a body centered cell consists of displacing every second sheet of units by 1/2 c. (see inside broken line, lower right of Figure 8) An occasional displacement of a whole volume of the crystal by 1/2 c would similarly leave the observed diffractions unchanged (see inside broken line, upper right of Figure 8).

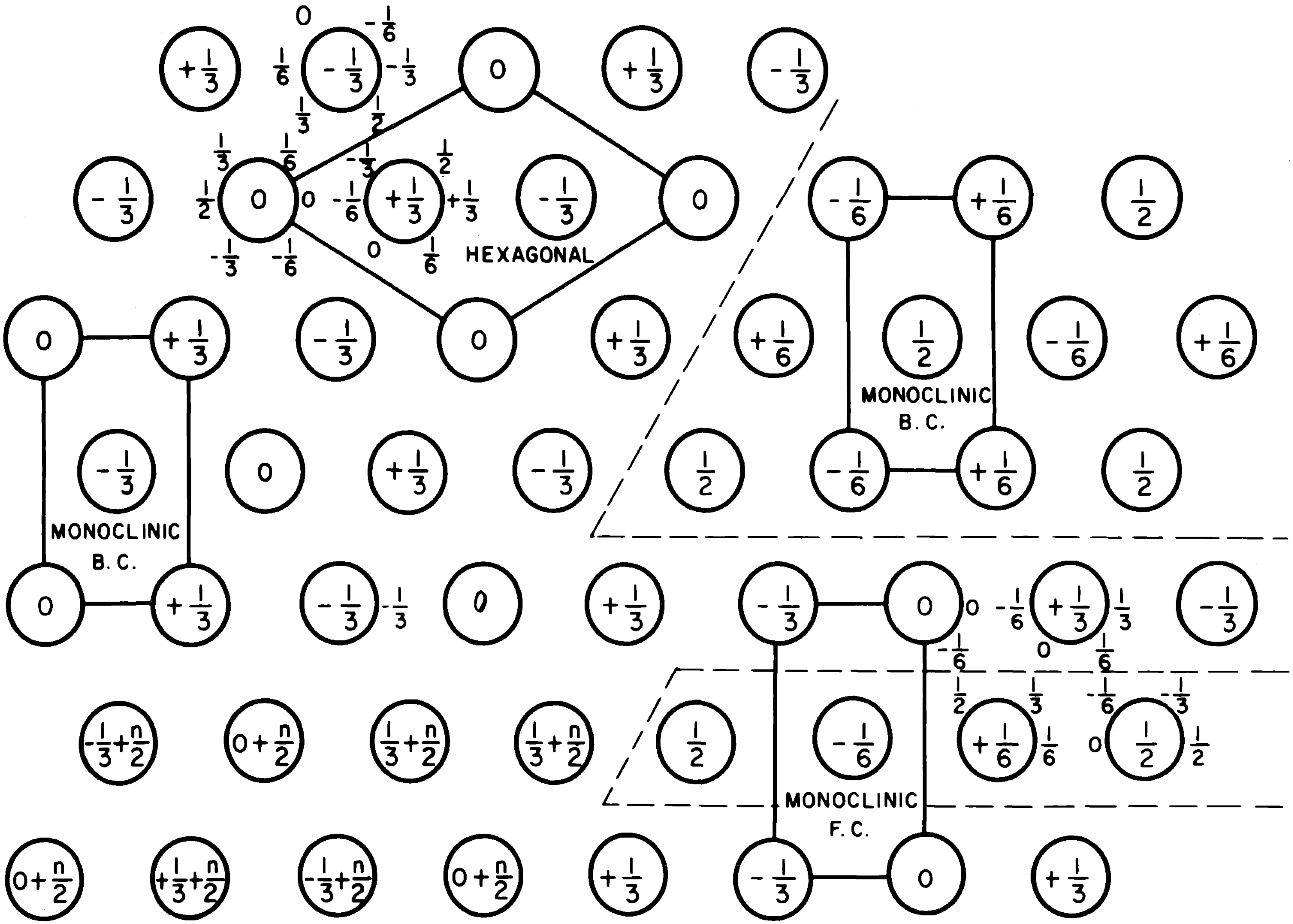
HEXAGONAL
MONOCLINIC B.C.
MONOCLINIC B.C.
MONOCLINIC F.C.

FIGURE 8

The fact that the 1st layer line is very sharp and yet shows no evidence of lattice sampling indicates that neither a regular face centered or body centered system exists. Rather very frequent defects involving displacements of individual units, sheets of units, or groups of units separately or in any combination are indicated. In such a system the intensity on even layer lines can be interpreted in terms of the structure factor of the unit cell and the lattice points and multiplicities. On the odd layer lines a continuous smoothly varying function takes the place of the lattice. When the number of defects is small a weak diffuse pattern is superimposed on the sharp pattern. The energy that is lost from the sharp pattern appears in the same area with a diffuseness that is a function of the frequency and type of defect.

In the case of the DNA B_3 pattern the dominant lattice, if there is one, is not known and the frequency and systems of defects are not known. Therefore, the effects of "lattice" on the intensity distribution on odd layer lines can not be specified. They may or may not shift the apparent structure factor maxima.

In Figure 21 pg. 148 the lattice points derived from the "parent" lattice are plotted along with the observed x-ray points and streaks and the optical diffractograph streaks from model #4.0. The multiplicity is always a multiple of three and the number of concentric circles at each point indicate the additional factor.

2. Acridine orange stained DNA pattern.

The diffraction pattern (2h, plate 2, pg 48) obtained from DNA stained with acridine orange can be indexed identically to B_3. The layer line spacing is 34 A but the distance between the axes of adjacent helices is only 21.4 A compared with 25 A for the B_3 pattern. The accuracy of measurement is not nearly so great as in the case of B_3 (pattern 2d) and the lattice may be slightly distorted from hexagonal.

3. The B_2 DNA pattern.

The lattice for the B_2 pattern, (1d, plate 1 and plate 3 also seen in mixtures with the A pattern) is apparently not hexagonal. The equatorial spot and the two 2nd layer spots can be indexed on the bases of a lattice with a square projection onto a plane perpendicular to the fiber axis ($a^{*\prime} = 0.082$, $a = 18.8$ A). The point on the 1st layer line does not agree well with this however having a measured X^* value of 0.038 and a predicted position of 0.029 or 0.065. The 1st layer line spot does appear streaked a bit on the mixed A and B_2 pattern and could be a result of a somewhat defective lattice combined with an apparent shift due to structure factor weighing. The layer-line spacing is 32.5 A. The other parameters should probably be considered as undetermined at present.

The form factor and molecular structure; general considerations for the DNA system.

1. Diffraction from helices; systems with a dyad axis.

The equations for diffraction from a discontinuous helix given by Crick, Cochran, and Vand (1952) are:

1. $I\left(R, \psi, \frac{l}{c}\right) = F^2\left(R, \psi, \frac{l}{c}\right)$

2. $F\left(R, \psi, \frac{l}{c}\right) = \sum_j \sum_n f_j J_n(2\pi R r_j) \exp i\left(n\psi - n\phi_{lj} + \left(\frac{1}{2}\right) n\pi + 2\pi l \cdot \frac{Z_{lj}}{c}\right)$

3. with the selection rule for n; $n = (l - Mm)/N$

I	Intensity
F	Structure factor
R, ψ	Radial and azimuthal cylindrical coordinates in reciprocal space
l	Layer plane index
c	Repeat period of the real space structure
j	A set of "atoms spaced periodically on a helix
n	Bessel function order
f_j	Atomic scattering factor of atoms of the set j
ϕ_{lj}	Azimuthal cylindrical coordinate of the first atom of set j.
Z_{lj}	The axial coordinate of the first atom of set j
M	The number of "atoms" of set j in one repeat period
m	Any integer
N	The number of turns of the helix in one repeat period
r	Radius of the helix

If we let A represent the amplitude term

4. $A_j = f_j \, J_n \, (2\pi \, R \, r_j)$

and let B represent the phase term

5. $B_j = \exp i \, (n\psi - n \, \phi_{1j} + (\frac{1}{2}) \, n \, \pi + 2\pi l \, \frac{Z_{1j}}{c} \,)$

6. then $F = \sum_j \sum_n A_{jn} \, B_{jn}$

Let ϕ_{oj} be the azimuthal coordinate of the helix on which the j set of atoms lie, when $Z = 0$, and let $Z_{1j}/c = z_{1j}$. Then

7. $\phi_{1j} = \phi_{oj} + 2 \, \pi \, N \, z_{1j}$

Substuting these in equation 5 and making use of the selection rule (eq. 3)

8. $B_j = \exp i \, (C + D)$

where $C = n \, (\psi + \pi/2)$

and $D_j = 2 \, \pi Mm \, z_{1j} - n \, \phi_{oj}$

In nucleic acid a major portion of the structure has a dyad symmetry such that each atom of set j has a counter part on set −j with $z_{-j} = -z_j$ and $\phi_{o-j} = -\phi_{oj}$ provided the proper reference system is chosen. In this case the structure-factor terms for the two sets can be conveniently combined by summing the phase terms with the result that

9. $B_{\pm j} = \exp i \, (C + D) + \exp i \, (C - D)$

Expanding this in terms of sines and cosines and combining terms

10. $B_{\pm j} = 2 \cos C \cos D_j + 2 \, i \sin C \sin D_j$

11. When $\psi = (2q + 1) \, \pi/2$, (q = any integer) which is the case when the X-ray beam is directed along a diad axis,

12. $\cos C = (-1)^{n(q + 1)}$ and $\sin C = 0$

The phase term of the structure factor thus becomes real with

13. $$B_{\pm j} = 2\,(-1)^{n\,(q\,+\,1)}\ \cos D_j$$

where q is to be interpreted as indicating the right and left hand sides of the pattern depending on whether it is odd or even.

When m = 0

14. $$D_{\pm j} = -\, n\, \phi_{oj}$$

15. and $$F = \sum_j \sum_n A_{jn}\ \ 2\,(-1)^{n\,(q\,+\,1)}\ \cos n\, \phi_{oj}$$

From the selection rule, n = 1/N, and therefore the diffraction from a pair of helices can be pictured in terms of a set of Bessel functions with their first maxima diverging from the center of the pattern. (Actually a straight line drawn through the maxima of the functions with index higher than one will extrapolate to intersect the axis at approximately 0.9 layer-line spacings away from the center of the pattern.) The coefficients of these Bessel functions will be modulated by a cosine term of "frequency" n ϕ_{oj} (and also by the factor ± 1).

When m = 1, n = (1 − M)/N and

16. $$D_{\pm j} = 2\,\pi\, M\, z_{1j} - n\, \phi_{oj}$$

In this case there will be a system of Bessel functions diverging from an 0 order function on the M th layer line. Again the Bessel function terms will be modulated by a cosine term of "frequency" n ϕ_{oj} (and the ± 1 term). In this case the cosine term is not unity at the J_o, as it always must be in the center of the pattern, but rather it is cos 2 π M z_{1j} at this point.

The entire pattern from a dyad related pair of helical systems can thus be considered to consist of various branches ascending and decending from J_o functions on the (Mm) th layer lines. Along each branch there is a cosine modulation of "frequency" $n\phi_{oj}$ and "phase" $2\pi M z_1$. It is because of this simplifying concept that the parameters ϕ_o and z_1 were chosen to specify the positions of the paired helical sets of atoms considered in this thesis.

2. Diffraction from helical systems of the DNA components; an optical diffractograph study.

To illustrate and analyze the complex cases of pertinence to the DNA analysis the Watson and Crick (1954) detailed model serves as a good object for study. In the following discussion their coordinates for the atoms in the backbone are used directly and the base-atom coordinates were derived from their plan figure. The carbon, nitrogen and oxygen atoms were given unit weight and the phosphorous weight two. The sodium ions and water were not included in their model. Hydrogen is neglected in this portion of the analysis.

From the outset it should be made clear that all of the patterns presented (except basal views) are from projections of the molecule along a dyad axis. Figure 11c (pg. 94) is a pattern from a projection along the helix axis and thus is a section of reciprocal space perpendicular to the helix axis and containing the equatorial line of the usual projections. The discussion of this pattern will be deferred until later.

Since the PO_4 is rather compact and yet distributed three dimensionally the diffraction from the two helical arrays of PO_4 groups might be expected to diffract in a manner similar to the ideal two helix case considered above. If we represent each PO_4 group by a spot at its center of gravity the simple case results. This is done in Figure 9b (pg. 88). The angle ϕ_0 (see pg. 84) is $0.23 \times 2\pi$ and thus intensity appears only on even layer lines near the center as it would everywhere with $\phi_0 = 0.25 \times 2\pi$. By the time the seventh layer

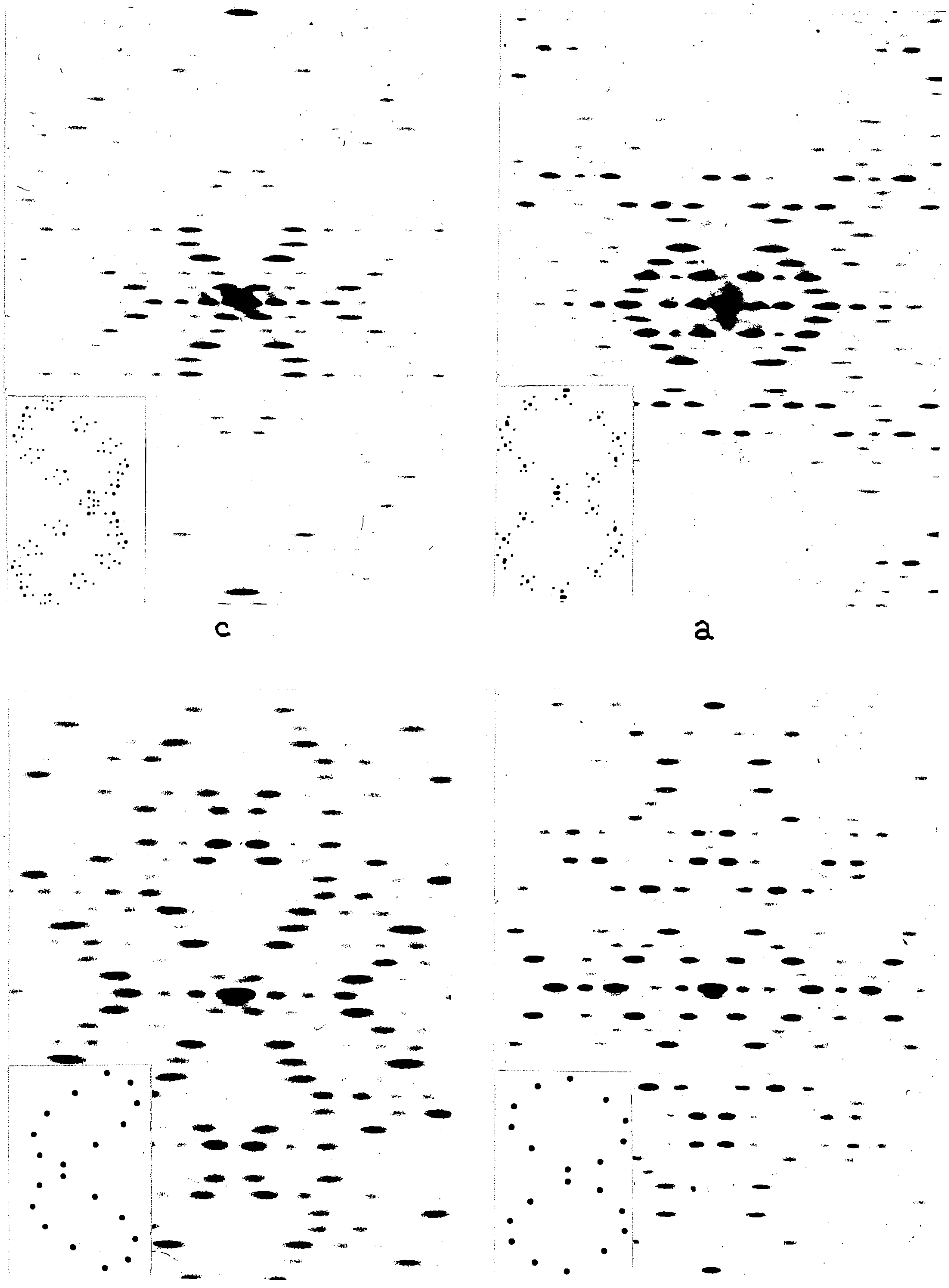

FIGURE 9

line is reached $n\ \phi_0 = 1.61 \times 2\pi$ rather than $1.75 \times 2\pi$ and so intensity can (and does) appear at the J_7 (X) maximum. All of the features can not be discussed and so it will only be noted that since $z_1 = 0.021$ $Mz_1 = 0.21$ and the 10th layer line has vanishingly little intensity on the meridian. Since ϕ_0 determines the frequency of variations of intensity along all branches of the pattern the alteration from weak to strong is also observed near the 10th layer line. Passing now to the more complete representation of the PO_4 group in Figure (pg. 88) (and comparing this with Figure 9b) the same general features are obvious. The similarity in areas dominated by the lower order J functions near the center of the pattern is most complete. The outer areas near the equator are somewhat modified. The intensity beyond the 10th layer line is strongly affected by a general decrease resulting from the spread of the scattering centers. In a loose analogy this is equivalent to diffraction from a small and large aperture resulting in a large and small central disk repsectively. Even at the 9th layer line the intensity is much less relative to the 1st than in the "schematic" center of gravity pattern. Actually the diffracted waves from the oxygen atoms are cancelling each other in this region and only the effect of the phosphorous remains.

An equivalent treatment of the deoxyribose group leads to similar results as shown in Figure 9c,d. For the center of gravity of this group $\phi_0 = 0.155 \times 2\pi$ and $z_1 = 0.023$. The 5 membered ring is a rather compact structure and more nearly planar than the PO_4

group. However, the nitrogen attached to C_1' was included in the group and the C_5' carbon is removed from the ring so that the fall off in intensity with distance from the center of the diffraction pattern is severe and not markedly directional, but somewhat so.

If the PO_4 and deoxyribose are both included in the diffraction mask the patterns of Figure 10c and 10d are obtained.

The intensity on the inner maxima of the 1st and 3rd layer lines from deoxyribose compliments the intensity on the 2nd layer line from the PO_4 and thus the first three layers all have intensity with little interaction between the components. On the 4th layer line both components have reflections and they thus interact. They happen to cancel each other rather effectively. On the 9th layer line they obviously add. On the 6th layer line evidently two sub threshold spots add and give rise to appreciable intensity.

The atoms within the base pairs are not strictly related by a dyad axis except for the nitrogens bound to the C_1' carbons. Furthermore there are two types of base pairs, adenine-thymine and guanine-cytosine, and they can have either one of two orientations at each level. The two types of pairs are very similar and all of the patterns and calculations in this thesis have used solely the guanine-cytosine pair. Experiments were carried out to determine the effect of random as opposed to regular arrangements of the bases, both diffracting by themselves and in combination with the backbone. The regular array had all guanine on one chain and the cytosine on the other. Two random orders were used in individual unit cells and the two types of unit cell were arranged at random in the one dimensional

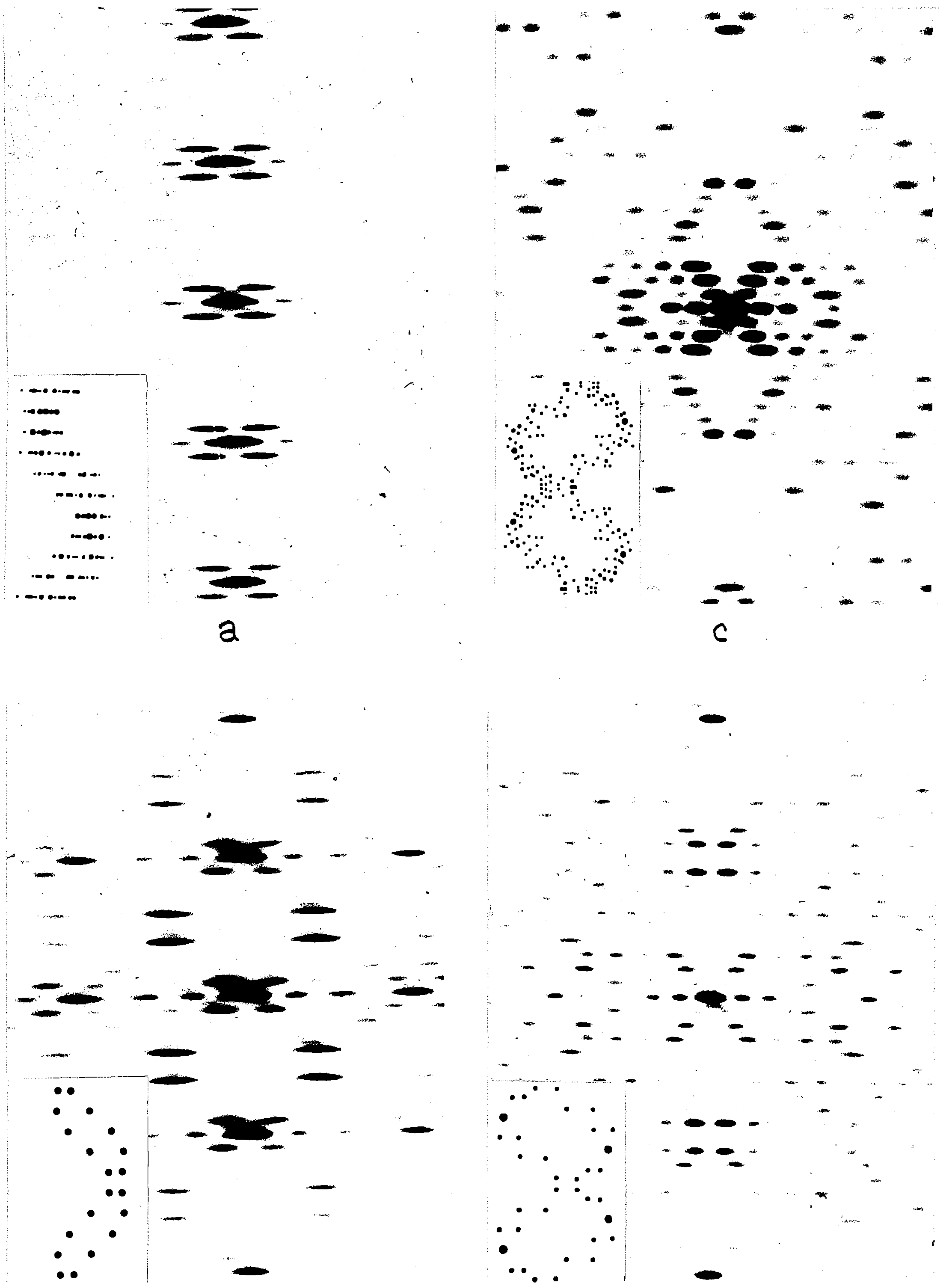

a

c

b

d

FIGURE 10

array of units normally used. The difference in the patterns were minor and seemed to affect mainly the weak 4th and 6th layer line diffractions. (In the patterns of Figure 11c has the regular array and a has the same random order in each cell.)

The schematic "equivalent" of the base pairs of Figure 10b was arrived at by considering all of the cytosine but only the 5 membered ring and N_3 of the guanine. In order to calculate the "average" center of gravity these were superimposed in the structure and a combined center of gravity was calculated. The total weight of the two groups was then distributed equally between the center of gravity calculated and its dyad related position.

The schematic representation then has $\phi_0 = 0.111 \times 2\pi$ and $z_1 = 0$. Since $z_1 = 0$, $Mz_1 = 0$ and the pattern around the origin is exactly repeated around the center of the 10th layer line. Since $\phi_0 = 0.111 \times 2\pi$ the 1st and 4th layer lines have strong first maxima and the 2nd and 3rd layer lines are weak. The lateral spread of the pattern is greater than that for either the PO_4 or the deoxyribose since the radius of the "center of gravity" of the bases is considerably less than that for the other components. The pattern from the atomic representation of the complete bases Figure 10a differs from the schematic markedly on the 4th, 6th, 14th, and 16th layer lines. This is due to the fact that the ϕ_0 values for the various atoms (as well as their radii) differ appreciably from the ϕ_0 of the center of gravity. On the 1st, 9th, 11th, etc. layer lines these differences are multiplied by one and the effect is not pronounced.

On the other layer lines mentioned the differences are multiplied by four and the result is that the diffractions from the various atoms cancel one another. For this reason a composite schematic should have the bases included when one is observing diffraction of low Bessel function orders and the bases should be omitted when considering reflections far off the meridian.

The composite model with all of the atoms of DNA (except the sodium) represented as in the Watson and Crick model is given in Figure 11a (pg. 94). In many positions of the pattern the intensity is due mainly to one of the three components considered above. In some cases several add, in others they cancel. Considering the 1st maxima on each layer line the following table summarizes the situation.

TABLE 5

1	PO_4	Deoxyribose	Bases	Total	Major Contributor
0	v. strong	v. strong	v. strong	v.strong	all add
1	v. weak	strong	strong	v.strong	R,B add
2	v. strong	weak	weak	strong	P
3	weak	strong	v. weak	strong	R
4	v. strong	medium	weak	v. weak	P, R cancel
5	v. weak	weak	v. weak	weak	R
6	medium	weak	weak	medium	P, R add
7	medium	v. weak	v. weak	weak	P
8	v. weak	weak	v. weak	medium	R
9	medium	weak	strong	strong	P,R,B add
10	v. weak	v. weak	v. strong	v. strong	B
11	weak	v. weak	strong	strong	B (P, R cancel)
12	v. weak	v. weak	v. weak	v. weak	none

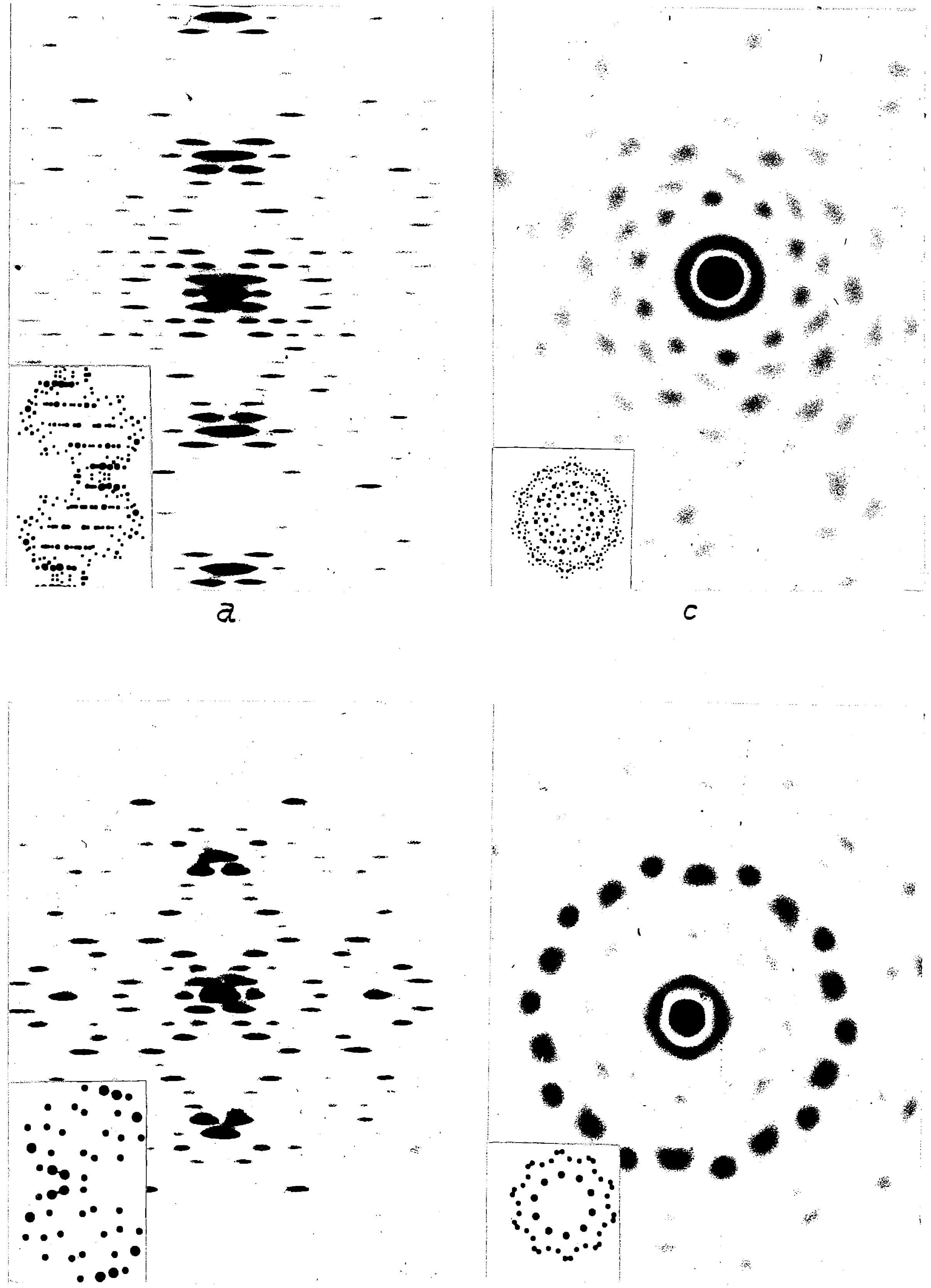

a c

b d

FIGURE 11

3. Treatment of the diffraction from the extensive water of hydration in DNA.

The diffraction from the water in the DNA structure, which amounts to roughly 40 per cent of the dry weight with DNA in the A form and 100 per cent of the dry weight in the B form, must be accounted for in some manner. The most rigorous way might be to place water molecules in a three dimensional model in accordance with principles known about water structure. Or the water might be treated as a liquid with boundaries determined by the DNA. A simpler method, which is based on a proposal by Wrinch (1950), was used in the present work.

The water was considered as a homogeneous electron gas of an average density corresponding to water. This electron gas is then pictured as filling a volume not excluded by the DNA. The diffraction pattern from the hydrated DNA can then be thought of as due to three parts. One is a homogeneous distribution of electrons filling all of the space. Its diffraction will all be in the central spot. The volume occupied by parts of the DNA then is a set of holes in the gas and by Babinet's principle these will diffract in the same manner as a set of homogeneous atoms (in regions devoid of diffraction from the space filling electron gas assumed above). The atoms themselves with the ordinary distribution of electrons will then be a third diffracting system. The diffractions from the atoms and the holes in the hypothetical electron gas will be 180° out of phase and thus subtract from each other. As an approximation the electrons of the atoms can be considered homogeneously distributed in the volume from which they exclude the water. This allows the water diffraction to be accounted for by a correction applied to the scattering power of each non-water atom. A reduced scattering factor is thus assigned to each atom and these may be negative.

Since the scattering power of the water atoms as well as that of the DNA atoms varies with diffraction angle the reduced atomic scattering factor should be computed for each such angle. The validity of this method is greatest at small angles where the effect of details of the shapes of excluded volumes and the true electron distributions are least. At larger diffraction angles the method is crude but would seem to be more legitimate than ignoring the water. With helical systems one might picture the water as a smooth helix and thus devoid of diffractions on all branches except the central X. However the volume occupied by the water does not necessarily have even approximately helical boundries. Wilkins and co-workers (Feughelman, et al, 1955) (~~in press~~) have used a treatment of the type applied here but have chosen to ignore the correction in the branches diverging from the 10th. layer line because the water does not penetrate between the adjacent atoms of the DNA molecules and it is short interatomic distances that are of importance in the pattern in the region involved.

A practical problem in applying this treatment to account for the water is that of assigning volumes to the atoms. Using the physical chemists partial molar volumes for dilute solutions directly lacks rigor in two respects. First, the "solution" is not dilute but rather parts of the configuration are completely analogous to ordinary dry crystals. Other parts may behave more like concentrated solutions with respect to excluding water from space. The second difficulty stems from the fact that the physical chemist is interested only in the total volume of a molecule and not the volume of the individual atoms. As a result corrections are applied for a ring. A nitrogen atom in a ring is assigned the same volume there as in an amino group. Then the ring correction is changed for heterocylic compounds to make the total volume calculated agree with measurements. The problem of the meaning of the physical chemists "covolume" per molecule when molecules are large and "bumpy" is left for conjecture.

An attempt was therefore made to assign more rational volumes to the various atoms in DNA. The bases were considered to occupy a solid volume 3.4 A thick and of cylindrical contour determined by Van der Waals radii. At the edges the thickness was slightly adjusted for the hydrogen atom so that its volume would correspond to the hydrogen volume usually assigned (3.1 ml/mole). Figure 12 shows the areas assigned to the various atoms in the base pair guanine-cytosine for the purposes of volume calculations. The solid lines are chemical bonds, and dashed lines show the areas assigned. The partial molar volume is given in ml. for comparison with physical chemical data. In practice it was convenient to group the atoms according to their assigned volumes and molecular species and then give each atom within the group an average volume. Table 6 characterizes these groups and gives the volumes assigned, the water correction and the reduced number of electrons. These values are applicable in diffraction when the unitary atomic structure factors are unity.

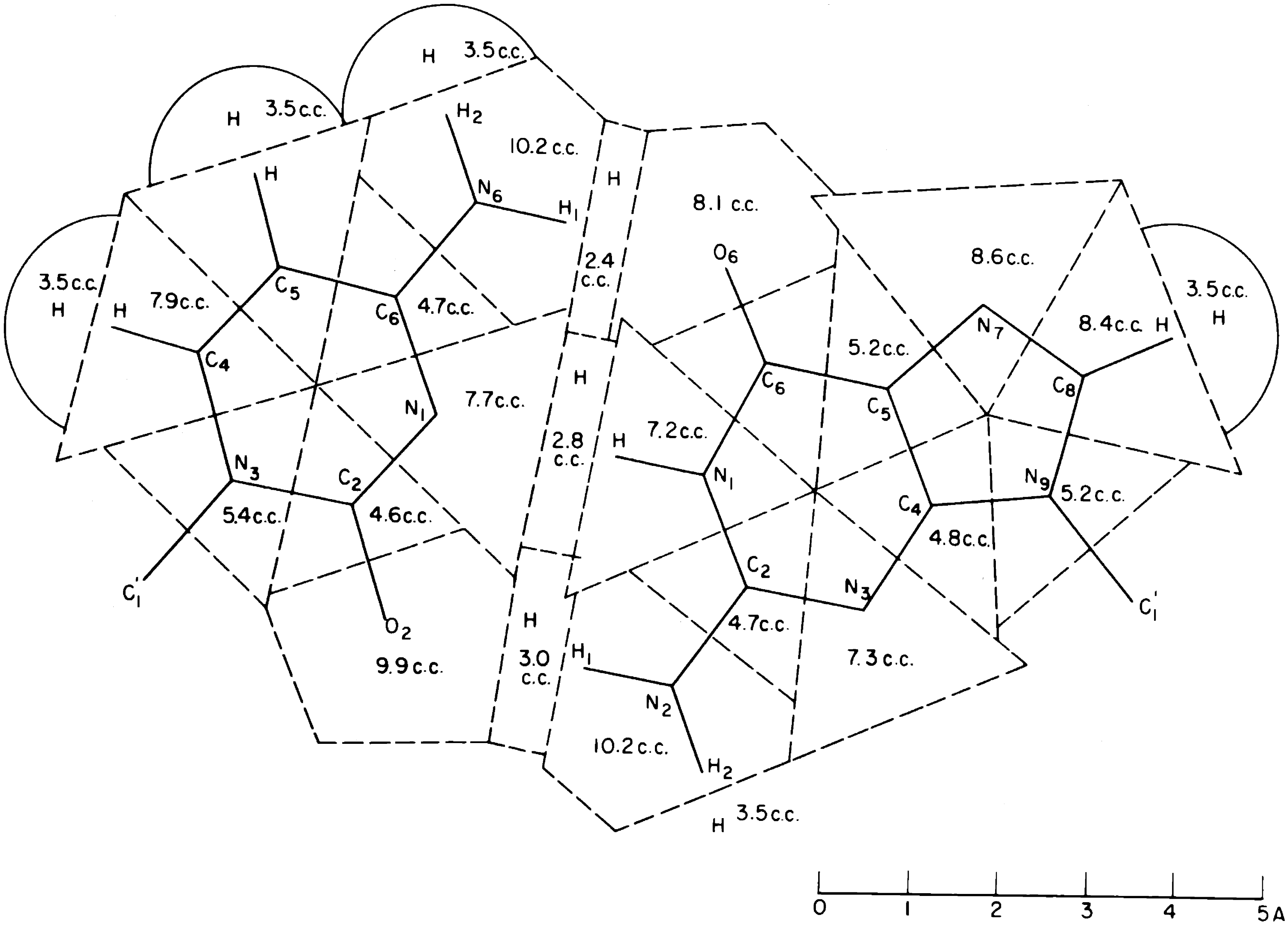
H
3.5 c.c.
H
3.5 c.c.
H$_2$
10.2 c.c.
H
N$_6$
H$_1$
3.5 c.c.
H
H
7.9 c.c.
C$_5$
C$_6$
4.7 c.c.
C$_4$
N$_1$
7.7 c.c.
N$_3$
C$_2$
5.4 c.c.
4.6 c.c.
C$_1'$
O$_2$
9.9 c.c.
H
2.4 c.c.
H
2.8 c.c.
H
3.0 c.c.
8.1 c.c.
O$_6$
8.6 c.c.
3.5 c.c.
H
5.2 c.c.
N$_7$
8.4 c.c.
H
C$_6$
C$_5$
C$_8$
H
7.2 c.c.
N$_1$
C$_4$
N$_9$
5.2 c.c.
4.8 c.c.
C$_2$
N$_3$
C$_1'$
4.7 c.c.
H$_1$
7.3 c.c.
N$_2$
10.2 c.c.
H$_2$
H
3.5 c.c.
0
1
2
3
4
5A

FIGURE 12

Table 6

			P.M.V. ml.	H_2O corr.	Red. # e^-
Bases					
H	All	———	3.1	−1.72	−.7
N	Amino	Cy − N_6, Gu − N_2	10.2	−5.66	1.3
N	In ring, no external bond or with 1 H external	Cy − N_1, Gu − N_1, N_3, N_7	7.5	−4.66	2.8
N	In ring, carbon external	Cy − N_3 Gu − N_9	5.3	−2.94	4.1
C	In resonant ring with H bound externally	Cy − C_4, C_5 Gu − C_8	7.8	−4.33	1.7
C	In resonant ring with no hydrogen attached	Cy − C_2, C_6 Gu − C_2, C_4, C_5, C_6	4.8	−2.66	3.3
O	= O	Gu − O_6, Cy − O_2	9.0	−5.0	3.0
Deoxyribose					
H	All				−.7
C	2 non hydrogen bonds	C_2', C_5'			1.7
C	3 non hydrogen bonds	C_1', C_3', C_4'			3.3
O	Ether type	O_1'	5.5	−3.06	4.9
Phosphate					
P		P	11.0	−6.1	8.9
O	All	O_3', O_5', O_I, O_{II}	5.5	−3.06	4.9
Sodium		Na^+	4.8	−2.7	8.3
Water		H_2O	18.0	−10	0

In the deoxyribose the oxygen was given the Traube (1899) volume for oxygen in ethers. The carbons were classified according to how many atoms other than hydrogen were bonded to them since it is mainly these atoms that decrease the volume assigned to the carbon. The atoms C_2' and C_5' were considered comparable to a resonant ring carbon with one H attached, and C_1', C_3', and C_4' were considered comparable to a resonant ring carbon with no hydrogen attached.

In the PO_4 group the phosphorous was considered to be about 10 per cent larger than carbon and in combination with Traube's solution volumes for carbon lead to the value for P given in the table. (This may be higher than proper in comparison with some of the other atoms, the C_5 carbon, for instance.) The ester-bond oxygen atoms were assigned volumes equal to Traube's ether-bond oxygen. The remaining two oxygens are perhaps equivalent to Traube's terminal carboxyl oxygens with average volume 2.95 ml, one at 5.5 ml. and the second at 0.4 ml. Why the second oxygen should effectively occupy such a small volume in the diester phosphate of the DNA system is not clear and both atoms were assigned the larger volume making them equivalent to the other two PO_4 oxygens.

The sodium ion was assigned a volume compatible with its small Van der Waals radius.

Electrostriction of the water around ions could be dealt with by reducing the volume of the ion. The appropriate reduction would depend on the amount of water surrounding the ion. At low angles of diffraction this would be justified but at higher angles the diffuseness of increased density of the water would tend to nullify the effect. Considering all of the approximations in the calculation electrostriction has generally been ignored but its possible significance has been estimated in some special circumstances.

As a check on the overall reasonableness of the volume assignments for the bases they were used to calculate the volume expected for guanine hydrochloride dihydrate. With $H_2O = 18.0$ ml. and $HCl = 16.3$ ml., with allowance made for the difference in bonding of the N_9 atom, and with allowance made for the additional hydrogen atom, the calculated volume was 144.0 ml. The volume of the unit cell of guanine hydrochloride dihydrate is calculated to be 142 ml. using Broomhead's (1951) data. The agreement is so close as to be fortuitous. Again, a summation of the assigned volumes for de~~s~~oxyribose and the phosphate together yields 90.2ml. In comparing the sum of Traube's (1899) physical chemical solution values with an estimate for phosphorous being larger than carbon and assuming the ring correction for a five membered ring to be 5 ml. (compared with 8.1 for hexamethylene) is 99 ml.

Calculating on the basis of the assigned volumes the number of residues per turn and the unit cell volume, in the B material (from lattice derived on pg. 76) water occupies 2.3 times the volume attributed to DNA. The calculated density is 1.29. Wilkins and co-workers (~~in press~~) (Feughelman, et al, 1955) report a density of 1.34 - 1.39 for their B material at 92 per cent relative humidity. They note that this would indicate 3 molecules instead of 2 in the basic unit and that therefore the interpretation of the density is suspect. If the density for A material is calculated using the assigned volumes and Franklin's (1953 d) unit cell dimensions a value of 1.48 is obtained. This compares favorably with Franklin's measured value of density of 1.47.

The assigned volumes would thus seem reasonable.

The molar volume of water is 18.0 ml. and there are ten electrons in the molecule. Since the scattering power at zero diffraction angle is equal to the number of electrons in the atom in correction to be applied to account for the water is ten eighteenths of the volume assigned to the atom.* The values for the volumes, correction terms, and reduced scattering power (number of electrons) for the various atoms of DNA are given in Table 7 . As stated above a different set of values should be used at each diffraction angle. Such a set was calculated for diffraction to the center of the 11th layer line as follows:

The scattering powers of the atoms of both DNA and water vary with diffraction angle. If the unitary atomic structure factors are divided by the weighted average unitary scattering factor for atoms of water relative unitary factors are obtained, valid at the chosen angle. Applying these factors to the scattering powers of the atoms at zero angle new relative scattering are obtained. The difference between these relative factors and the zero angle scattering power is then applied as an additional correction to the values corrected for water. These calculations are presented in Table 8 . The largest corrections are $-1.1\ e^-$ to be applied to carbon and $+ 1.0\ e^-$ to be applied to the

---

* The immersion fluids used in this thesis are alcoholic solutions. The average electron density in the fluid of "hydration" is therefore not known precisely. The electron density for water is 0.55 e^-/ml., for ethanol 0.44 e^-/ml. and for 70 per cent ethanol 0.49 e^-/ml.

Table 7

Guanine

	wt.*	wt.*	spot
N_1	2.8	2.1	2
H_{n1}	-0.7		
C_2		3.3	3
N_2	1.3	-0.1	0
H_{n21}	-0.7		
H_{n22}	-0.7		
N_3		2.8	2.6
C_4		3.3	3
C_5		3.3	3
C_6		3.3	3
O_6		3.0	3
N_7		2.8	2.6
C_8	1.7	1.0	1
H_{c8}	-0.7		
N_9		4.1	4
		28.9	27

Cytosine

	wt.*	wt.*	spot
N_1		2.8	2.6
C_2		3.3	3
O_2		3.0	3
N_3		4.1	4
C_4	1.7	1.0	1
H_{c4}	-0.7		
C_5	1.7	1.0	1
H_{cs}	-0.7		
C_6		3.3	3
N_6	1.3	-0.1	0
H_{n61}	-0.7		
H_{n62}	-0.7		
		18.4	17.6

Phosphate

P	8.9	8
$O_{3'}$	4.9	4
O_5	4.9	4
O_I	4.9	5
O_{II}	4.9	5
	28.5	26

Sodium

Na	8.3	8

Deoxyribose

C_i	3.3	2.6	2.4
H_{c1}	-0.7		
C_2	1.7	0.3	0
H_{c21}	-0.7		
H_{c22}	-0.7		
C_3	3.3	2.6	2.4
H_{c3}	-0.7		
C_4	3.3	2.6	2.4
H_{c4}	-0.7		
O_1		4.9	4.5
C_5	1.7	0.3	0
H_{c51}	-0.7		
H_{c52}	-0.7		
		13.3	11.7

*Weights are corrected for water. Unitary atomic structure factors are unity.

sodium ion. The other corrections are less than 1/3 electron per atom. The general effect will be to decrease the weighting of the bases and deoxyribose compared to the PO_4 group. For comparison with lower layer line intensities the effective unitary factor for water is to be applied in addition to the above. This has been done for the group weights in Table 10.

Table 8

	$\hat{f}_o$	n	f	f'_o	f'	$f'-n$
H	0.63	1	0.63	0.860	0.86	−0.14
C	0.60	6	3.60	0.818	4.91	−1.1
N	0.70	7	4.90	0.955	6.69	−0.3
O	0.76	8	6.08	1.035	8.28	+0.3
P	0.74	15	1.11	1.010	15.15	+0.15
Na	0.80	11	8.80	1.090	11.99	+1.0
H_2O	0.734	10	7.34	1.000	10.00	0

$\hat{f}_o$ – unitary atomic structure factor at 11th layer line (3.1A)

n – atomic structure factor at zero angle ($\#e^-$ in atom)

f – atomic structure factor (at 3.1A)

f'_o – f_o normalized to $H_2O = 1.000$

f' – $n f'_o$, normalized atomic structure factor

$f'-n$ – correction to be applied to the reduced weighting factors of Table 7 for relative calculations in the vicinity of the 11th layer line.

In calculations all atoms including hydrogen were treated independently. In making optical diffractograph masks negative values could not be represented properly. Fixed sized spots were used having

Table 9

	wt.*	Guanine wt.*	spot size
N_1	2.5	1.7	1
H_{N1}	-0.8		
C_2		2.2	2
N_2	1.0	-0.6	0
H_{N21}	-0.8		
H_{N22}	-0.8		
N_3		2.5	2
C_4		2.2	2
C_5		2.2	2
C_6		2.2	2
O_6		3.3	3
N_7		2.5	2
C_8	0.6	-0.2	0
H_{C8}	-0.8		
N_9		3.8	3
Total		21.8	19

	Phosphate	
P	10.	8
O_3'	5.2	4
O_5	5.2	4
O_I	5.2	4
O_{II}	5.2	4
	30.8	24

	Sodium	
Na	11.2	8 (9)

	wt.*	Cytosine wt.*	spot size
N_1		2.5	2
C_2		2.2	2
O_2		3.3	3
N_3		3.8	3
C_4	0.6	-0.2	0
H_{C4}	-0.8		
C_5	0.6	-0.2	0
H_{C5}	-0.8		
C_6		2.2	2
N_6	1.0	-0.6	0
H_{N61}	-0.8		
H_{N62}	-0.8		
Total		13.0	12

		Deoxyribose	
C_1	2.2	1.4	1
H_{C1}	-0.8		
C_2	0.6	-1.0	0
H_{C21}	-0.8		
H_{C22}	-0.8		
C_3	2.2	1.4	1
H_{C3}	-0.8		
C_4	2.2	1.4	1
H_{C4}	-0.8		
O_1		5.2	4
C_5	0.6	-1.0	0
H_{C51}	-0.8		
H_{C52}	-0.8		
Total		7.4	7

* Weights are corrected for water and also for atomic structure factors at 3.1 A.

areas from 1 to 16 in integral steps. The negative hydrogen atoms were considered as part of the carbons to which they are bonded with no correction being applied to the position of the carbon. Remaining negative values were ignored. The groupings, combined weights and spot sizes used for all of the atoms are given in Tables 7 & 9 (pg 103, 105) with water corrections applied and with both water and structure factor corrections applied respectively.

In Table 10 the diffracting power of the components of DNA are compared with each other at zero angle with and without the water correction and at the 11th layer line with the water and unitary structure factor corrections applied. The relative diffracting power of the deoxyribose is very greatly diminished, of the bases is greatly diminished, of the phosphate is greatly increased, and of the sodium is very greatly increased by the corrections.

Table 10

Scattering powers of the components of DNA

	uncorrected	corrected for water	corrected for water and f_j at 3.1 Å
Guanine	77	28.9	16.0
Cytosine	57	18.4	9.5
2 Deoxyribose	90	26.6	10.8
2 PO_4	94	57.0	45.1
2 Na	22	16.6	16.4
	340	148.5	97.8
In parts per hundred:			
Guanine	23 } 40	20 } 33	16 } 26
Cytosine	17	13	10
2 Deoxyribose	26	18	11
2 PO_4	28 } 35	38 } 49	46 } 63
2 Na	7	11	17

4. Comparison of the optical diffractograph "sections" with X-ray "rotation" patterns.

Before comparing an optical diffractograph pattern with an x-ray diffraction fiber pattern the fact must be considered that the former is from a single projection of the molecule where as the fiber pattern is a rotation pattern involving all orientations of the molecule with a fixed axis. Figure 11c as mentioned before is a pattern from a basal projection of the Watson and Crick model. It is thus an intensity plot on a $(\mathbf{R},\psi)$ section of diffraction space. The most striking feature of this pattern is its ten fold symmetry. Of almost equal note is the lack of the appearance of this ten fold symmetry in the central disk and the first ring. In the structure factor equations, the symmetry of the model is contained in the phase term in which the angle ψ is multiplied by the Bessel function order of the term being considered. The central maximum and first ring are dominated by J_o (X) functions and thus have circular symmetry $(n\psi = o)$. The outer maxima are dominated by J_{10} (X) functions and thus over a complete 360° plot of ψ the phase term will go through ten cycles. (In the compound helix case where some heavy component has a large radius compared to the average radius the 10 fold symmetry may have a pronounced effect on the first ring.)

In comparing the basal projection pattern of Figure 11c with the equatorial line of the dyad axis projection of Figure 11a it is seen that on the latter the first strong ring of spots from the former is completely absent and the next two rings are both sampled. Patterns for layer planes other than the equatorial plane can not be obtained directly with the optical diffractograph unless a precession system is used since no matter what projection of the structure is taken the section of diffraction space sampled always includes the origin. By referring to the equations for the whole diffraction space we can determine what to expect from this sort of effect on the other layer lines.

The exp~~p~~ression for the phase term B given on page 84 Eq 10 for a pair of diad related helices is

$$B_j = 2\,\overset{\cos C}{\wedge}\cos D_j + 2\,i \sin C \cos D_j$$

where $C = n\,\psi + \frac{1}{2}\,n\,\pi$

and $D_j = n\,\phi_{oj} - 2\,\pi\,\mathrm{Mm}\,z_{1j}$ (page 84-8)

or $B_j = 2 \cos D_j \left\{ \cos \left[n(\psi + \pi/2) \right] + i \sin \left[n\,(\psi + \pi/2) \right] \right\}$

In the treatment and projections considered earlier in this thesis the expression in curly brackets was $(-1)^n$. This is no longer so since ψ is not fixed at $\pi/2$. Since this term is always independent of D_j the summation for all j sets of atoms will be of the form

$$\left(\sum_j \right)_n = \left[\sum f_j\, J_n\,(x)\; 2 \cos \text{ equation on separate line } D_j \right] \{\,\}_n$$

so that the summation is a sum of real numbers. The summation for various n values can be treated as follows. On a given layer plane at any given value of X the expression for terms from various branches of the pattern (various n values) are simply expressions for vectors in the complex plane of magnitude $J_n\,(X) \cos D_{jn}$ (maintaining the sign) and phase angle $\theta_n = n\,(\psi + \pi/2)$.

Considering the two terms with smallest $|n|$ values, as ψ sweeps through 360° the vectors add to give a range of values between the sum and difference of the two vectors. Since the signs of n are always opposite for its two smallest absolute values the vectors rotate in opposite direction as ψ is changed. There will be $|n_1| + |n_2|$ peaks and valleys in the curve as ψ makes a complete cycle and $|n_1| + |n_2|$ equals M. The positions of the maxima and minima will be given by the two equations

$$\text{a.)}\ n_1 (\psi + \pi/2) = n_2 (\psi + \pi/2) + q (2\pi)$$

and $$\text{b.)}\ n_1 (\psi + \pi/2) = n_2 (\psi + \pi/2) + q (2\pi) + \pi$$

where q is any integer. Which of the two will give the positions of maxima and which the position of minima will depend on the signs of the other terms in the total expression. Solving these equations with $q = 0$ and employing the relation, $n_1 - n_2 = M$, and the fact that $M = 10$ in DNA the equation

a.) has the solution $\psi = -\pi/2$

and b.) has the solution $\psi = -4\pi/10$.

Since there is a ten fold symmetry all of the solutions can be obtained by repeatedly adding $2\pi/10$ to these specific solutions. Thus a.) has as solutions all odd tenths of $\pm \pi$ and b.) has as solutions all even tenths of $\pm \pi$. Thus two projections, one with ψ equal to an even tenth of 2π, and the other with ψ equal to an odd tenth of 2π, will contain the maximum and minimum intensities for all values of l and R at which only two Bessel function terms are significant.

The mean intensity value at any given l and R value will be of the form——

$$\int A^2 \, d\,\omega / \int d\,\omega$$

where $A^2 = (A_1 + A_2 \cos\omega)^2 + A_2^2 \sin^2\omega$

and this reduces to $A_1^2 + A_2^2$ when integrated from 0 to $q\,\pi$.

The maximum intensity value is $(A_1 + A_2)^2 = A_1^2 + 2\,A_1\,A_2 + A_2^2$

The minimum intensity value is $(A_1 - A_2)^2 = A_1^2 - 2\,A_1\,A_2 + A_2^2$

The average of the maximum and minimum values is $A_1^2 + A_2^2$ which is precisely the mean intensity value. The optical diffractograph pattern that should be compared with the x-ray pattern is thus the sum of the patterns obtained with each of two projections. If M is odd only one projection is needed since the two halves of the diffraction pattern corresponds to the two projections. If M is even the two projections can be the sine and cosine projections of the structure referred to the dyad axis as above. (Because of the symmetry involved when M is even only one half of a turn need be calculated and plotted in making the mask.)

The equatorial plane is a special case where considering two n values is not sufficient since n = 0, ± M either 1 term dominates or three are probably involved. Taking the terms with n = ± M together

$$n = +M \text{ when } m = -1, \quad n = -M \text{ when } m = +1$$

$$B_{j+M} = 2\cos D_{j+M} \left\{ \cos M\,(\psi + \pi/2) + i \sin M\,(\psi + \pi/2) \right\}$$

$$B_{j-M} = 2\cos D_{j-M} \left\{ \cos\,(-M)\,(\psi + \pi/2) + i \sin\,(-M)\,(\psi + \pi/2) \right\}$$

$$= 2\cos D_{j-M} \left\{ \cos M\,(\psi + \pi/2) - i \sin M\,(\psi + \pi/2) \right\}$$

Where $D_{j+M} = M\,\phi_{oj} - 2\,\pi\,M\,(\,-1\,)\,z_{1j}$

$$= M\,\phi_{oj} + 2\,\pi\,M\,z_{1j}$$

$$D_{j-M} = -M\,\phi_{oj} - 2\,\pi\,M\,(\,+1)\,z_{1j}$$

and therefore $\cos D_{j+M} = \cos D_{j-M}$

Before combining these functions they must be multiplied by

$$A = f_j J_n (X)$$

since $J_{-n} (X) = (-1)^n J_n (X)$

when M is even $J_{-n} (X) = J_n (X)$

and $F_{j \pm M} = 2 f_j J_M (X) 2 \cos D_{j \pm M} \cos M (\psi + \pi/2)$

When n = 0 all of the sine and cosine arguments become 0 and $F_{j,0}$ $= 2 f_j J_0 (X)$ $\therefore$ $\frac{1}{2 f_j} F_{j,0,\pm M} = J_0 (X) + 2 J_M (X) \cos D_{j \pm M} \cos M (\psi + \pi/2)$

The extremes of this function as ψ is varied will clearly be given by $M (\psi + \pi/2) = q 2 \pi$

and $M (\psi + \pi/2) = q 2 \pi + \pi$

These expressions are identical to those arrived at for the interaction of two functions of different n. The same conclusions do not hold however since in the previous case the parameter that assumed extreme values was the magnitude of a vector whose length could never be zero between the extremes. In this case the parameter is a cosine term in a real expression whose value can be zero between positive and negative extremes. Thus the intensity which is the square of F can have 2 M zero values with M extremums of one value and M extremums of a different or like value. Since a basal projection is relatively simple to prepare, this is preferred to taking extra dyad axis type projections for the sake of equatorial intensity evaluations.

Generally areas other than in the equatorial plane where terms with three values of n are significant are not particularly significant on the X-ray pattern. Such cases will be therefore ignored.

The form factor and molecular structure; the DNA B_3 pattern

1. Analytic description of the DNA B_3 pattern. A light and a dark enlarged print of the DNA B_3 pattern are presented in Plate 4 page 113. This pattern was obtained under conditions given in the "Results" section of this thesis. It is pattern 1 b (Plate 1). This DNA, B_3 x-ray pattern can be analytically described as follows:

a. The X shaped distribution of intensity on the lower layer lines is characteristic of a helix.

b. The strong meridianal "cap" of intensity on the 10th layer line is characteristic of a discontinuous helix. The precision of the layer positions 1, 2, and 10 indicates that there are an integral number of residues per turn or more than 10 turns per repeat. (see page 78) The number of residues per turn is probably 10 but 9 or 11 can not be a priori eliminated. From the layer line positions the pitch is 34 A.

c. The equator and the 2nd layer line exhibit strong lattice sampling effects. The other layer lines show no distinct lattice effects. Thus a lattice with a "quantized" type of defect exists. The lattice analysis (see page 76) shows that the projection on the plane perpendicular to the fiber axis is hexagonal with a 25.0 A separation between centers of equivalent units.

d. The lattice limitations to the radius of the helix combined with the rough angle of the central X indicate a basically single strand helix of radius 8 to 11 A.

e. There is only one strong spot on the equator and in particular the 2nd and 3rd spots allowed by the lattice are absent or at least less than 1/50 the intensity of the 1st spot. These sampling positions will be referred to as EI, EII, EIII, and the significance of the intensity

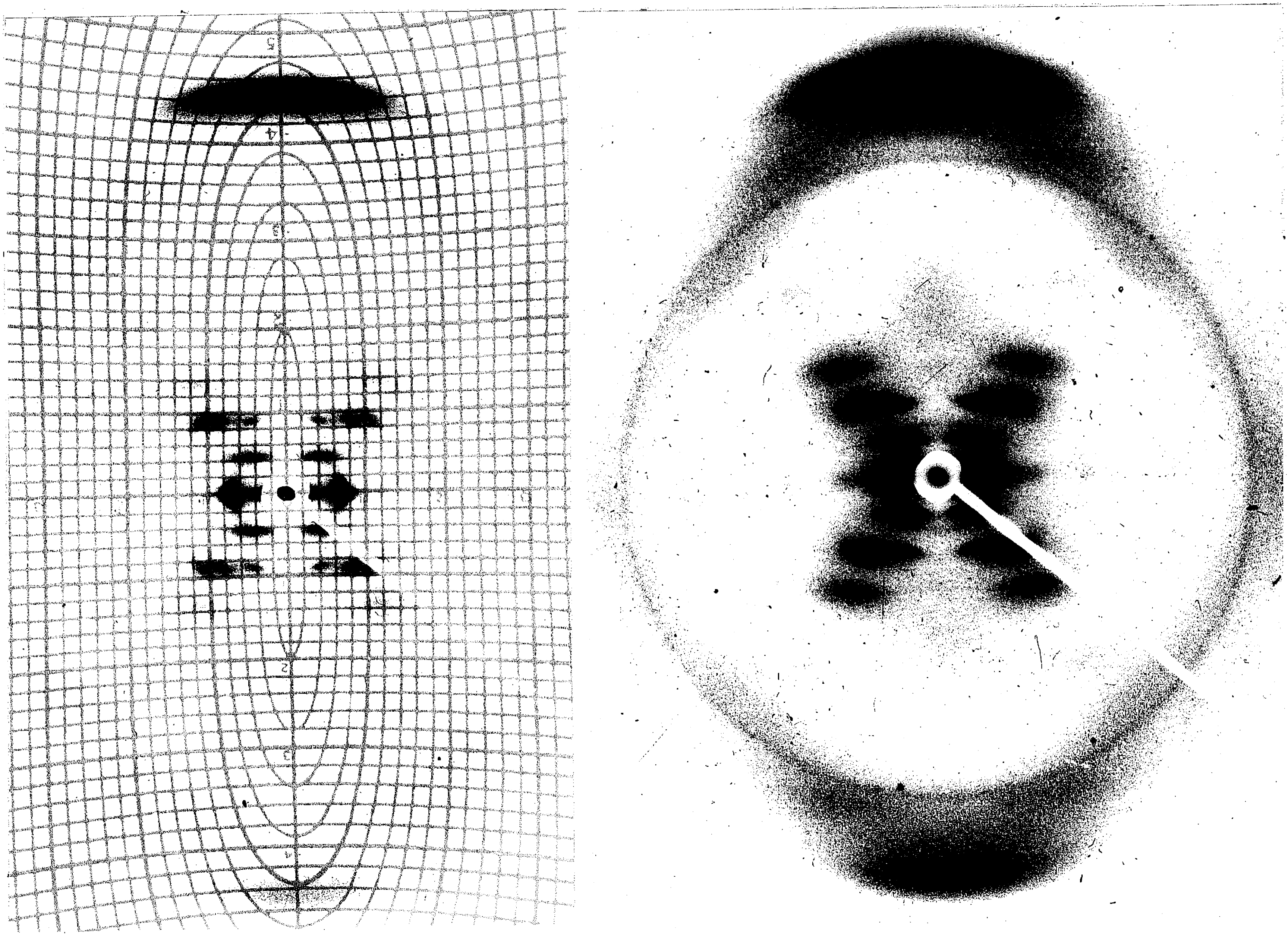

a (1b)

b (1b)

PLATE 4

ratio EI/EII will be discussed later.

f. There is no intensity observed on the 11th layer line. The significance of the ratio of intensities L 10/L 11 will be discussed later.

g. The relative intensities of the first six layer-line "inner maxima" runs; medium, strong, medium weak, very weak (absent), weak, very weak. A strong 2nd layer line would be obtained from dyad related helices with $2\phi_0 = 1/2 \times 2\pi$. The 1st-layer-line intensity would come from helices with $2\phi_0$ closer to 0. (See page 83 for discussion of form factor equations and the meaning of ϕ_0.) The absence of 4th-layer-line intensity would come from helices with $2\phi_0$ = odd 1/8 ths of 2π. Medium intensities on the 3rd and 5th layer lines would exist with $2\phi_0 \neq 1/3$ rds of 2π and $\neq 1/5$ths of 2π respectively. The absence on the "inner maximum" position on the 6th layer line is more difficult to interpret since it depends on both ϕ_0 and z_1 (the position of the discontinuity along the helix). These requirements are conflicting if a single value of ϕ_0 is sought. Since there are about 30 atoms with separate (not dyad related to any of the 29 other atoms) coordinates in NaDNA, exclusive of water, further discussion is most profitably related to complete or schematic models taking size, shape and other normal stereochemical factors into consideration.

h. The positions of intensity maxima on the various layer lines do not indicate strictly the same radius. In particular the 1st and 2nd layer lines would emphasize larger helices than the 3rd and 5 layer line intensities.

i. There is a diffuse band of intensity descending and diverging from the 10th layer line reflection.

j. In the diffuse area intensification is observed on the 8th layer line.

k. With the specimen tilted to bring the 10th layer line meridian into reflection position (see pattern 2e, page 48) no splitting of the broad 10th layer line diffraction is seen.

l. With the specimen as in k. a weak sharp band is seen near the meridian of the 9th layer line.

m. A weak blurr of diffraction is observed in the forbidden region between the branches of the X in the region starting midway between the 2nd and 3rd layers and terminating between the 5th and 6th layers. From specimens tilted 5° this intensity would appear to be meridional and near meridional.

The conclusions drawn from points a through c would appear to be quite firm and are assumed to be fact in the following discussion. Points e through h are the main observational facts on the basis of which models will be evaluated and modified. Points i through m are left for any who will to ponder.

2. Evaluation of the Watson and Crick model as the source of the DNA B_3 X-ray pattern. The Watson and Crick model of DNA was built to fit only a small portion of the data now available from diffraction patterns of DNA (see page 17). Points a and b above and the approximate radius indicated in point d were essentially all that they had to base their model on. In addition there was a good deal of information available about the structure of the constituents and a variety of accessory data from physical chemical, optical, electron optical, and chemical studies. Also there was information available as to the biological activity of DNA in a variety of cases. Many of the facts were quite remarkable and

equally as puzzling. It was their genius to bring these together with known stereochemical principles and facts and create a model which was reasonably in the light of practically all of the data and conversely led to plausible explanations of the manifold phenomena previously so difficult to interpret. Since detailed diffraction data was not available to Watson and Crick it is not surprising that their model does not fit these data as the following discussion shows.

With reference to the intensity ratio of the equatorial spots EI and EII as presented in point e above the Watson and Crick model is particularly in contradiction to the data. E II which should have no intensity falls in the middle of the first ring outside of the central disk. Spot E I falls near the edge of the central disk where the PO_4 and deoxyribose are significantly opposing the diffraction from the base pair. The calculated value of the intensity ratio EI/E II, assigning weights of one to the carbon, nitrogen and oxygen and two to the phosphorus, is 0.65. When the detailed atomic weighting factors with the water correction applied are used the ratio is reduced to 0.1. If the sodium is placed at 12.5 A radius the intensity at E I vanishes and if placed 4 A the ratio improves, becoming unity. The sodium would have to be placed at 1 or 2 A radius with an added allowance for maximal electrostriction around the sodium ion with none around the PO_4 to make E II vanish and this certainly is unreasonable.

The ratio of the intensity on the 10th and 11th layer lines is in the proper direction but no intensity is observed on the 11th layer line in the X-ray patterns. Sampling effects would tend to make the Watson and Crick pattern poorer in this respect. The water and atomic structure factor corrections will weaken the base effects compared to the PO_4 by a factor of five or six at the 10th layer line (intensity wise). As seen in Table 5 and Figure 10 the 10th and 11th layer line reflections from the Watson and Crick model both come predominantly from the bases as compared to the second layer line domination by the PO_4. Thus the water and atomic structure factor corrections will not change the L 10/L 11 ratio. They will change the L 2/L 11 ratio by a factor of ten however. Thermal effects will further weaken the 11th layer compared to the 2nd. The more diffuse character of the radiation on the higher layer lines makes it more difficult to detect. By itself, then, the observed intensity on the 11th layer line of the optical diffractograph pattern is not serious enough to rule out the model but it is not in completely satisfactory agreement with the x-ray observations.

The relative intensities on the first six layer lines is not in accord with the x-ray patterns. The 1st layer line is much too strong compared to the 2nd and 3rd. The 2nd is too weak compared to the 3rd. In the projection tested, the 6th layer is much stronger than the 5th and the x-ray pattern shows the reverse. The main point of agreement is the lack of intensity on the 4th layer line. The water corrections will change the amplitude of diffractions from the PO_4 compared to the bases in this portion of the pattern by a factor of 1.8. The ratio of the 1st to 2nd layer intensities would be improved by this but not completely corrected. The sodium could be used to supplement the PO_4 diffraction by 25 per cent.

The intensity on the 1st layer line spreads out much too far on the optical diffractograph pattern. On the second layer line one of the observed x-ray spots falls closer to the meridian than the first diffractograph streak, one falls in the center of the streak, and the third falls midway between the first and second streaks. The 3rd layer line intensity is in the proper place.

The conclusion must therefore be drawn that the Watson and Crick model is not satisfactory but it remains to be seen whether or not this type of model can be made to fit the data and if so how slight a change will suffice.

3. Evaluation of modifications of the Watson and Crick model. Two methods were used, in conjunction with each other to arrive at and evaluate the stereochemical feasibility of detailed models, namely construction and measurement of a three dimensional model system and calculation of bond angles and distances between atoms. Calculation is particularly useful in assigning limiting values to certain selected parameters on the basis of Van der Waals approaches. The three dimensional model is useful in determining detailed atomic positions and backbone configurations where many bond rotations and even bond angles are variable. It also provides a visual guide to, and check on, calculations.

In correlating the changes in diffraction pattern to be expected with changes in the model two techniques were particularly valuable in addition to the optical diffractograph study of schematic, partial atomic and full atomic models discussed previously. (see page 87.) One technique was simply to focus on the relative intensity of two spots on the equator E I and E II and to plot the structure amplitudes at each spot from each major component of the model as function of a radial coordinate. The other technique was to make a z vs ϕ plot of the model and to construct on this a simple system of phase maps for the positions of the various Bessel function maxima.

The overall picture is presented most easily through the last technique and the justification for concentrating on the equatorial intensities first comes out of this picture.

a. Phase maps in the ϕ vs z plane. If a helix is plotted in terms of z vs ϕ a straight line is obtained. This simplification is the reason for Bear's (private communication) and Cohen's (1954) extensive use of what they term the "helix net." A set of nodes on a helix becomes a net in this plot and from this it is apparent that there are many ways to connect the points in straight line (and thus helical) systems. Many ambiguities in the interpretation of x-ray patterns follow from this. In particular Bear and Cohen were concerned with the right and left handed helices with minimum pitch angles and associated these with the presence of J_1 functions.

It can readily be shown that every possible set of helices has a whole set of J functions associated with it. Furthermore the phase map used to derive the amplitude of a given Bessel function (the phase term of the structure factor equation is the major factor in determining the coefficient of the Bessel function) is a set of lines parallel to the helix associated with it. For the first Bessel function of each set the helices drawn through all of the points of the net are the zero-angle lines. For the second Bessel function additional zero-angle lines are added midway between these, etc.

Figure 13 shows one zero-angle line for the phase maps for each Bessel function as indicated. A plot of the "center of gravity" schematic representation of the Watson and Crick model is shown along with lines representing the chemical connections (and the extent of the bases). The dashed lines indicate the right handed genetic helices for the various

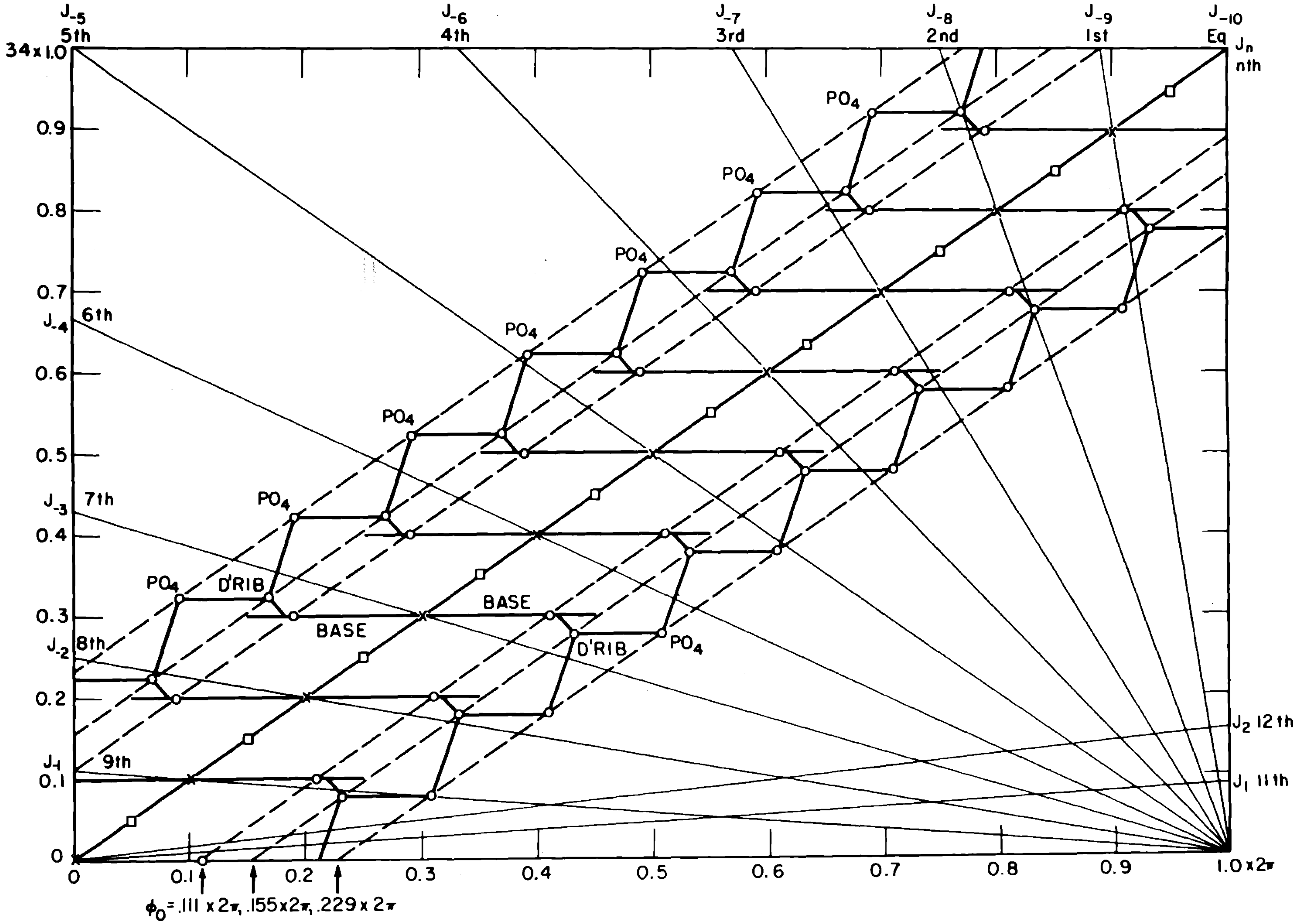
J-5
5th
J-6
4th
J-7
3rd
J-8
2nd
J-9
1st
J-10
Eq
J_n
nth
34x1.0
0.9
0.8
0.7
0.6
0.5
0.4
0.3
0.2
0.1
0
J_{-4} 6th
J_{-3} 7th
J_{-2} 8th
J_{-1} 9th
J_2 12th
J_1 11th
PO4
D'RIB
BASE
0
0.1
0.2
0.3
0.4
0.5
0.6
0.7
0.8
0.9
1.0x2π
ϕ_0=.111 x 2π, .155x2π, .229 x 2π

FIGURE 13

components. The left handed genetic helices would have ten turns per repeat and be parallel to the zero-angle line for J_{-1} on the 9th. Helices could be drawn through the points, parallel to all of the other zero-angle lines. The number of helices needed to connect all of the points is related to the J function order, n. In interpreting the position of a node relative to the zero-angle lines it is well to remember that the combined effect of a node and its dyad related node decreases to zero and continues to decrease until a negative extremum is reached as one moves away from the zero-angle line. In the Figure the X's indicate the set of dyad axis, one of which has been repeatedly referred to. There is another set of dyad axis indicated by ⊡'s that relate C_1' carbons for example to the C_1' carbons of the odd levels above. The first set relate C_1' carbons to counterparts in even levels. It can be noted that the two projections needed to arrive at an average value for diffraction from all projections, derived on page 109, are both projections along dyad axes, one from each set.

b. The effect of motions of the components of DNA on the diffraction pattern. Tilting of the bases through a negative angle will increase their inclination to the zero-phase-angle line for J_1 on the 11th layer and thus increase the spread in phase angles for this layer and accordingly increase cancelling. At the same time the inclination to the zero-angle line for J_{-1} on the 9th layer will decrease, the phase angles will be more tightly bunched, and the intensity will increase on the 9th layer line. The bases already make an appreciable angle with the zero angle line for J_1 on the 1st layer line. For this reason and because of the large spacing of the latter phase lines the 1st layer line will not be so sensitive to tilt as the higher layer lines. The intensity will decrease slightly with negative tilt.

Moving the base pair toward the helix axis will cause a spreading of the ϕ coordinates of the various atoms. This would cause weakening of the diffraction from the bases on all layer lines except the 0, 10th, 20th etc. since the bases are inclined to all other zero-phase-angle lines.

Motion of the PO_4 group in the z direction will change its diffraction in the region of the 10th layer line very rapidly while making little change near the center of the diffraction pattern. Such motion could be obtained either by tilting the bases or changing the rotation of the deoxyribose about the $C_1' - N$ bond. Without changing the configuration of the components there is not much freedom in rotation of the deoxyribose. The PO_4 position relative to the bases is such that with zero or negative tilt of the bases either the PO_4 contribution on the tenth layer line is weak or it is opposed to the base diffraction. The same applies to the deoxyribose.

The fact that the bases are already at a large angle to the dyad axis genetic helix makes the ϕ_o coordinate of the PO_4 rather insensitive to negative tilting of the bases. The value of ϕ_o is rather critical when details of the intensity distribution on the first five layer lines is considered so that slight tilting may help in fitting these data. The way that ϕ_o of the PO_4 can be most readily altered is by changing the position of the bases relative to the axis.

c. Radial parameters and the equatorial intensity problem. The intensity distribution on the equator, especially at spots E I and E II is dependent largely on the radial coordinates of the atoms. Since the ϕ_o values also seem to be most strongly effected by the position of the bases, the allowable tilt is affected by the radius, and the ratio of

E I/ E II is the most pronounced defect in the Watson and Crick model, it therefore is expedient to consider this problem in detail.

If the bases are paired in the stipulated manner and specific hydrogen bond lengths and angles are assumed, and the bases are in a plane perpendicular to the fiber axis, then three parameters serve to define their position. In the central area of the basal projection pattern one radial parameter is all that is significant. The structure factor for the bases at a sampling spot can therefore be plotted as a function of one radius alone. Such a plot for the equatorial sampling spots E I and E II is shown in Figure 14. The calculations were made with the aid of a rotating template centered at the various axial positions located on one basal plot of the bases. Similar curves for the other components are included. The deoxyribose weight was assumed to be centered in the O_1' oxygen. The phosphate oxygens were located as in the basal projection of the Watson and Crick model and the radius was measured to the phosphorus atom. The radial parameter used in the calculations for the bases was the radius to the center of the line joining the C_1' carbons. The curve was sensibly symmetrical about a value for this parameter, $y_B = 1.6$ A. The curves are plotted with a common center of symmetry and 1.6 A must be added to the coordinate of the graph to obtain y_B values. Negative y_B values indicate that the body of the base pair is on the side of the $C_1' - C_1'$ line opposite the axis. The weighting of each atom is that given in Table 7 (page 103) as corrected for water.

The Watson and Crick position of the bases, deoxyribose and PO_4 are indicated by X's on the curves and on the horizontal bar labeled W. and C. The corresponding partial and total structure factors are tabulated above and below the bar and the ratio of intensities (EI/EII) is

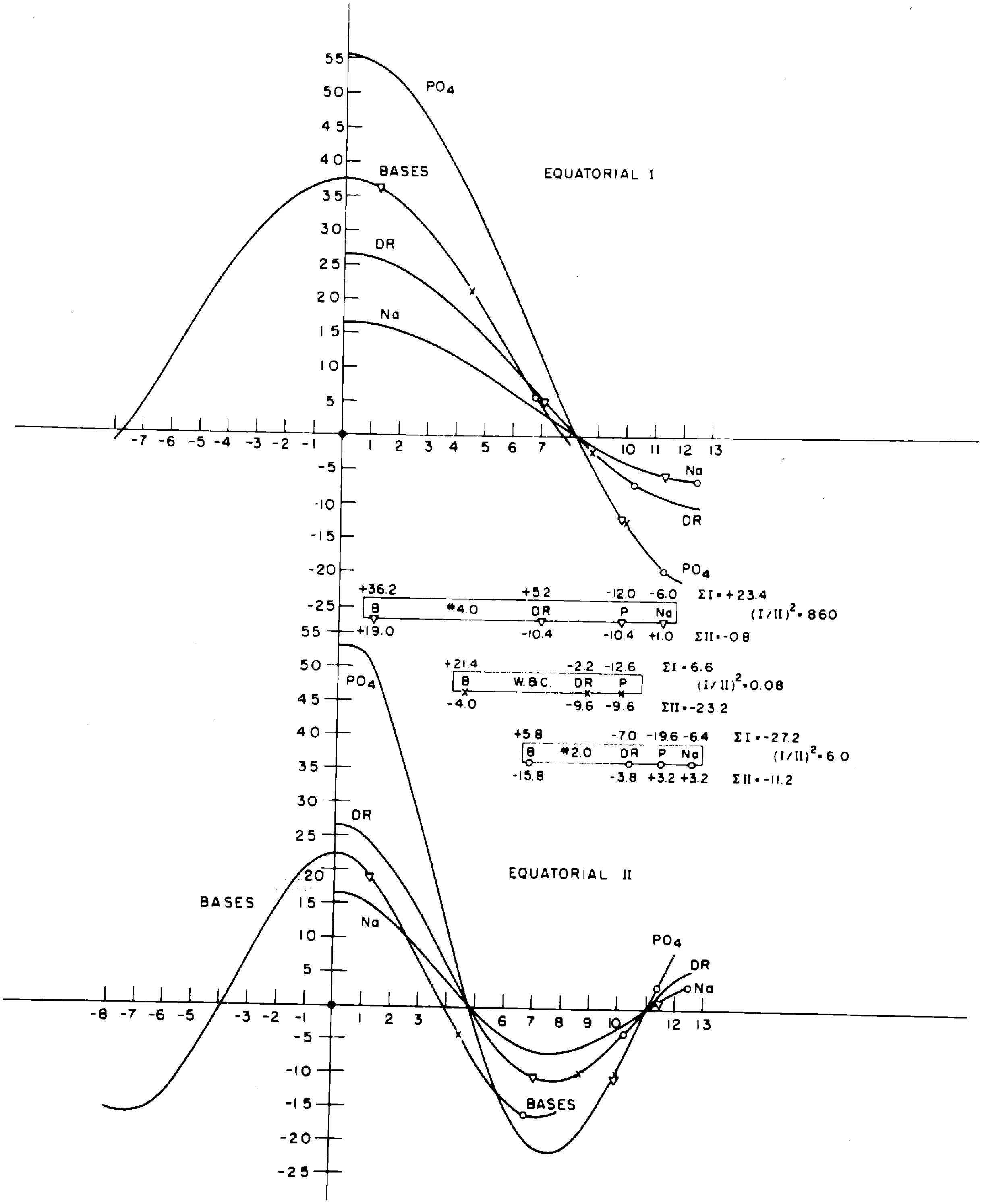
EQUATORIAL I
PO4
BASES
DR
Na
55
50
45
40
35
30
25
20
15
10
5
-5
-10
-15
-20
-25
-7 -6 -5 -4 -3 -2 -1 1 2 3 4 5 6 7 10 11 12 13
+36.2 +5.2 -12.0 -6.0
B #4.0 DR P Na
+19.0 -10.4 -10.4 +1.0
ΣI = +23.4
(I/II)² = 860
ΣII = -0.8
+21.4 -2.2 -12.6
B W.B.C. DR P
-4.0 -9.6 -9.6
ΣI = 6.6
(I/II)² = 0.08
ΣII = -23.2
+5.8 -7.0 -19.6 -6.4
B #2.0 DR P Na
-15.8 -3.8 +3.2 +3.2
ΣI = -27.2
(I/II)² = 6.0
ΣII = -11.2
EQUATORIAL II
PO4
DR
BASES
Na
-8 -7 -6 -5 -3 -2 -1 1 2 3 6 7 8 9 10 12 13
BASES

FIGURE 14

calculated. The intensity at the inner sampling point on the 2nd layer line suggests that the backbone is at a larger radius than in the Watson and Crick model. Clearly moving the components to larger radii will rapidly change the intensity of E I to zero and then to appreciable values again. At the same time the intensity at E II would change slowly because the contribution of the bases would become more strongly negative as the phosphate and ribose change in the opposite sense.

The Θ 's and bar labeled #2.0 show an extreme case of such a shift derived from a detailed model. In order to increase the radius of the phosphate the model had to be based on eleven residues per turn and even so the backbone was slightly stretched. Furthermore the size is so large that packing against the adjacent molecule would involve the oxygen atoms of one finding small cavities in the surface of the other in order for the structures to overlap slightly. The intensity ratio E I/E II including contributions from the sodium ions was increased to 6.4 by these changes in radii, a distinct improvement over the Watson and Crick model but still poor considering the X-ray pattern. With eleven residues per turn there is a J_0 on the 11th layer line (where there is no reflection on the X-ray pattern) and a J_1 on the 10th. Because of arcing of the pattern on the one hand and off meridional sampling on the other it can not be said with certainty that the intensity on the 10th layer line is associated with a J_0 and therefore this model can not be eliminated for that reason. (A J_2 function can probably be excluded.) In model # 2.0 the bases were tilted 5° in order to accommodate eleven pairs per turn, maintaining inter plane spacings of 3.4 A. This desirably weakens the base diffraction to the 11th layer line as mentioned previously. The phosphate opposes the bases on the 11th layer line and the sodium was positioned to best advantage so that the cancellation was complete at the center of the eleventh layer. The PO_4 and sodium are at such different radii from the bases that they cannot effectively counteract the bases at all R values. In particular intensity remains at the inner sampling areas predicted from the imperfect lattice. In spite of this the 10th layer line diffraction was calculated to be appreciably stronger than the 11th by approximate calculations. When an optical diffractograph pattern of this model was taken it became immediately obvious that no further effort should be expended on it. The pattern is shown in Figure. 15

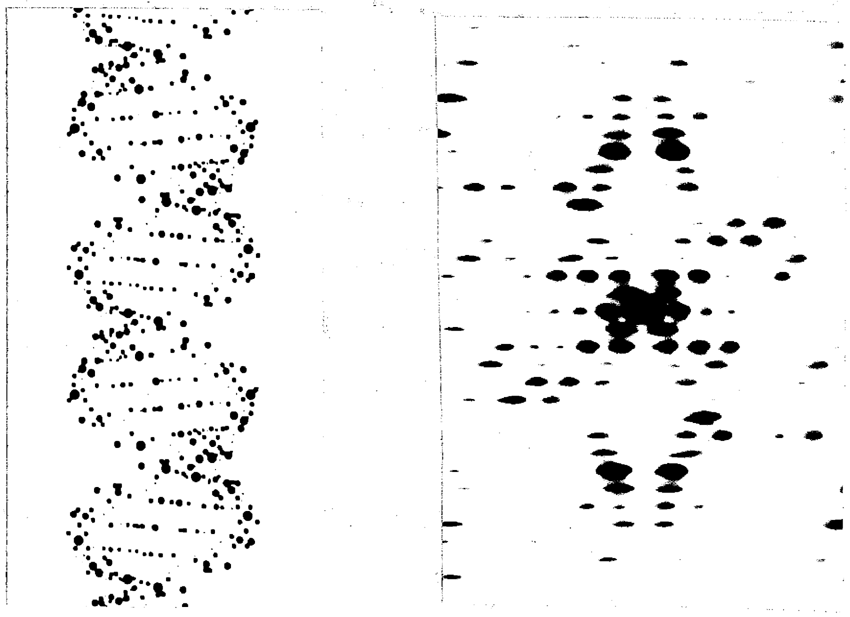

Figure 15

The ninth layer line is considerably stronger than the 10th and the pattern in general is more reminiscent of the A X-ray pattern than the B pattern.

The next alternative is to make the radius smaller. The intensity at E I will clearly increase rapidly if this is done. The intensity at E II might slightly increase and then decrease, eventually to zero. Actually the base coordinate decreases more rapidly than the phosphate radius since the former moves along a radius and the latter moves more or less tangential to a large circle. A model was set up with $y_B = 3.0$ and the PO_4 radius was then 8.1 A with a very close packed structure. In fact there was no room for the hydrogen attached to C_3' of the deoxyribose. The ratio of intensity E I/E II was 10 without the sodium, increasing to 13 with the sodium at 12.5 A radius. If there were a large amount of electrostriction of the water around the sodium ion and very little around the PO_4 ion the ratio could be doubled. If y_B is increased to 4.0 there is a possibility of finding a structure that is not prohibitively crowded (as with $y_B = 3.0$) but the intensity ratio E I/E II drops to 3 with or without the sodium contribution when this is done. The optical diffractograph pattern of the model with $y_B = 3.0$ did have interesting features, in particular a very broad intense band on the 10th layer line with practically no intensity on the 11th. The breadth of the band was comparable to that observed on the x-ray patterns. As mentioned above the diffraction from the bases would concentrate on the 10th layer line decreasing on the 1st, 9th, and 11th as they were moved toward the axis. This result should have been anticipated but attention had been focused on the equatorial problem and the diffractograph served to point up this salient feature.

d. Calculation of certain stearic limitations to modification of the model. All of the structures mentioned so far have been built with the components in the configuration similar to that found by Furberg for cytidine, in crystalline form, except for freedom to rotate about the C_1' – N bond. Cytidine contains ribose rather than deoxyribose. Considering this and the fact that the furanose ring contains only single bonds it may be that some other configuration exists in the polymer of the phosphate with its peculiar stresses and strains.

Before attempting to build models with hypothetical configurations of the furanose ring it would be good to have a more firm basis for rejecting the known configuration than the statements given above. The weakness of the position is that although in the models build Van der Waals approaches were prohibitively close when the X-ray data was within sight of being fitted there always remains the possibility that the right model was not tried. By setting the problem up mathematically in the form of deriving firm exclusions for ranges of values of selected parameters the position can be solidified.

It is assumed that the bases are paired with a fixed configuration and that they are in planes perpendicular to the helix axis at 3.4 A intervals. The $N - C_1'$ bonds and the backbone chains are dyad related one turn helical structures with pitch 34 A. The cytosine and deoxyribose configurations are taken to be precisely those given by Furberg (1950) with freedom of rotation about $C_1' - N$ added and the $(OH)_2$ replaced by hydrogen to convert from ribose to deoxyribose. Hydrogen atoms in the deoxyribose were located by assuming their bond angles with the non H bonds to be 109.5°. In the bases they were placed in the plane of the bases and with equal angles to the two adjacent bonds. The bases were paired with the $O - - H - N$ bonds 2.80 A and the $N - - H - N$ bonds 3.05 A. The $C_1' - C_1'$ distance was 11.1 A and the $C_1' - N$ bond was at 41° to the dyad axis (based on the cytosine—quanine pair).

With these assumptions all of the Van der Waals conflicts except those involving O_5', P, O_I, O_{II}, H_{C51} and H_{C52} can be expressed as a function of two variables, the radial position of the bases, y_B, and the rotation angle about $C_1' - N$, ϵ. By considering the appropriate atoms pairwise, boundaries can be derived in the ϵ vs y_B plane inside of which sufficiently severe Van der Waals conflicts exist so as to preclude further consideration. Allowance can be made for reasonable minor distortions by taking Van der Waals radii 0.2 A smaller than normal* and by considering the number and type of conflicts in questionable areas.

The easiest exclusions to calculate are those involving conflicts between the deoxyribose and the base to which it is bonded since they are independent of the radius. Next, selected conflicts with the base below can be considered using the three dimensional model as a guide.

Another type of limitation which is very useful but slightly more involved to calculate is that derived from the maximum possible distance between O_3' and C_5' as determined by the extension of the $- P - O_5' -$ bridge. The requirement that the $C_3 - O_3 - P$ and $C_5 - O_5 - P$ bond angles must be reasonable is ignored at this point. This calculation yields a closed curve in the ϵ vs y_B plane outside of which structures can not be built. There will be two such curves corresponding to connecting the O_3' from below to the C_5' from above and vice versa.

All calculations were based on right handed helices. Model building seemed to readily preclude left handed arrangements but a set of calculations would be reassuring.

Figure 16 presents a group of curves showing certain conflicts and exclusions that limit variations in y_B and ϵ in models of the Watson and Crick type. The structure must fall inside the curve labeled

---

* Normal Van der Waals radii were obtained from Pauling (1948) pg 189. – H=1.2 A, O= 1.4 A, N= 1.5 A, C= 1.8 A.

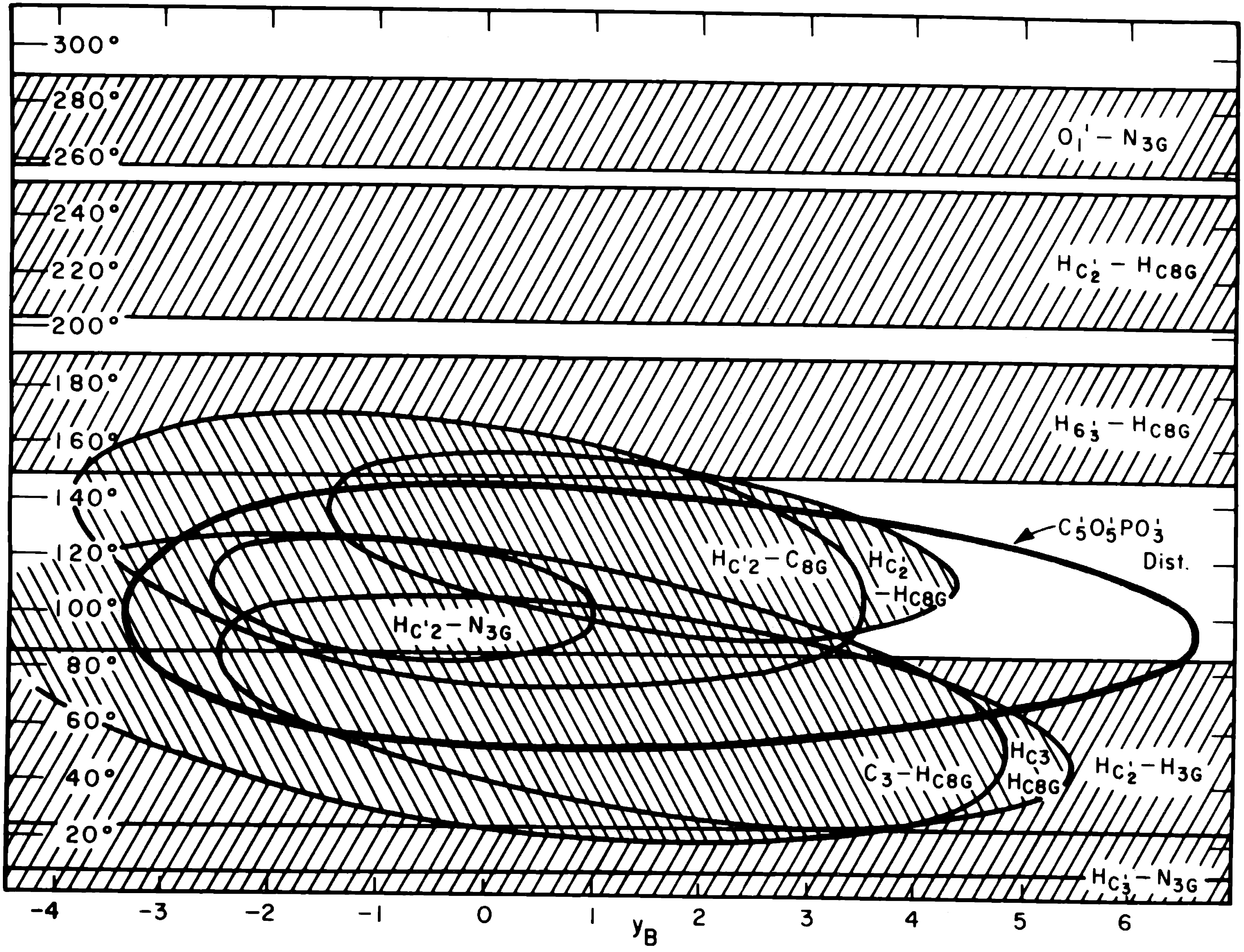
300°
280°
260°
240°
220°
200°
180°
160°
140°
120°
100°
80°
60°
40°
20°
$O_1' - N_{3G}$
$H_{C_2'} - H_{C8G}$
$H_{6_3'} - H_{C8G}$
$C_5'O_5'PO_3'$ Dist.
$H_{C'2} - C_{8G}$
$H_{C_2'} - H_{C8G}$
$H_{C'2} - N_{3G}$
$C_3 - H_{C8G}$
$H_{C3} - H_{C8G}$
$H_{C_2'} - H_{3G}$
$H_{C_3'} - N_{3G}$
-4
-3
-2
-1
0
1
2
3
4
5
6
y_B

FIGURE 16

"$C_5'O_5'PO_3'$ distance" and outside of the shaded areas. From these considerations alone it can be seen that y_B cannot be larger than 6.65 A nor smaller than 3.35 A. At the lower limit the distance from the center of H_{C2}' of the one deoxyribose would be 2.6 A from the center of the C_8 atom of quanine in the residue below. Also the C_3' carbon would be 2.6 A from the H_{C8} of the quanine below. There is no guarantee that at the stipulated value of ϵ the backbone could be connected with proper bond angles and with no serious Van der Waals conflicts but the angle is near that used in model # 3.0 referred to above.

Since the equatorial intensities in model # 3.0 were still in substantial conflict with the observed X-ray intensities and since y_B was 3.0 compared with the minimum discussed above of 3.35 it can be concluded that the Watson and Crick model can not be shifted to fit the data without appreciable distortion of some component or bond angle.

e. Configuration of the pentose; configuration of non-resonant-ring structures with five members. The configuration of the furanose ring is perhaps the least reliable of the major assumptions used above and therefore possible distortion of deoxyribose from this configuration must be considered. The following data may be used as a guide in this endeavor.

The structure of a number of compounds containing five membered single bonded rings has been determined crystallographically. In each case the ring has been non planar and by striking the proper plane it can be said that four atoms are close to planar and the fifth is nearly 0.5 A out of the plane. Also the generalization can be made that the average of the internal bond angles is less than 109°, being more nearly 105°. For a plane configuration the average internal angle would be 108° and whether the puckering is the result of the bond angles seeking to become smaller or of stearic and strain considerations within or external to the ring is problematical.

In Furberg's (1950) structure for cytidine the C'_3 carbon is 0.5 A out of the plane of $C'_4O'_1C'_1C'_2$ on the same side as N_3. The average internal bond angle in the five membered ring is 105°.

In Beevers and Cochran's (1947) structure for sucrose a furanose ring also occurs. C'_4 is about 0.5 A out of the plane of $C'_5O'_2C'_2C'_3$ on the side of O_1 of the glucose residue and the average internal angle is 104°.

In the structure for 2' : 3' iso propylidene 3 : 5' cycloadenoside iodide determined by Zussman (1953) the furanose ring is puckered with $O'_1C'_1C'_2C'_5$ in a plane and C'_4 is about 0.5 A away from this plane. The average internal angle is 105°.

"Cis naphodionane," which is bi 1,5 dioxaclyco pentyl (2), contains two identical 5 membered rings, each containing two oxygen atoms and three carbons. The C_4 carbon is between the oxygens and bonded to the C'_4 carbon of the second ring. It lies "about 0.6 A out of the plane of the other 4 atoms" according to Furberg and Hassel (1950). The average internal angle is 106°.

Proline contains a 5 membered ring which is puckered.

In penicillin there is a five membered ring containing one sulfur and one nitrogen atom and no double bonds. In the figure given by Crowfoot, Dunn, Rogers-Low, and Turner-Jones (1949) the C_5 carbon appears to be considerably out of the rough plane of $C_6S_9C_{10}N_{11}$. The average internal angle given for the sodium salt is 106° and for the potassium salt 108°.

4. A molecular model for DNA with a modified deoxyribose configuration.

a. Modification of the furanose ring. For the reasons given above a hypothetical deoxyribose residue was constructed with a puckered configuration and an average internal bond angle of less than 108°. The C_3 carbon and the hydrogen attached were a source of trouble when trying to make the DNA model diameter small. The C_3 atom was therefore placed on the side of the plane of the other four from opposite its position in the ribose of cytidine. The configuration was constructed as follows: All bond lengths were standard as given by Pauling; C – C = 1.54, C – O = 1.43 C – H = 1.07. All bond angles between external and internal bonds were 109.5°. The five membered ring was given an internal dyad symmetry with C_2', C_3' and O_1' in a plane and with the dyad axis bisecting $C_2'C_3'$ and passing through O_1'.

If angles $C_1' - C_2' - C_3'$ and $C_2' - C_3' - C_4'$ are made 105° and C_1' and C_4' are in the plane then the C_1' C_4' distance is such that the remaining angles are all 109.5°. If the angles at C_2' and C_3' are decreased to 102° the angle at O_1' reduces to 102° and the remaining two increase to 117°, maintaining the average at 108°. By rotating C_1' and C_4' in opposite direction about the $C_2'C_3'$ axis the C_1' C_4' distance is increased and the angle at O_1' is opened up. The average angle also decreases and the angles at C_1' and C_4' are rapidly decreased. With C_1' and C_4' 0.32 A from the plane the angle at O_1' is 105° and at C_3' and C_4' the angles are 111°. This is the configuration adopted as a trial structure. With C_1' displaced in the same direction as the nitrogen attached to it a puckered configuration very similar to that found in cytidine is formed. The opposite displacement therefore gives the desired trial configuration. When a plane is placed through C_1' C_3' and C_4' it is found that O_1' is only 0.13 A from this plane and C_2'

is 0.45 A removed. If instead the reference plane were located through C_1' C_2' and C_4' then C_3' would be 0.45 A from the plane and O_1' would still be 0.13 A from the plane. (C_3' would be on the opposite side of the plane from the base attached to C_1'.) Thus in the trial configuration it can either be said that C_2' is 0.45 A from the approximate plane of the other four atoms or that C_3' has this distinction.

b. Model building with hypothetical deoxyribose. With this configuration for deoxyribose the DNA model building is considerably modified because the $C_3' - O_3'$ bond direction and position is quite different from before. This seems to be more significant than the removal of Van der Waals conflicts between C_3' and the bases. As illustrated above two different atoms can be made to deviate from the rough plane of the other four with a single configuration and thus there are five rather than ten markedly different configurations of the five membered ring. There are of course many more than ten detailed configurations that can be hypothesized. For each configuration of the deoxyribose there are four types of DNA model to be considered, right and left handed helices with two directions for the backbone linkage in each case.

With the hypothetical deoxyribose discussed above calculations were carried out to determine some of the limitations to y_B* and ϵ* for right handed helices as was done with the previous configuration. Only two types of constraint were considered. Those arising from Van der Waals conflicts between the deoxyribose and the base to which it

* y_B is a radial parameter for the base pair

ϵ is an angular coordinate for rotation around the $C_1' - N$ bond is bound, and the limitations imposed on the position of the bases and the deoxyribose by the necessity of chemically connecting the O_3' of one residue to the C_5' of the next through a – P – O_5' – linkage. In Figure 17 the shaded areas are excluded by the former and the area outside the closed curves is excluded by the latter. In comparing this figure with Figure 16 (the scales differ by a factor of two) it can be seen that in the lower curve the angular range not excluded by the O_3'–C_5' distance is different for the old and new deoxyribose configurations. Furthermore the range of y_B values not excluded is much greater than previously. Some consideration was given to models in the area of the upper curve with the backbone running in the opposite sense to that of the Watson and Crick model but the lower area looked more promising.

A model was set up with the backbone running in the Watson and Crick direction. The new deoxyribose configuration allows a greater spread between the radial parameter of the bases and the PO_4 group and makes the situation with regard to equatorial intensity on the X-ray pattern quite different than it was before. In the discussion of the Watson and Crick model it was pointed out that the intensity at the second spot, E II, was much too high. When the radius was either increased or decreased the change in contribution of the bases to this spot was always initially in apposition to the change in the phosphate contributions. As a result the radius could not be decreased enough to make the model conform with the data. Now the bases can be moved inward considerably without moving the phosphate and the problem vanishes. Moving the bases inward also improves the relative intensity on the 10th and 11th layer lines and weakens the 1st as is

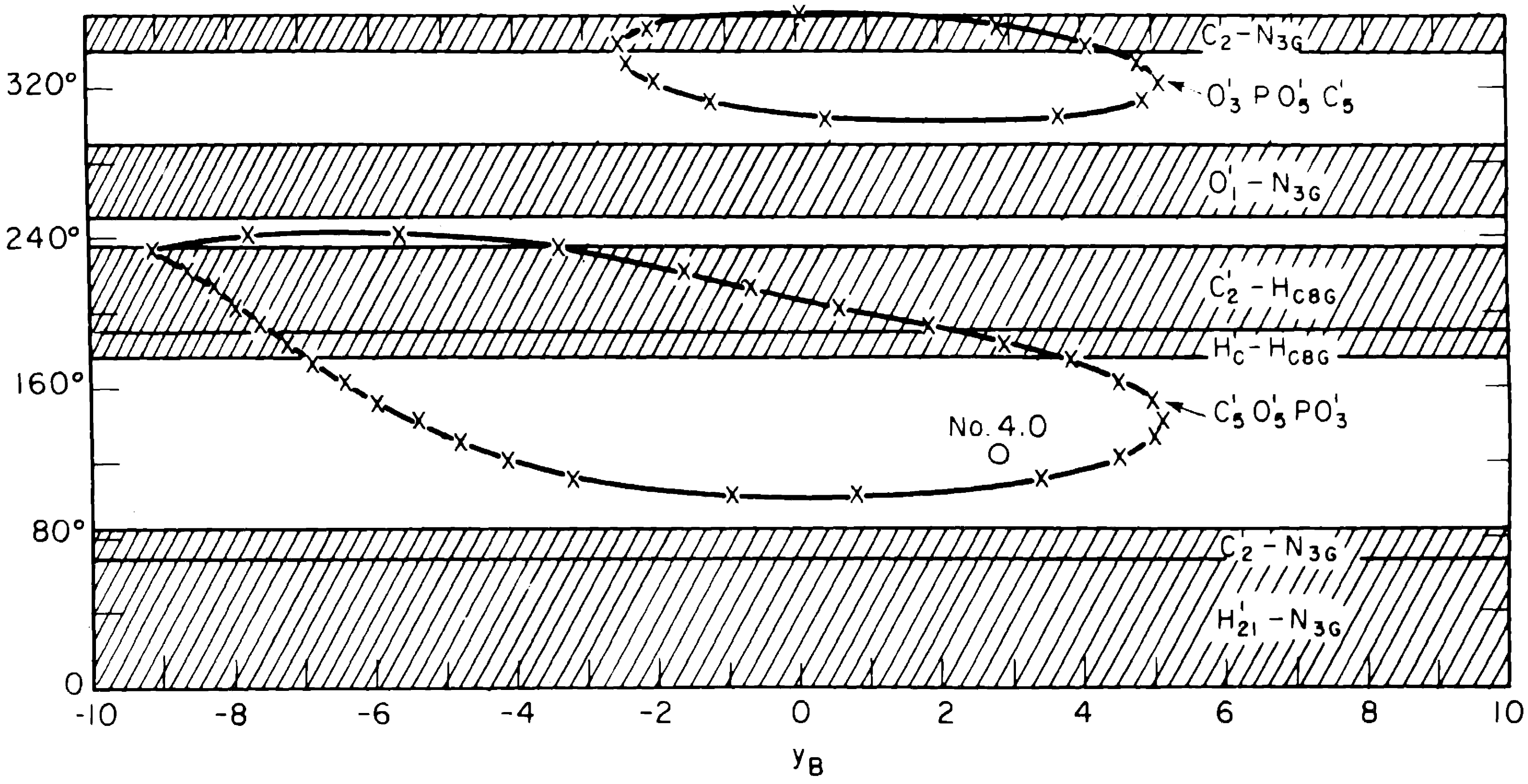
$C'_2 - N_{3G}$
$O'_3 P O'_5 C'_5$
$O'_1 - N_{3G}$
$C'_2 - H_{C8G}$
$H'_C - H_{C8G}$
$C'_5 O'_5 P O'_3$
No. 4.0
$C'_2 - N_{3G}$
$H'_{21} - N_{3G}$
320°
240°
160°
80°
0
-10
-8
-6
-4
-2
0
2
4
6
8
10
y_B

FIGURE 17

desired. There is intensity well in on the 2nd layer line of the X-ray pattern and the 1st layer line intensity is also close to the meridian so that it is desirable to have the backbone at a large radius for these reasons.

Thus the new configuration of the deoxyribose allows and the X-ray evidence suggests a model with the bases close to the axis and the PO_4 group as far from the axis as possible.

The analysis of the X-ray intensities on layer lines 1 through 5 led to the conclusion that for a single dyad related pair of helices the best fit would be obtained with $\phi o = 0.205 \times 2\pi$ (see Figure 9b for the pattern from such an arrangement with $\phi o = 0.23 \times 2\pi$). This was kept in mind when considering where the phosphate groups should be.

A model was thus considered with y_B equal to 2.0. For stearic reasons y_B was then increased to 2.8. The angular rotation of the deoxyribose about the $C_1' - N$ bond was considered in the regions allowed by the curve of Figure 17. The O_3 to C_5 distance was calculated for several promising rotations and the dihedral angle of O_3'–P–O_5'–C_5' was estimated graphically. Working between the three dimensional model and semigraphical calculations of Van der Waals approaches, bond distances, and bond angles a fixed rotation about $C_1' - N$ was chosen and the position of atoms in the backbone refined with some adjustment of bond angles permitted in the flexible link. No adjustments were made in the other components.

C. Model # 4.0

The model arrived at, # 4.0, has serious Van der Waals conflicts (C – C distance of 2.94A) in the region between the C_2' carbon of one residue and the C_8 of the guanine below (C_4 of cytosine). One singly bonded oxygen in the backbone is too close to a carbon atom ($C_3' - O_I$ distance 2.58A) but this does not appear to be serious. Other more minor difficulties exist.

Considering the improvement in the diffraction pattern obtained with this model (see discussion on page 142) and the number of adjustments that can be made along with the number of possible configurations that must be investigated, the Van der Waals difficulties encountered can not be considered to negate the value of further analysis. Rather it would appear that the model in its present state is worthy of presentation as a stepping stone toward a more satisfactory solution. Certainly it is indicated that no more drastic changes than those discussed above warrant consideration before extensive work has been done within the present framework.

Figure 18 is a basal projection of two layers of the structure with the lower in fine lines. Van der Waals radii are drawn at the inner edge of the upper base pair and at the outer edge of the backbone. Elevations referred to the lower base pair are indicated. For reference, circles are drawn through the innermost atom, the terminals of the C_1' – N bond, the phosphorous atom, and at 12.5 A which is the half separation between adjacent molecules. The general appearance of the structure is also seen in the pictures of the masks used for the optical diffractograph study presented in Figures 19 and 20. Coordinates of all the atoms are given in Table 11. Bond lengths and angles in the backbone, derived from the coordinates, are given in Table 12. Some interatomic distances are also given in this Table. The radial positions of the components are indicated in Figure 14 (page 124) where a comparison with the Watson and Crick model and Model # 2.0 can readily be made.

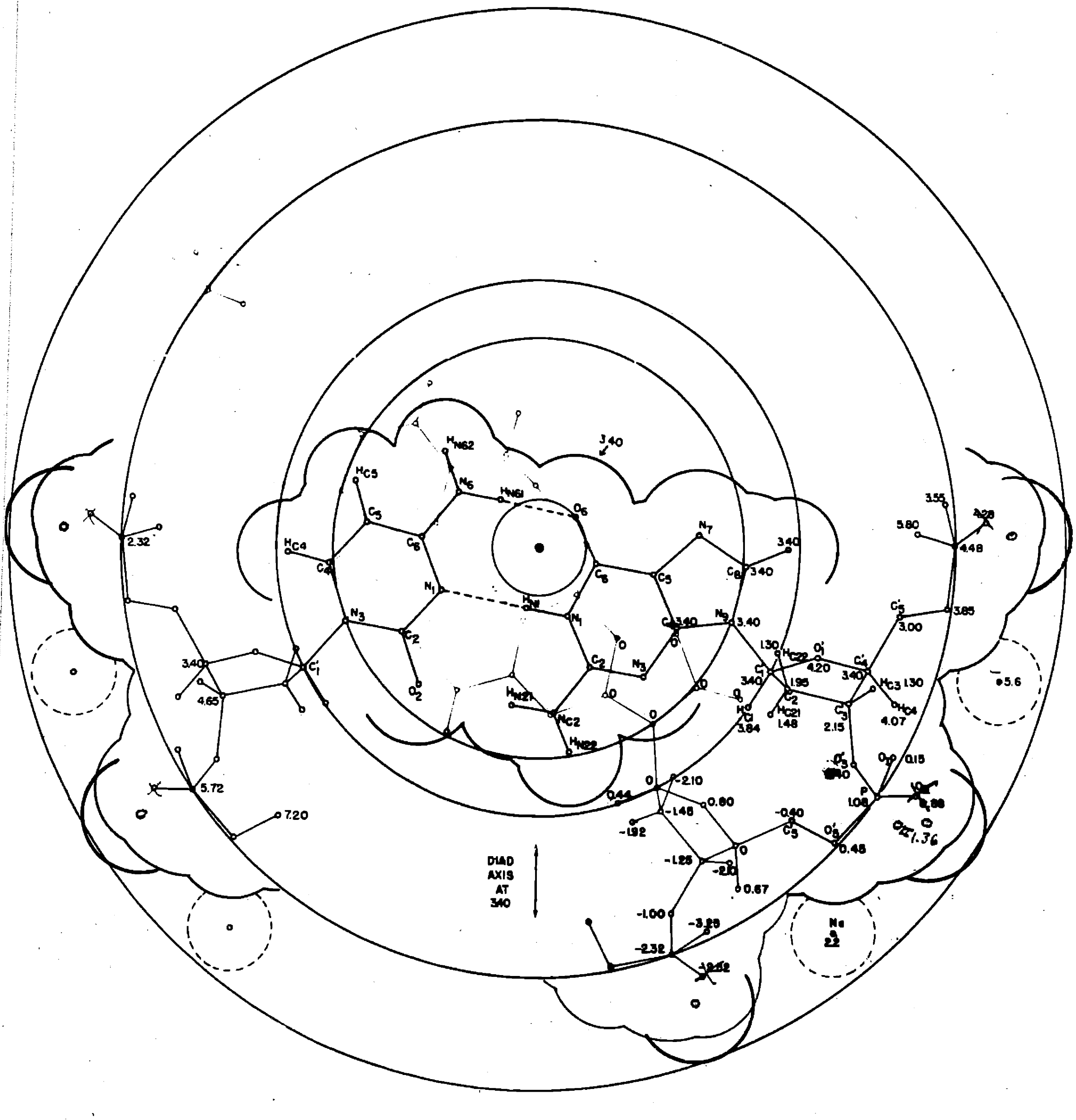
3.40
H_{N62}
H_{C5}
N_6
H_{N61}
O_6
C_5
C_6
N_7
H_{C4}
C_4
N_1
H_{N1}
C_8
C_5
N_3
C_2
N_9
C_1'
O_2
H_{N21}
N_{C2}
H_{N22}
C_2
N_3
2.32
3.40
4.65
5.72
7.20
3.55
5.80
4.28
4.48
C_5'
3.00
3.85
1.30
H_{C22}
O_1'
4.20
C_4'
3.40
C_1'
1.95
C_2'
H_{C21}
1.48
H_{C1}
3.84
C_3'
2.15
H_{C3}
1.30
H_{C4}
4.07
O_3'
O_{II}
0.15
P
1.08
O_I
O_{I} 1.36
O_5'
0.48
C_5
-0.40
0.44
-2.10
-1.48
0.80
-1.92
-1.25
-2.10
0.67
-1.00
-3.28
-2.32
5.6
Na
22
DIAD
AXIS
AT
3.40

Figure 18

Table 11

	X	−Y	Z
		Guanine	
N_1	0.68	1.56	0
H_{N1}	−0.28	1.40	0
C_2	1.22	2.76	0
N_2	0.38	3.82	0
H_{N21}	−0.60	3.66	0
H_{N22}	0.76	4.72	0
N_3	2.50	2.96	0
C_4	3.28	1.80	0
C_5	2.74	0.58	0
C_6	1.44	0.36	0
O_6	0.86	−0.74	0
N_7	3.80	−0.34	0
C_8	4.94	0.38	0
H_{C8}	5.96	−0.02	0
N_9	4.60	1.68	0
		Phosphate	
P	9.90	−0.18	1.08
$O_{3'}$	9.00	−0.44	2.40
$O_{5'}$	9.74	1.28	0.45
O_I	9.57	−1.15	0.07
O_{II}	11.28	−0.42	1.36
		Sodium	
Na	11.00	2.96	2.20

	X	−Y	Z
		Cytosine	
N_1	−2.32	0.98	0
C_2	−3.24	1.96	0
O_2	−2.82	3.20	0
N_3	−4.58	1.72	0
C_4	−4.98	0.36	0
H_{C4}	−5.94	0.10	0
C_5	−4.10	−0.58	0
H_{C5}	−4.36	−1.54	0
C_6	−2.80	−0.24	0
N_6	−1.92	−1.28	0
H_{N61}	−0.92	−1.10	0
H_{N62}	−2.24	−2.22	0
		Deoxyribose	
C_1	5.54	2.80	0
H_{C1}	5.02	3.64	0.44
C_2	5.96	3.20	−1.45
H_{C21}	5.56	3.80	−1.92
H_{C22}	5.72	2.38	−2.10
C_3	7.44	3.54	−1.25
H_{C3}	7.98	3.18	−2.10
C_4	7.88	2.76	0
H_{C4}	8.50	3.54	0.67
O_1	6.68	2.48	0.80
C_5	8.60	1.50	−0.40
H_{C51}	—	—	—
H_{C52}	—	—	—

The PO_4 group is at the same radius as in the Watson and Crick model, being at 9.9 A. The O_1' atom of deoxyribose is at 7.6 A. The center of the line joining C_1' carbons of a pair of residues is 2.8 A from the axis ($y_B = 2.8$). The line joining the PO_4 groups attached to the C_5' carbons of a given pair of residues comes within 0.6 A of the axis and is tilted so that one phosphorous atom is 1.08 A above the plane of the bases involved. ($z_{1P} = 0.0318$). The helices on which the PO_4 is located are 0.442 of a turn apart in the axial direction ($\phi o = 0.221 \times 2\pi$). With the PO_4's being practically straight above each other their separation along a line parallel to the axis is alternately 15 A and 19 A.

The deoxyribose is rotated about the $C_1' - N$ bond so that C_4' lies in the plane of the bases and at a greater angle from the dyad axis than C_1'. The plane of $C_1'\ C_3'\ C_4'$ is inclined at 60° to the plane of the bases.

All of the atoms of the base pair with the exception of two hydrogen atoms have their centers within 5 A of the axis. There would appear to be room for about one water molecule per base pair within this same radius.

Table 12

$C_4'C_5'$	– 1.51	$C_4'-C_5'-O_5'$	– 110°	$C_2'-C_{8G}$	– 2.93
$C_5'O_5'$	– 1.44	$C_5'-O_5'-P$	– 117°	$C_2'-C_{4C}$	– 2.90
$O_5'P$	– 1.60	$O_5'-P-O_3'$	– 114°	$C_3'-O_I$	– 2.57
PO_3'	– 1.62	$P-O_3'-C_3'$	– 109°	$C_2'-C_5'$	– 3.87
$O_3'C_3'$	– 1.42	$O_3'-P-O_I$	– 110°	$Na-O_{II}$	– 3.49
PO_I	– 1.44	$O_5'-P-O_I$	– 108°	$Na-O_3'$	– 3.95
PO_{II}	– 1.43	$O_3'-P-O_{II}$	– 110°	$Na-O_5'$	– 2.73
		$O_5'-P-O_{II}$	– 109°	$Na-O_{II}$*	– 5.62
				$Na-O_3'$*	– 5.10

C. Model #4.0 and the DNA B_3 pattern.

A variety of optical diffractograph patterns of Model #4.0 and its components are presented in Figure 19 and 20 (pg. 143 and 144). Enlargements of one or two unit cells of the masks from which these patterns were obtained are included.

The patterns 19a and 19b are from two projections of the model perpendicular to the axis, one along a dyad axis and the other perpendicular to it. As discussed on pg. 109 the mean intensity value on a given layer line at a given radius for all projections is the average of the intensity from these two projections. This average is therefore to be compared with the X-ray patterns on pg. 143 which are a light and a dark print of the same negative. In making the optical diffractograph masks the atoms were weighted as indicated in Table 7 (pg. 103) with the correction for the diffraction from water applied and with unitary atomic structure factors unity. The patterns are strictly applicable only at small diffraction angles because of the latter fact.

The patterns a, b, and c, and d of Figure 20 are patterns from the bases alone, the backbone alone, the backbone with the sodium ions included, and the total structure, respectively. The projection is the same as in pattern 19a. Pattern 20e is from a basal projection of the complete model. The weights used in Figure are those of Table 9 (pg. 105). As well as having been corrected for the water effect these have also been adjusted for diffraction to the center of the 11th layer line (3.1 A).

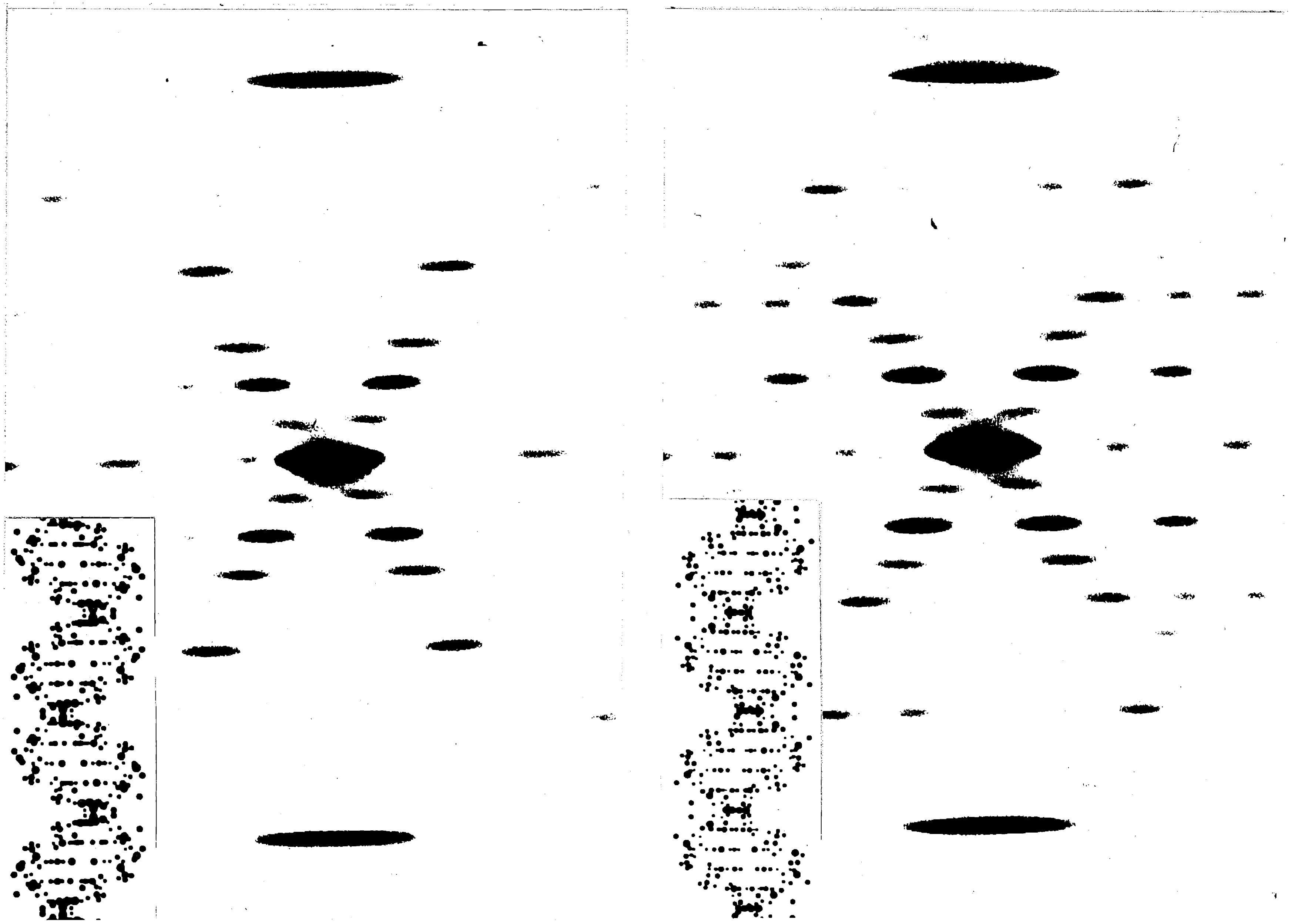

a

b

FIGURE 19

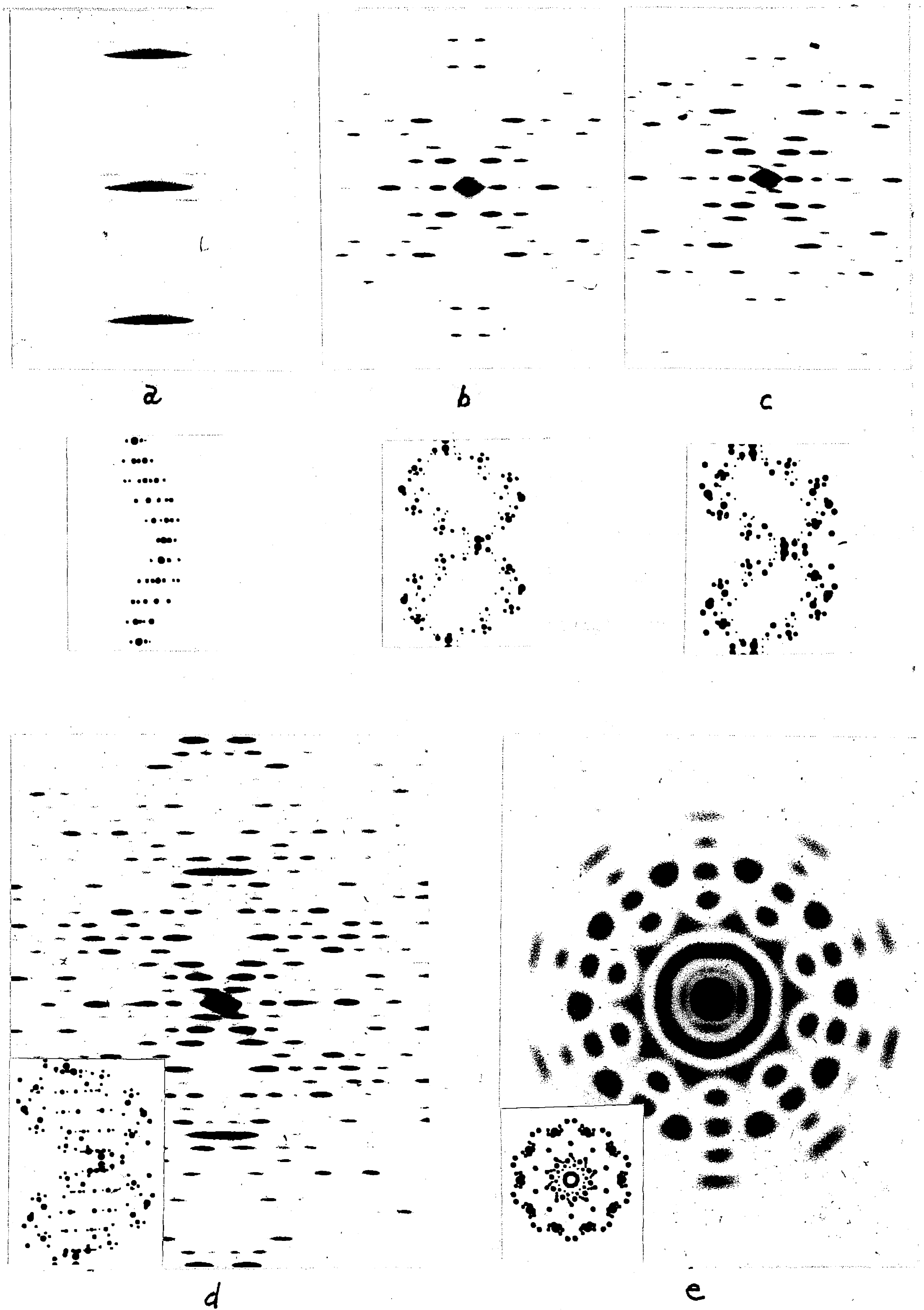

FIGURE 20

Referring to the analytical description of the DNA B_3 pattern, pp. 112-115, the data in points a, b, c, and d are inherently met in the basic assumptions of the model building. The calculated ratio of intensities at E I and E II is 860 as given in Figure 14 and thus point e is met in this respect. Rather good agreement is obtained elsewhere on the equator as well. The diffractograph pattern shows a very high ratio of intensity on the 10th and 11th layer lines and point f is met satisfactorily.

The relative intensities on the first six layer lines are correct in that the 2nd is appreciably stronger than the 1st and 3rd, the 4th (inner maxima) is weaker than the 5th and the 6th is absent. Thus the data of point seven are qualitatively matched but the 1st layer line is perhaps too weak on the diffractograph pattern and the 4th and 5th are certainly too strong. The disagreement is such that a smooth but rapid fall off applied to the optical results would substantially improve the situation. The fall off must not be applied to the 10th layer line since the water and atomic structure factor corrections would already be acting in this direction and the agreement here is already reasonable. If anything, it might be desirable to counteract the latter effects by reducing the second layer line intensity, for example, without reducing the 10th. It would almost seem that a reduction by a factor $(1/n)^3$ applied when n is not 0 would be in order.

Comparing the relative intensity of the second spot on the second layer line, L_2II, with the 1st spot on the equator, E I, (which was not done in the listing of features) another difficulty comes to the fore. The ratio of E I/L_2II is about 10 as estimated from an X-ray exposure time series. The calculated ratio of E I/L_2II taking multiplicity of lattice sampling into account is 1:1.17. Thus a fall off factor of $(1/n)^3$ as suggested above would be useful in this respect also.

There are several ways in which intensity changes of the type desired could be obtained. One would be to orient the helices in the unit cells in such a manner that the lattice sampling points on the 5th layer line would fall on minima of the structure factor expression as much as possible. A second would be to assign a much higher anisotropic temperature factor to the backbone than to the bases. Another possibility would be to hypothesize a lattice defect in the axial direction (in addition to the defect already used in the lattice analysis) quantized in tenths of the repeat period. This would leave the 10th layer line sampling sharp and make the 5th layer line sampling more diffuse. Such a quantized defect could arise from the forces between a PO_4 on one helix and the base pairs in the adjacent double helix. A fourth possibility would be that much more of the material in the fiber is contributing to the equatorial and 10th layer line intensities than to the 2nd, 3rd, and 5th layer lines. The possibility remains that the model is wrong, (a small change in the z coordinate of the phosphate or a different positioning of the sodium could help) or that it is incomplete. A second component could be cancelling on the 2nd and 5th layers.

There is rather good agreement between the optical and X-ray patterns in the distribution of intensity along the layer lines. The data from the X-ray patterns and the two optical patterns of Figure 19 are transposed to Figure 21. The positions of intensity on the X-ray pattern are indicated by crosses and the bars with uprights at the end. These are placed on the layer lines. Above these, the positions of intensity on the two optical patterns are indicated by two parallel lines (with no uprights). In between the X-ray and optical data the position and multiplicity of the lattice sampling points derived from the "parent" lattice (see Figure 8) are indicated by circles. The number of concentric circles at each point is one third of the multiplicity. The position of the first layer-line streaks on the X-ray and optical diffractographs agree very well. Calculation of the intensities on the 2nd layer line neglecting the bases and using centers of gravity for the backbone components (including Na) give relative intensities at the three spots of 1:4:3. This includes multiplicity considerations. The inner spot appears relatively stronger than this but agreement is substantial. Perhaps some components of the structure should be at a slightly larger radius. The third layer line intensity is very close to the proper location, especially if the position of the sampling points has meaning. The model should be slightly smaller, if anything, to match this datum. On the 5th layer line the fit would also be improved by a slight decrease in radius but again the sampling might work in the proper direction to obviate this shift.

In general the data relative to point h (pg. 114) are thus matched quite well by the model with an indication that the various components of the backbone may have to be shifted in different directions to improve the picture.

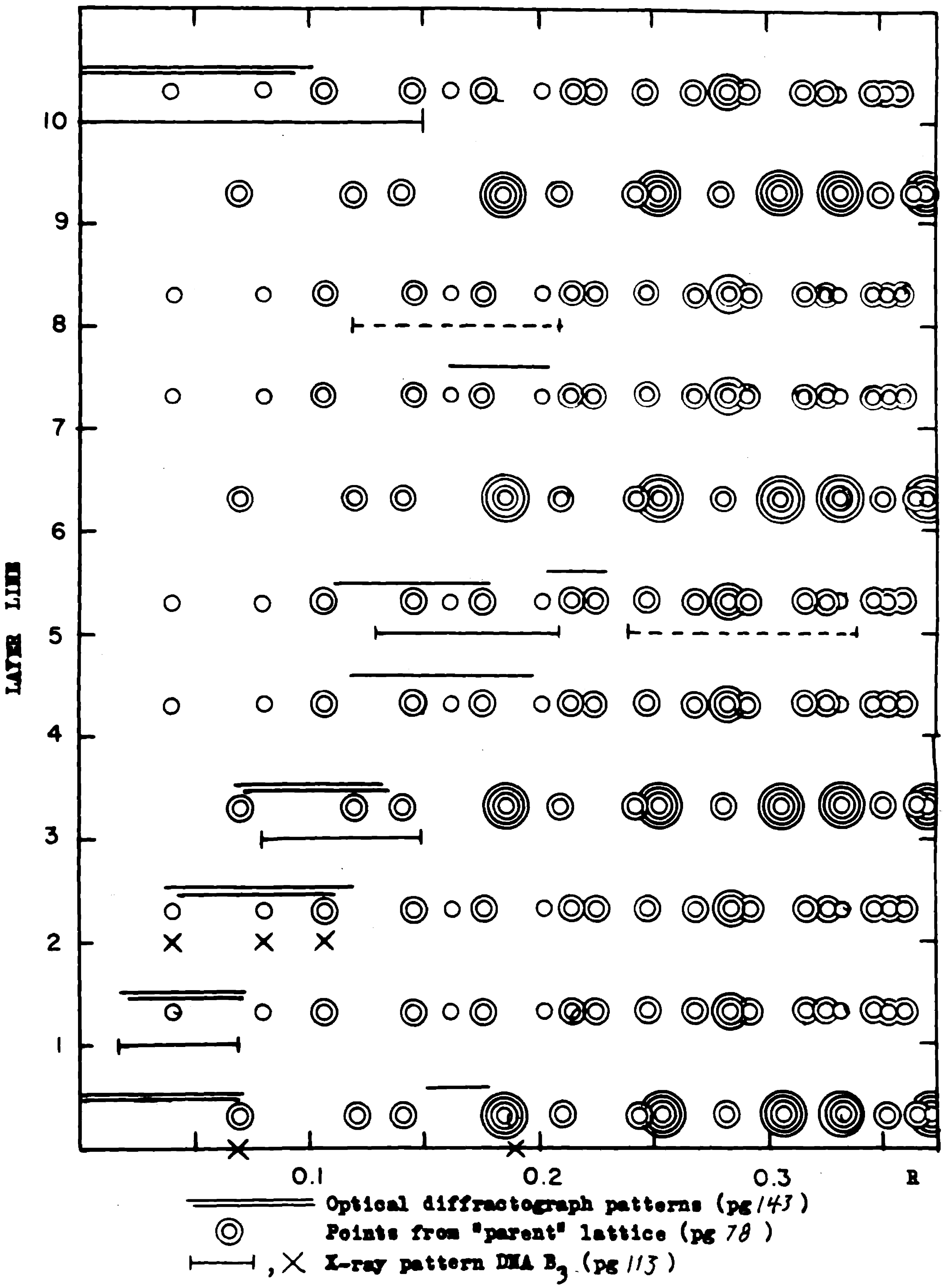
LAYER LINE
1
2
3
4
5
6
7
8
9
10
0.1
0.2
0.3
R
Optical diffractograph patterns (pg 143)
Points from "parent" lattice (pg 78)
, X X-ray pattern DNA B_3 (pg 113)

FIGURE 21

The points i through m will be ignored except to indicate that the intensification in the diffuse region of the 8th layer line is not at all indicated on the optical diffractograph patterns. In the course of analysis no obvious way of getting intensity there with minor shifts was noted.

In conclusion it can be said that changing of the pentose configuration has modified the model building considerably. Substantial improvement in the correlation of optical and X-ray diffraction patterns has been obtained with a detailed model containing a hypothetical deoxyribose. Van der Waals conflicts do exist and the X-ray data is not fitted perfectly. The intensity distributions in the optical patterns along the equator and the 1st, 2nd, and 10th layer lines agree very well with the X-ray data. The diffuse intensity on the 3rd and 5th layer lines is not quite so well matched. The intensities on the layer lines, relative to one another, would be improved by a general rapid fall off to a minimum intensity on the 5th layer line, returning to a maximum on the 10th. Several possible ways of obtaining this are suggested.

5. Consideration of the acridine-orange-stained-DNA diffraction pattern in terms of the DNA model #4.0.

Two X-ray patterns from DNA stained with acridine orange (AO) were presented in Plate 2 (Patterns 2h and 2i, pg48). On page 81 the lattice was analysed to be sensibly the same as that of the B_3 pattern except for a lateral shrinkage. If it is assumed that the DNA did not change its shape when the acridine orange was added partial structure factors from the DNA (and water) can be calculated for the new sampling positions. Using the graphs of Figure 14 (pg124) with an adjusted scale for radial values the partial factors in the following table were obtained. For ready comparison the values for model #4.0 with the B_3 lattice are also tabulated.

Table 13

	I		II	
	AO	#4.0	AO	#4.0
Bases	35.6	36.2	23.2	19.0
Deoxyribose	-0.2	5.2	-10.4	-10.4
PO_4	-20.2	-12.0	4.8	-10.4
Na	-5.2	-6.0	3.6	1.0
Total	10.0	+23.4	21.2	-0.8

When the acridine orange was added to the DNA the observed equatorial intensity was greatly weakened (relative to the 2nd layer line) at the first sampling point and not markedly changed at the second sampling point. On the basis of the assumption used above this would imply that the acridine was present in large quantity and placed so that diffraction from it would cancel the DNA (with the new sampling points) diffraction at the second equatorial spot and not markedly affect the intensity at the first spot. With the "center of gravity" of the acridine orange at about 7 A radius it would act in this direction changing the structure factor to 10.5 at E I and 7 at E II. The ratio of the two intensities would then be 2.3 in the proper direction. A larger ratio than this exists on the X-ray pattern. If the acridine orange displaced the sodium from the structure the effect would again be in the desired direction, changing the ratio $(EI/EII)^2$ to 25. This figure is of the right order of magnitude. The removal of the sodium would intensify the first spot somewhat leaving a net reduction of intensity at EI by a factor of 2.4 which is perhaps a little too small.

The acridine orange is about the same size as a base pair and somewhat thicker. At the ends there are two dimethyl amino groups that could interact with two phosphate ions, perhaps through a water bridge. In the middle of one side there is an NH group capable of hydrogen bonding to the bases. The acridine orange has an internal dyad symmetry and if the dyad axis is placed perpendicular to the fiber axis with the more hydrophilic edge of the molecule near the inner edge of the base pair a plausible structure results. If the plane of the acridine orange is tilted 5° to the plane of the bases the interplanar spacing will be 3.7 A at 5.5 A radius and a tightly packed structure will be obtained with one acridine orange for each base pair. If the acridine orange is tilted 22° in the opposite direction the same interplanar spacing will be obtained with one acridine orange molecule for every two pairs of bases. In either arrangement the nonpolar faces would extensively overlap one another. The outside edge of the complex would be nonpolar where the acridine was located and the shrinkage of the lattice might be a result of this.

The possibility of having only one acridine orange for every four phosphate ions provides a plausible explanation of the complexing ratio of 4.0 as found in solution by the partition method discussed on pg 70. The data is not conclusive in either area but it would appear to be possible by means of extended and refined experiments of the types employed here to come to a firm conclusion. Halides of the acridine derivatives might prove useful in this respect and other mutagens, carcinogens, pharmacueticals, or dyes of similar structure could also be profitably investigated.

SUMMARY

Two types of x-ray diffraction patterns obtained from DNA have been reported in the literature. Type A is obtained at 75 per cent relative humidity and comes from well defined crystallites (within a fiber). The structure is helical with a pitch of 28.1 A and two distances are observed between the axes of adjacent helices, 22.0 A and 22.7 A. The type B pattern is obtained at 92 per cent relative humidity and comes from a structure that is not as well ordered as the A material. The structure is helical with a pitch of 34 A. The distance between helices is variable and had not previously been specified. (See, however, Page 23 concerning a paper by Feughelman, Langridge, Seeds, Stokes, Wilson, Hooper, Wilkins, Barclay, and Hamilton, May 14, 1955).

1. The following patterns have been presented in this thesis, obtained from bundles of fibers of DNA which were immersed in alcoholic solutions and maintained under constant tension during the exposures:

a. DNA A pattern (See Plate 1). A pattern that was indistinquishable from the A pattern of the literature was obtained with specimens immersed in 80 or 85 per cent ethanol.

b. DNA B_3 pattern (See Plate 4). Patterns similar to the B patterns of the literature were obtained with specimens immersed in 65 to 70 per cent ethanol. The periodicity of the structure in the direction of the axis (the helix pitch) is 34.2 A. These patterns contain more detail than any patterns previously available and it was derived that the lateral separation of the centers of adjacent helices is 25.2 A (at 70 per cent ethanol). The helix axes are in a hexagonal array. Each helical unit (consisting of two coaxial DNA chains) can be in one of two positions along its axis as discussed on Page 78.

c. DNA B_2 pattern (See Plate 3). A pattern partly of the B type but distinctly different from any in the literature was obtained by mechanically stretching material in the A form (immersed in 85 per cent ethanol). The material in the stretched form is crystalline. The periodicity of the structure in the direction of the fiber axis is 32.5 A. The helix axes are not in a hexagonal array.

d. DNA-AO pattern (See Plate 2). When DNA in the B_3 form was "stained" with acridine orange (dissolved in the immersion fluid), a modified pattern was obtained. The modifications consisted of intensity changes and an isotropic lateral shrinkage of the array of axes to a new separation of 21.4 A. The repeat period along the axis remained at 34 A and the arrangement of helical units (DNA double chains) along their axes remained unchanged.

e. DNA-Hg pattern (See Plate 2). When $HgCl_2$ was added to the immersion fluid, the pattern deteriorated essentially leaving only the indication of a lateral repeat period. The same result was obtained with $AgNO_3$.

2. A new molecular model that is in substantially better agreement with the X-ray data than the Watson and Crick model was derived from a detailed analysis of the DNA B_3 pattern. The basic assumptions of the Watson and Crick model were maintained, but it was found necessary to assume a new puckered configuration for the deoxyribose. Details of the complete model are diagramed in Figure 18, and atomic coordinates are given in Table 11. There are 10 residues per turn and the pitch is 34 A. The phosphate group is at the same radius as in the Watson and Crick model, but the base pair is displaced three and a half angstroms toward the axis so that it overlaps the axis appreciably, and all of the atoms (except two hydrogens) are within 5.1 A of the axis.

The phosphorus atoms are 1.1 A from the plane of the bases and lie nearly above one another with alternating 15 A and 19 A separations.

3. Many aids were developed in the course of the analysis that will be useful in any structure determination involving DNA.

a. The optical diffraction method of testing models was refined so that it can be used with models as complex as those of DNA. The technique involves photographic reduction of a large model and oil immersion of the resulting mask. A suitable apparatus for obtaining the optical diffraction patterns was designed, developed, and permanently installed in the laboratory. In the case of DNA with its two related chains, calculations show that the average of only two optical diffraction patterns is necessary to evaluate the average obtained in an X-ray fiber pattern at all points of significance except for the equatorial plane. An optical diffraction pattern from a projection of the model along its axis will give the complete pattern in this plane.

b. An optical diffractograph study of the diffraction from the components of DNA, the bases, the pentose, and the PO_4 group, in the Watson and Crick positions is presented in Figures 9, 10, and 11 and summarized in Table 5. The diffraction from each of these components (with water taken into account as below) to two critical sampling positions on the equator was calculated as a function of radial position. These "group structure factor" values are plotted in the graphs of Figure 14 with the values for several specific models indicated.

c. A detailed method was developed for taking account of the extensive water of hydration in DNA by means of adjusting the weights assigned to the various atoms of the DNA structure. The corrections and adjusted weights for all of the atoms of DNA are listed in Tables 6, 7, and 9. The effects of the corrections on the scattering power of the various components of DNA are given in Table 10.

d. Making use of the relationship between the two chains in DNA, the equations of diffraction from helices were simplified. A simple graphical method of interpreting the phase relations expressed in these equations in terms of straight-line-contour maps on a special plot of the model (a projection on to a cylindrical surface which is then "unwrapped") was developed. (See pp. 119-121)

e. A three dimensional model kit was designed and constructed with the centers of all of the atoms represented and with all of the allowed rotations and bond-angle adjustments provided. In addition a system was set up for calculating and graphically representing many limitations to model building in terms of two major variables, the radial position of the base pair and the rotation of the pentose about the C_1'-N bond. (See pp. 128-131)

4. Through mechanical and optical studies the observed transition from the A to the B_2 X-ray pattern, obtained by stretching of the fiber bundle, was correlated with the optical and physical transitions observed (under different conditions) by Wilkins and Seeds (1951) and Fraser and Fraser (1951). The mechanical, optical, and X-ray studies all indicated that the transition involved was of a discontinuous nature. The X-ray data provides direct evidence of an elongation of the helix. The gross reversible elongation of the fibers (100 per cent) was, however, of a different order of magnitude than the reversible change in the axial repeat period (16 per cent) obtained directly from the X-ray data. Unless the coherently diffracting molecules have been stretched by a factor of approximately two and rearranged to have a repeat period involving about half as many residues as formerly then it must be inferred

that one or both of the sharp X-ray patterns are obtained from only a portion of the DNA present. The 100 per cent elongation could then be attributed to a "non-diffracting" moiety.

5. The complexing of acridine orange with DNA (see pg 70) was investigated in dilute acqueous solution by estimating the free acridine orange through its partition equilibrium in a two phase system of butanol and water. Saturation of the binding cites occurred with approximately one acridine orange molecule for each four phosphate groups but a direct phosphate estimation was not carried out. Binding decreased sharply when the DNA was denatured by boiling, indicating that the complexing depends on the physical structure of the DNA. A model for the DNA-acridine orange complex, based on X-ray data from DNA stained with acridine orange, is discussed on page 150. A plausible explanation of the acridine orange to phosphate ratio of 1:4 results. In the model the acridine orange assumes a position similar to that proposed by Feughelman, et al, (1955) for the protamine in nucleoprotamine.

6. Spectroscopic studies (see pg 70) of the interaction of $MgCl_2$ with DNA (prepared by the Mirsky-Pollister method) in dilute solution indicates complexing and thus qualitatively confirms Cavalieri's (1952) observations. The observations were extended to heat denatured DNA with the same evidence for complexing being found.

7. It was observed that DNA can apparently be maintained molecularly disperse in alcoholic media containing very little water (see pg 63). This provides an opportunity to study optical and other physical chemical properties of the isolated molecule in the media used in the X-ray studies presented above.

Bibliography

1. Allgen, L. G., 1954. Biochim Biophys. Acta 13, 446.
2. Astbury, W. T., and Bell, F. O., 1938a. Nature 141, 747.
3. Astbury, W. T., and Bell, F. O., 1938b. Cold Spring Harbor Symp. 6, 109.
4. Beevers, C. A. and Cochran, W., 1947. Proc. Roy. Soc. A. 190, 257.
5. Blout, E. R., and Lenormant, H., 1954. Biochim Biophys. Acta 15, 303.
6. Bragg, W. L., and Stokes, A. R., 1945. Nature 156, 332.
7. Broomhead, J. M., 1948. Acta Cryst. 1, 324.
8. Broomhead, J. M., 1951. Acta Cryst. 4, 92.
9. Brown, D. M., Michelson, A. M., Todd, A. R., 1954. Trans. Faraday Soc. 50, 291.
10. Cavalieri, Liebe F., 1952. J. of American Chem. Soc. 74, 1242.
11. Chargaff, E. and Davidson, J. N., 1955. The Nucleic Acids; Chemistry and Biology, vols I and II. New York: Academic Press.
12. Clews, C. J. B., and Cochran, W., 1948. Acta Cryst. 1, 4.
13. Clews, C. J. B., and Cochran, W., 1949. Acta Cryst. 2, 46.
14. Cochran, W., 1951. Acta Cryst. 4, 81.
15. Cochran, W., Crick, F. H. C., and Vand, V., 1952. Acta Cryst. 5, 581.
16. Cohen, Carolyn, 1954. Ph.D. Thesis. M. I. T.
17. Crick, F. H. C., and Watson, J. D., 1954. Proc. Roy. Soc. A. 223, 80.
18. Crowfoot, D., Bunn, C. W., Rogers—Low, Turner—Jones, 1949. The Chemistry of Penicillin, Princeton U. Press. 310.
19. Doty, P., and Rice, S. A., 1955. Biochim. Biophys. Acta. 16, 446.
20. Feughelman, M., Langridge, R., Seeds, W. E., Stokes, A. R., Wilson,

H. R., Hooper, C. W., Wilkins, M. H. F., Barclay, R. K., and Hamilton, L. D. 1955. Nature. 175, 834.

21. Franklin, R. E., and Gosling, R. G., 1953a. Nature. 171, 740.
22. Franklin, R. E., and Gosling, R. G., 1953b. Nature. 172, 156.
23. Franklin, R. E., and Gosling, R. G., 1953c. Acta Cryst. 6, 673.
24. Franklin, R. E., and Gosling, R. G., 1953d. Acta Cryst. 6, 678.
25. Franklin, R. E., and Gosling, R. G., 1955. Acta Cryst. 8, 151.
26. Fraser, J. F., and Fraser, R. D. B., 1951. Nature. 167, 761.
27. Frick, G., 1954. Biochim. Biophys. Acta. 13, 41.
28. Frick, G., 1954. Biochim. Biophys. Acta. 13, 374.
29. Furberg, S., 1950. Acta Cryst. 3, 325.
30. Furberg, S., 1952. Acta Chem. Scand. 6, 634.
31. Furberg, S., and Hassel, O., 1950. Acta Chem. Scand., 4, 1584.
32. Hooper, C. W., Seeds, W. E., Stokes, A. R., 1955. Nature. 175, 679.
33. Jacobson, B., 1953. Nature, 172, 666.
34. James, T. W., Mazia, D., 1953. Biochim Biophys. Acta. 10, 367.
35. Laland, S. G., Lee, W. A., Overend, W. G., and Peacocke, A. R., 1954. Biochim. Biophys. Acta. 14, 356.
36. Lipson, H. and Cochran, W., 1953. The Determination of Crystal Structures. London: G. Bell.
37. Mirsky, A. E., and Pollister, A. W., 1946. J. Gen. Physiol. 30, 117.
38. Overend, W. G., Peacocke, A. R., and Stacey, M., 1954. Trans. Faraday Soc. 50, 305.
39. Parry, G. S., 1954. Acta Cryst. 7, 313.
40. Pauling, L., 1948. The Nature of the Chemical Bond, 2nd ed. Ithaca: Cornell University Press.
41. Pauling, L., and Corey, R. B., 1953. Proc. N. A. S. 39, 84.

42. Peacocke, A. R., and Schachman, H. K., 1954. Biochim. Biophys. Acta. 15, 198.

43. Pitt, G. J., 1948. Acta Cryst. 1, 168.

44. Reichman, M. E., Bunce, B. H., Doty, P., 1953. J. Polymer Sci. 10, 109.

45. Riley, D. P., and Oster, G., 1951. Biochim. Biophys. Acta. 7, 526.

46. Schwander, H., and Signer, R., 1950. Helv. Chim. Acta. 33, 1521.

47. Shack, J., Jenkins, R. J., and Thompsett, J. M., 1953. J. Biol. Chem. 203, 373.

48. Thomas, R., 1954. Biochim. Biophys. Acta. 14, 231.

49. Traube, J., 1899. Samml Chem u Chem Tech Vorträge. 4, 255.

50. Watson, J. D., and Crick, F. H. C., 1953a. Nature. 171, 737.

51. Watson, J. D., and Crick, F. H. C., 1953b. Nature. 171, 964.

52. Watson, J. D., and Crick, F. H. C., 1953c. Cold Spring Harbor Symp. 18, 123.

53. Wiegand, R. G., 1953. Master of Science Thesis, M. I. T.

54. Wilkins, M. H. F., 1951. Pubbl. Staz. Zool. Napoli 23 Suppl. 104.

55. Wilkins, M. H. F., Gosling, R. G., Seeds, W. E., 1951. Nature 167, 759.

56. Wilkins, M. H. F., Seeds, W. E., Stokes, W. E., Wilson, H. R., 1953. Nature. 172, 759.

57. Wilkins, M. H. F., Stokes, A. R., Wilson, H. R., 1953. Nature 171, 738.

58. Williams, R. C., 1952. Biochim. Biophys. Acta. 9, 237.

59. Wrinch, D., 1950. Acta Cryst. 3, 475.

60. Zamenhof, S., Griboff, G., and Marrullo, N., 1954. Biochim. Biophys. Acta. 13, 459.

61. Zussman, J., 1953. Acta Cryst. 6, 504.

Biography

Born: December 3, 1926, Niagara Falls, New York.

Secondary School: was graduated from Niagara Falls High School January 1944.

Undergraduate Study: Attended Antioch College, Yellow Springs, Ohio, March 1944 to December 1948, majoring in physics, leading to a B.S. degree, awarded in June 1949.

Graduate Study: Attended Massachusetts Institute of Technology, Cambridge, Mass., January 1949 to June 1955.

Employment: As part of the Antioch College program the following positions were held: Junior Research Engineer in Metallurgy, P.R. Mallory and Co., Indianapolis (6 months 1944–45); Academic Laboratory Assistant in Physics, Antioch College (1 year half-time, 1945–46); Laboratory Assistant in physics, Linde Air Products Laboratory, Tonowanda, New York, (5 months, 1946–47); Technician in Psychometrics, Illinois Institute of Technology Psychological Service Center, Chicago, Illinois, (2½ months, 1948); Research Assistant in Biology, Massachusetts Institute of Technology, 1948–

During postgraduate studies the position of Research Assistant in Biology at Massachusetts Institute of Technology has been maintained, 1949–1955. Also consulting work has been done for Jarrell Ash Co., Scientific Specialties Co., and Tufts College Dental School.

Publications: Wyckoff, H.W. Hydrogen arc ultraviolet source. Mass. Inst. Tech. Res. Lab. of Elec. Quart. Progress Report, July 1949.

Wyckoff, H.W. High intensity wide angle hydrogen arc source of the ultraviolet continuum. J. Opt. Soc. Am. 41:293 (abs.), 1951

Wyckoff, H.W. The M.I.T. Recording Microspectrophotometer. Lab. Invest. 1:115, 1952